



Aalborg Universitet

**AALBORG UNIVERSITY**  
DENMARK

## **Microcalorimetric Evaluation of Wettability Alteration and Geothermal Brine Reinjection**

Cobos, Jacquelin

*Publication date:*  
2020

*Document Version*  
Publisher's PDF, also known as Version of record

[Link to publication from Aalborg University](#)

*Citation for published version (APA):*  
Cobos, J. (2020). *Microcalorimetric Evaluation of Wettability Alteration and Geothermal Brine Reinjection*. Aalborg Universitetsforlag. Ph.d.-serien for Det Ingeniør- og Naturvidenskabelige Fakultet, Aalborg Universitet

### **General rights**

Copyright and moral rights for the publications made accessible in the public portal are retained by the authors and/or other copyright owners and it is a condition of accessing publications that users recognise and abide by the legal requirements associated with these rights.

- Users may download and print one copy of any publication from the public portal for the purpose of private study or research.
- You may not further distribute the material or use it for any profit-making activity or commercial gain
- You may freely distribute the URL identifying the publication in the public portal -

### **Take down policy**

If you believe that this document breaches copyright please contact us at [vbn@aub.aau.dk](mailto:vbn@aub.aau.dk) providing details, and we will remove access to the work immediately and investigate your claim.





# **MICROCALORIMETRIC EVALUATION OF WETTABILITY ALTERATION AND GEOTHERMAL BRINE REINJECTION**

**BY  
JACQUELIN ELIZABETH COBOS MORA**

**DISSERTATION SUBMITTED 2020**



**AALBORG UNIVERSITY**  
DENMARK



---

---

# Microcalorimetric Evaluation of Wettability Alteration and Geothermal Brine Reinjection

---

---

Ph.D. Dissertation  
Jacquelin Elizabeth Cobos Mora

Dissertation submitted November 30, 2020

Dissertation submitted: November 30th, 2020

PhD supervisor: Prof. Erik Gydesen Søgaard  
Aalborg University

PhD committee: Associate Professor, Saqib Toor (chairman)  
Aalborg University

Vural Sander Suicmez, General Manager  
Middle East Operations at QRI, Houston – Texas

Associate Professor, Antje van der Net  
Norwegian University of Science and Technology

PhD Series: Faculty of Engineering and Science, Aalborg University

Department: Department of Chemistry and Bioscience

ISSN (online): 2446-1636  
ISBN (online): 978-87-7210-849-0

Published by:  
Aalborg University Press  
Kroghstræde 3  
DK – 9220 Aalborg Ø  
Phone: +45 99407140  
aauf@forlag.aau.dk  
forlag.aau.dk

© Copyright: Jacquelin Elizabeth Cobos Mora

Printed in Denmark by Rosendahls, 2020

# Abstract

The increased global demand for energy has spurred intense research in both non-renewable and renewable sources. Low salinity waterflooding is a low cost and environmentally friendly technology that could improve oil recovery by about 5-38%, which is above the established waterflooding technique. Carbonate reservoirs are promising targets for this type of enhanced oil recovery (EOR) method because they hold more than 60% world's oil reserves. Core-scale laboratory tests and field-scale trials have demonstrated the success of low salinity waterflooding but also its failure. Therefore, identifying which component/components of the crude oil+brine+rock system (COBR) responsible for the observed enhance oil recovery is extremely important but also hard to determine. It is because of the complexity of calcite bearing formations, crude oil, aqueous phase, and interactions among components. Another source of energy is Salt-Power, which uses the osmosis principle to produce clean and CO<sub>2</sub> free energy. In recent years, it has been shown the potential of hypersaline brines to produce electricity if they are mixed with fresh water. Geothermal brines are highly saline fluids (salinity more than 15%), normally reinjected back in the same reservoir after heat extraction, that could be used to produce more energy through osmosis. However, large amounts of diluted brine shall be handled properly to avoid environmental issues. Reinjection can be considered as the most feasible disposal option; nonetheless, complex fluid-fluid and rock-fluid interactions that take place upon reinjection make unclear the assurance of the overall reservoir.

The understanding of complex rock-fluid and fluid-fluid interactions is crucial for energy production from both non-renewable and renewable sources. This thesis deals with both research topics by using microcalorimetry, which is a universal tool that could be used to meet the challenge of assessing complex interactions in a reasonable time frame. Isothermal Titration Calorimetry (ITC) is a microcalorimetric analysis that measures directly the heat absorbed or released during physical or chemical process. The ITC experiments require small amounts of rock and fluids. Moreover, ITC gives both fluid-fluid and rock-fluid interactions with high accuracy. The heat response registered in a microcalorimeter could be used to determine enthalpy changes, which are related to

adsorption energies, and the detachment of loosely attached particles within the porous media.

The experimental results show that effectively isothermal titration calorimetry could be used to measure the adhesion energies, related to changes in wetting properties of a COBR system. It was found that those energies (enthalpy changes) vary significantly depending on the ionic composition of the injection fluid. In this sense, the performance of 10 times diluted seawater (10D\*SW) is much higher than the modified seawater (spiked with sulfate). Minor differences in enthalpy were also detected depending on the composition of outcrop and synthetic chalk samples. The reason why diluted seawater performs much better than modified seawater seems to be related to fluid-fluid interactions. By isolating rock-oil, ions/mixtures-oil interactions, it was confirmed that crude oils with high interfacial activity form micro-dispersions when the injection fluid has low salinity. It was found that the total energy required to create and stabilize a micro-dispersion follows:  $\text{Mg}^{2+} > \text{Ca}^{2+} > \text{Na}^+$ . The same trend has been reported from rheology and coalescence measurements, which indicate that a less rigid interface is obtained for  $\text{Mg}^{2+}$  than other water-soluble ions. It was also found that pair creation processes affect fluid-fluid interactions. If  $\text{SO}_4^{2-}$  is added to an aqueous phase containing either  $\text{Ca}^{2+}$  or  $\text{Mg}^{2+}$ , the endothermic enthalpy creation for mixture 2 ( $\text{Mg}^{2+} - \text{SO}_4^{2-}$ ) is lower than for mixture 1 ( $\text{Ca}^{2+} - \text{SO}_4^{2-}$ ). It is suspected that it is easier for water molecules to push away ion pairs with a neutral charge into the oil phase than to disrupt the existing hydrogen bonding (HB) network. More fundamental wettability studies confirm that the injection of fresh crude oil favors the wettability alteration of outcrop carbonate rocks. Further crude oil injections into the rock+brine system give exothermic peaks, which could suggest that carboxylic groups bond strongly to the limestone lattice due to acid/base interactions.

In the reinjection feasibility analysis of concentrated and diluted geothermal brines, it was found that an ion exchange process stabilized authigenic clays that are loosely attached to the pore surface. It is because divalent cations present in geothermal and diluted geothermal brines are adsorbed onto the negatively charged clay particles. The main issue with the reinjection of diluted geothermal brines coming from SaltPower electricity generation is iron precipitation inside the porous media, which causes a permeability reduction. Citric acid, an iron-control agent in oil field treatments, could be potentially used to keep Fe(II) in solution. This acid also dissolves iron-bearing carbonate cement (siderite and ankerite) which improves the rock properties. It was determined that effectively the usage of citric acid could be decreased very much after the first injection because of a permeability and porosity improvement. This, in turn, makes half diluted geothermal brine with citric acid an ideal choice to overcome the very often scaling problems that occur in reinjection wells.

# Resumé

Det stigende globale behov for energi har bevirket intens forskning i såvel ikke-vedvarende som alternative og vedvarende energikilder. Waterflooding med lavt saltindhold er en billig og miljøvenlig teknologi, som kan forbedre udvindingen af olie fra oliereservoirs med omkring 5-38%, hvilket er over den nuværende etablerede waterfloodings teknik. Karbonat reservoirs er velegnede mål for denne type af forøget olie indvinding (EOR), fordi de indeholder mere end 60% af verdens kendte olie reserver. Laboratorieprøver og test i core-plug skala og undersøgelser i fuld skala i oliefelter har demonstreret succes af waterflooding med lavt saltindhold, men der er også forekommet fejl. Derfor er det meget vigtigt men også et omfattende arbejde at identificere hvilken komponent eller komponenter af råolie+brine+mineral systemer (COBR), der er ansvarlige for den observerede forøgede olieudvinding. Dette skyldes også kompleksiteten af de kalcit bærende formationer, råolie, den vandige fase bestående af formationsvand og vand fra waterflooding. En anden kilde til energi er Salt-Power, som udnytter osmoseprincippet til at producere ren og CO<sub>2</sub> fri energi. I de seneste år er potentialet for koncentreret brine til at producere elektricitet, når det blandes med fersk vand gennem en halv gennemtrængelig membran, blevet vist. Geotermisk brine er brine med høje saltindhold (saltindhold mere end 15%), hvilket normalt bliver reinjiceret tilbage til det samme reservoir efter ekstraktionen af varme. Denne brine kan nu anvendes til at producere mere energi gennem osmose. Imidlertid skal de store mængder brine behandles rigtigt og med omhu for at undgå miljøproblemer. Reinjection kan betragtes som den mest optimale behandling; ikke desto mindre udgør komplekse væske-væske- og mineral-væske vekselvirkninger, som finder sted efter reinjektionen en uklar udfordring for hele reservoiret.

Forståelsen af komplekse mineral-væske- og væske-væske-interaktioner er afgørende for energiproduktion fra både ikke-vedvarende og vedvarende kilder. Denne afhandling behandler begge forskningsemner ved hjælp af mikrokalorimetri, som er et universelt værktøj, der kan bruges til at imødekomme udfordringen med at vurdere komplekse interaktioner inden for en rimelig tidsramme. Isotermisk titreringskalorimetri (ITC) er en mikrokalorimetrisk analyse, der direkte måler varmen, der absorberes eller frigives under en fysisk eller kemisk proces. ITC-eksperimenterne kræver små mængder mineral

og væsker. Desuden giver ITC både væske-væske- og mineral- væske vekselvirkninger med høj nøjagtighed. Resultatet registreres af mikrokalorimeteret og kan bruges til at bestemme entalpiændringer, der er relateret til ion- indkorporeringsenergi og løselighed af løst fastgjorte partikler i det porøse medium. De eksperimentelle resultater viste, at effektiv isothermisk titreringskalorimetri kunne bruges til at måle adhæsionsenergiene relateret til ændringer i befugtningsegenskaber i et COBR system. Det blev fundet, at disse energier (entalpiforandringer) varierer betydeligt afhængigt af den ioniske sammensætning af injektionsvæsken. I denne forstand er ydelsen for 10 gange fortyndet havvand (10D \* SW) meget højere end for modificeret havvand (tilsat sulfat). Mindre forskelle i entalpiændringer blev også påvist afhængigt af sammensætningen af outcrop og syntetiske kridtprøver. Årsagen til, at fortyndet havvand klarer sig meget bedre end modificeret havvand synes at være relateret til væske-væske-interaktioner. Ved at isolere mineral-olie, ion- blandinger-med olie-interaktioner blev det bekræftet, at råolie med høj grænsefladeaktivitet danner mikrodyspersioner, når injektionsvæsken har lavt saltindhold. Det blev fundet, at den samlede energi, der kræves for at skabe og stabilisere en mikrodyspersion, følger:  $Mg^{2+} > Ca^{2+} > Na^{+}$ . Den samme tendens er rapporteret fra målinger af reologi og koalescens, som indikerer, at der opnås en mindre stiv grænseflade for  $Mg^{2+}$  end for andre vandopløselige ioner. Det blev også fundet, at pardannelsesprocesser påvirker væske-væske-interaktioner. Hvis  $SO_4^{2-}$  tilsættes til en vandig fase, der indeholder enten  $Ca^{2+}$  eller  $Mg^{2+}$ , er den endoterme entalpiændring for en blanding af  $Mg^{2+}$  og  $SO_4^{2-}$  lavere end for blanding af  $Ca^{2+}$  og  $SO_4^{2-}$ . Det antages, at det er lettere for vandmolekyler at skubbe ionpar med en neutral ladning ind i mikroemulsionen end at lade det forstyrre det eksisterende hydrogenbindingsnetværk (HB). Mere grundlæggende fugtighedsundersøgelser bekræfter, at injektionen af frisk råolie favoriserer fugtighedsændringen af outcrop-karbonat. Yderligere råolieinjektioner i mineral + saltvandssystemet giver exotermiske toppe, hvilket kan antyde, at carboxylsyregrupper binder sig stærkt til kalkstensgitteret på grund af syre / base-interaktioner.

I analysen af effekten af koncentreret og fortyndet geotermisk saltvand blev det fundet, at en ionbyttingsproces stabiliserede authigenisk ler, der er løst bundet til poreoverflader. Det skyldes, at divalente kationer, der findes i geotermisk og fortyndet geotermisk brine adsorberes på de negativt ladede lerpartikler. Hovedproblemet med reinjektion af fortyndet geotermisk saltvand, der kommer fra SaltPower elproduktion, er jernudfældning inde i det porøse medium, hvilket medfører en permeabilitetsreduktion. Citronsyre, et middel til at kontrollere opløst jern i kemikaliebehandling af oliefelter, kan potentielt bruges til at holde Fe (II) i opløsning. Denne syre opløser delvist også jernholdigt karbonatcement (siderit og ankerit), hvilket forbedrer reservoiret. Anvendelsen af citronsyre i starten vil sandsynligvis effektivt kunne reduceres meget efter den første injektion på grund af den resulterende permeabilitetsforøgelse og porøsitetsforbedringen. Dette gør igen halvt fortyndet geotermisk saltvand med citronsyre til et ideelt valg til at overvinde de skaleringsproblemer, der ofte opstår i reinjektionsbrønde.



# Thesis Details

**Thesis title:** Microcalorimetric evaluation of wettability alteration and geothermal brine reinjection

**PhD student:** Jacquelin Elizabeth Cobos Mora

**Supervisor:** Prof. Erik Gydesen Søgaaard

The main body of this thesis consist of the following papers (in the order of logical narrative of the thesis):

- (I) **Cobos, Jacquelin**, Peter Westh, and Erik G. Søgaaard. “Isothermal Titration Calorimetry Study of Brine–Oil–Rock Interactions”, *Energy&Fuels*, Vol. 32, pp. 17338-7346, 2018.
- (II) **Cobos, Jacquelin**, and Erik G. Søgaaard. “ Impact of Compositional Differences in Chalk and Water Content on Advanced Waterflooding: A Microcalorimetric Assessment”, *Energy&Fuels*, Vol. 34, pp. 12291–12300,2020.
- (III) **Cobos, Jacquelin**, and Erik G. Søgaaard. “ Effect of individual ions on Rock-Brine-Oil Interactions: A Microcalorimetric Approach”, Under review in *Fuel*
- (IV) **Cobos, Jacquelin**, Martine Sandnes, Marianne Steinsbø, Bergit Brattekås, Erik G. Søgaaard, and Arne Graue. “ Evaluation of Wettability Alteration in Heterogeneous Limestone at Microscopic and Macroscopic Levels” Under review in *Journal of Petroleum Science and Engineering*
- (V) **Cobos, Jacquelin**, and Erik G. Søgaaard. “ Study of geothermal brine reinjection by microcalorimetry and core flooding experiments”, *Geothermics*, Vol. 87, pp. 101863, 2020.

- (VI) **Cobos, Jacquelin**, and Erik G. Søgaaard. “ Systematic Study of Geothermal Brine Reinjection for SaltPower Generation Purposes: Citric Acid as a Potential Iron Control Agent” Under review in *Geothermics*.

In addition to the journal article, following selected oral presentations have also been made:

- (VII) **Cobos, Jacquelin**, and Erik G. Søgaaard. “ Synergy of Microcalorimetry and Zeta Potential Measurements to Study Chalk-Brine Interactions”, *Oral presentation*, 81st EAGE Conference and Exhibition, 3-6 June 2019
- (VIII) **Cobos, Jacquelin**, and Erik G. Søgaaard. “ Geothermal Brine Reinjection from SaltPower Generation: A Microcalorimetry Study”, *Oral presentation*, 12th Annual Meeting InterPore, 31 August-4 September 2020

# Acknowledgments

First of all, I would like to express my sincere gratitude to my supervisor Prof. Erik G. Søgaaard for believing in me and providing me the freedom I need to be creative. I always felt your office was open for any kind of discussion. Thank you for being more than a supervisor but a friend who I share this extraordinary journey with. You inspired me to always strive towards excellence.

I would like to thank my fellow PhD students, and other co-workers. I enjoyed working next to Linda Madsen and Dorte Spangsmark. They were always helpful in the lab and genuinely showed me how to perform my own measurements. My special thanks also go to Mahdi Nikbakht Fini, Nikos Montesantos, Iveth Romero, Navid Bayati for academic discussions and wonderful times. Many thanks also to Heidi Thomsen for all the administrative paperwork and to all my colleagues at the department. Not lastly to Luis Garcia, Thomas Hansen, Evi Peshkepia, Maria Jørgensen, Arun Selvam, Kenneth Simonsen, and Tanzila Sharker who I shared countless experiences with.

During my studies I was fortunate to spend three months at University of Bergen, Norway. I would like thank everyone at the Department of Physics and Technology for your hospitality. A special thanks to my lab partner, Martine Folgerø Sandnes for all the great time we spent together and enriching my stay in Norway with your friendship. To my supervisor at University of Bergen, Prof. Arne Graue, I would like to say this: working with you has been an amazing experience. I will be forever grateful for your support and guidance all this time long.

My heartfelt gratitude goes to my family, specifically my parents, Gorqui Cobos and Mariana Mora, and my brother, Fernando Cobos for supporting my dreams and believing in me. You always encourage me to keep going, to keep believing in myself no matter the life's vicissitudes.

Finally, I thank God for giving me a second life chance for making this work possible. He was a very present help in trouble, my strength and refuge.



# Preface

“A theory is the more impressive the greater the simplicity of its premises, the more different kinds of things it relates, and the more extended its area of applicability” **Albert Einstein**.

This thesis is submitted to the Doctoral School of Engineering and Science in partial fulfillment of the requirements for the degree of Doctor of Philosophy at the Department of Chemistry and Bioscience, Aalborg University, Denmark. The Ph.D. project was performed under the supervision of Professor Erik Gydesen Sogaard from the section of Chemical Engineering at Aalborg University as the principal supervisor. The research was carried out in the period spanning from September 2017 to November 2020 at the section of Chemical Engineering at Aalborg University in Esbjerg, Denmark.

The work concerns the use of microcalorimetry in combination with other apparatus to evaluate wettability alteration processes and geothermal brine reinjection. This thesis is structured as a collection of scientific papers and divided into III parts. In the first part, the framework of the thesis and its research objectives are presented. It includes an introduction to the challenges of energy production from non-renewable and renewable sources (Chapter 1), relevant literature for carbonate and sandstone rocks (Chapter 2 and 3) and applied materials and methods (Chapter 4). For the information on the applied materials and methods, the reader is referred to the main body of this thesis. Part II summarizes the main findings of this PhD work, which is divided into a chapter for wettability alteration in carbonate rocks and a chapter for geothermal brine reinjection in sandstone rocks. Each chapter of this part tackles an individual research goal that was investigated and presented as an individual scientific paper. Those chapters were followed by the main conclusions and ending with an outline for future work in both research areas. Part III consists of a number of scientific papers that have been published or submitted to peer-reviewed journals. Those papers are sorted out depending on the rock type.

Jacquelin Cobos M.  
Aalborg University, November 26, 2020



# Contents

Abstract	iii
Resumé	v
Thesis Details	vii
Acknowledgments	ix
Preface	xi
I Framework and Background	1
1 Introduction	3
1 Research objective	6
1.1 Thesis outline	7
References	10
2 Carbonate Rocks	13
1 Introduction	13
2 Properties and Minerals	13
3 Classification of Carbonate Rocks	15
3.1 Limestone	15
3.2 Chalk	16
4 Wettability	18
4.1 Wettability measurement	19
5 Advanced Waterflooding	21
5.1 Suggested recovery mechanisms	22
References	27

<b>3</b>	<b>Sandstone Rocks</b>	<b>33</b>
1	Introduction . . . . .	33
2	Porosity and Permeability . . . . .	33
3	Minerals and Properties . . . . .	35
4	Formation Damage . . . . .	35
4.1	Mechanisms . . . . .	36
5	Geothermal Energy . . . . .	37
	References . . . . .	39
<b>4</b>	<b>Methodology</b>	<b>41</b>
1	Rock Samples . . . . .	41
1.1	Carbonate rocks . . . . .	41
1.2	Sandstone rocks . . . . .	42
2	Fluids . . . . .	43
2.1	Wettability alteration brines . . . . .	43
2.2	Geothermal brine . . . . .	44
2.3	Crude oil . . . . .	44
3	Microcalorimeter Apparatus . . . . .	45
4	Core Flooding Systems . . . . .	45
	References . . . . .	48
<b>II</b>	<b>Main Findings</b>	<b>49</b>
<b>5</b>	<b>Wettability Alteration</b>	<b>51</b>
1	Isothermal Titration Calorimetry for Wettability Studies . . . . .	51
2	Compositional Differences in Chalk and Water Content on Advanced Waterflooding . . . . .	54
3	Contribution of Individual Ions and Mixtures of Ions to Adhesion Energies . . . . .	59
3.1	Adhesion energies for oil-individual ions . . . . .	59
3.2	Adhesion energies for oil-mixture of ions . . . . .	64
3.3	Adhesion energies for chalk-individual ions/mixtures . . . . .	66
4	Wettability Alteration of Strongly Water-Wet Edwards Limestone . . . . .	68
4.1	Change in boundary conditions for imbibition experiments . . . . .	70
4.2	Wettability alteration towards less oil-wet conditions . . . . .	72
	References . . . . .	72
<b>6</b>	<b>Geothermal Brine Reinjection</b>	<b>77</b>
1	Half Diluted Geothermal Brine Reinjection Feasibility . . . . .	77
1.1	Microcalorimetric evaluation of rock-fluid and fluid-fluid interactions . . . . .	77
1.2	Brine permeability flow test . . . . .	80
2	Citric Acid as a Potential Iron Control Agent . . . . .	83



Contents	xv
2.1 Brine permeability flow test . . . . .	86
References . . . . .	91
<b>Conclusions</b>	<b>93</b>
<b>Future Perspectives</b>	<b>95</b>



# Part I

## Framework and Background

The motivation behind the current thesis is the need for a better understanding of the mechanisms by which a fluid alters physically and chemically the rock lattice of carbonates and sandstone reservoirs for energy production. A short introduction to the problem is followed by a general description of carbonate and sandstone rocks. This is followed by a presentation of the state-of-the-art in wettability alteration by advanced water flooding in carbonates and re-injection of geothermal brine in sandstone reservoirs. Lastly, the research goals and thesis structure will be presented.



# Chapter 1

## Introduction

The global energy demand has increased rapidly due to a robust population and economic growth. In this sense, the energy consumption was near twice the average rate of growth since 2010 [7]. Around 158 terawatt-hour (TWh) of energy was needed to maintain the lifestyle of 7.7 billion people worldwide in 2019 [13]. This is because the global population quadrupled and the world energy demand went up 16 times [9]. In the 20<sup>th</sup> century, fossil fuels play a dominant role in the global energy mix with an overall share that has not changed over the last 25 years. The strong rise of renewable energies will only reduce its demand to around 60% based on a sustainable development scenario presented by the International Energy Agency [8]. This scenario sets desired outcomes according to the sustainable goals of the United Nations (UN SDGs). The sustainable development scenario shows how the energy sector would need to adapt to reach those objectives in an integrated and cost-effective manner by reducing the CO<sub>2</sub> emissions and keeping the global temperature well below 2 °C.

Figure 1.1 shows how the energy demand between 2025 to 2040 in the sustainable development scenario. As observed, the demand for crude oil reaches a peak, and then it begins to decline. Coal, on the other hand, moves back to when the global economy was a quarter the size of today. Due to environmental advantages in comparison to other fossil fuels, the consumption of natural gas barely changes. The forecast also shows that the demand for renewable energy, such as hydro, modern biomass, and other (i.e wind, solar) increases more than 50% between those years.

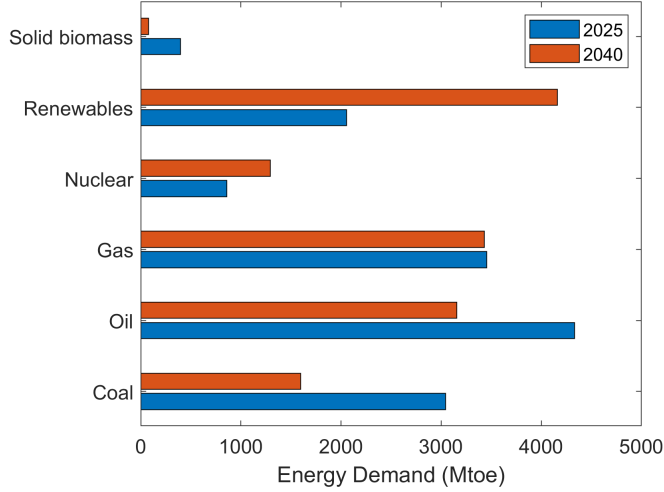


**Fig. 1.1:** World primary energy demand by a sustainable development scenario in million tones of oil equivalent (Mtoe). Based on data from IEA [7]

As shown by the most conservative forecast, the primary energy demand will still depend on fossil fuels in the near future. The declining rate of new oil reserves discoveries urges to explore new technologies to improve the oil recovery in reservoirs with high residual saturations economically and feasibly. Carbonate reservoirs (chalk, limestone, and dolomite) are considered promising targets because those reservoirs hold more than about 60% world's oil reserves. Nevertheless, the ultimate recoveries are very low [15].

Technical and economical challenges have narrowed the application of enhanced oil recovery (EOR) methods in carbonate reservoirs. Only a few projects have included chemical flooding (surfactants and polymers) from the 1990s to the 2000s. For instance, Yates field in Texas [18], Cottonwood Creek in Wyoming [17], and Mauddud carbonate in Bahrain [21]. Besides the high cost, there are several reasons for not using chemical flooding in carbonate reservoirs, such as a contrast in permeability (low-permeability matrix and high-permeability fractures), highly saline formation brines, and elevated reservoir temperatures [12]. Other EOR technologies, like hydrocarbon miscible gas injection (HC), water-alternating-gas injection (WAG), simultaneous water-and-gas injection (SWAG), and foam-assisted WAG injection (FAWAG) have been implemented in the North Sea region. The main constraints of those applications have been injectivity issues, reservoir heterogeneities, high permeability channels, and lack of a suitable injection-system monitoring [2]. According to Awan [2], most of the EOR field applications in the North Sea have been of the WAG type since 1975. In this sense, among the 19 EOR field applications, 48% were WAG due to a better microscopic/macroscopic

efficiency and flexibility when implementing WAG-injection cycles.  $\text{CO}_2$  injection has not yet been implemented in the North Sea region due to the limited availability of that gas offshore.

Most of the field developments have been limited to waterflooding, which is used for pressure maintenance and to displace the oil trapped in the pore space. This practice has left behind in the reservoir  $\sim 2/3$  OOIP [16]. In other words, only 30-40% of the original oil in place (OOIP) has been produced by primary recovery and conventional waterflooding, leaving a large amount of oil trapped in the pore space [3]. Nevertheless, the injection of seawater seems to be very promising and visible in many carbonate reservoirs. A good example is the fractured chalk Ekofisk reservoir in the North Sea, which has been submitted to seawater injection since 1987 [1]. An increase in oil rates, dramatic drops in the gas-oil ratio (GOR), and limited water breakthrough were observed in individual wells in the Ekofisk field in the Norwegian North Sea sector [6]. According to the Norwegian Petroleum [1], the expected final recovery factor for this field is nowadays over 50%, which is well above the established waterflooding technique. A better chemical understanding from laboratory experiments and field experience have shown that the ionic composition of the injected water has an impact on the wetting properties of carbonate reservoirs. The crude oil, brine, rock system (COBR) was brought into a new equilibrium state since the injected fluid has a different composition than the original formation brine. Therefore, it is important to characterize those interactions reliably and accurately in order to understand the reason for such tremendous success

According to the sustainable development scenario presented by the International Energy Agency [8], the power mix could be pushed to two-thirds by 2040 if additional measurements are taken to incentive the investment in renewables energies (based on geothermal heat, solar, biofuels, and electrification). Salinity Gradient Energy obtained by mixing fluids with a different salinity can also contribute to the energy transition from fossil fuels to more sustainable and environmentally friendly energies. In this sense, salinity gradient energy can be produced continuously, 365/24, with a low carbon footprint. It is completely independent of whether the sun is shining or the wind blowing [11]. This type of energy could be produced by pressure retarded osmosis (PRO), which is a membrane-based technology that utilizes the osmotic pressure difference between the draw (high salinity fluid) and the feed (low salinity fluid) [11, 20]. More energy is available for utilization by exploiting a larger salinity gradient. For instance, the Dead Sea, the Great Salt Lake, Lake Torrens in Australia, salt domes, natural subterranean formations of solid salt. By mixing freshwater with a hypersaline solution of 5.3 M NaCl, the energy of mixing is 11 times greater than for seawater [19]. Madsen et al. [10] also mentioned that this type of energy also called “SaltPower electricity generation”, is economically viable by using hypersaline fluids. This is because the PRO process can be operated at pressures up to 70 bar with power densities above  $5 \text{ W/m}^2$ .

Heat depleted geothermal brines are a good example of hypersaline fluids ( $>15$  wt % NaCl) that could be mixed with freshwater to produce “green energy”. However, this mixing process for power generation would produce large amounts of diluted geothermal brine that should be managed most environmentally. Reinjection is considered the most suitable option. However, the integrity of the geothermal reservoir should be assessed in advance to avoid operational and environmental issues [4]. This is because the chemical composition of geothermal fluids is quite diverse and it depends on the geochemistry of the reservoir. Normally, large concentrations of sodium, calcium, chloride, iron, and sulfide are present in the geothermal water since the reservoir rocks contain those ions [5]. Consequently, complex rock-fluid and fluid-fluid interactions should be determined in an accurate manner before reinjection.

Calorimetry which is defined as “the measurement of heat” (Sarge) [14] could provide the complex rock-fluid and fluid-fluid interactions observed in both non-renewable and renewable energy sources. Self-made calorimeters were used fifty years ago before the commercial production of those instruments. Since then, the development of sophisticated electronics has allowed reliable and accurate measurements within a short interval of time. This has made possible the development of new calorimeters and opened up new fields of applications. Scientific interest has also increased because calorimetry is a very easy and powerful method for different kinds of research [14]. Modern calorimetry has been successfully applied in different fields, such as life sciences (medicine, biology, and biochemistry), material science, pharmacy, and food science. However, it has not been widely used in the field of Geosciences. Therefore, this technique was used throughout this PhD study to meet the challenge of assessing complex rock-fluid and fluid-fluid interactions in a reasonable time frame for non-renewable and renewable energy production.

## 1 Research objective

The interaction between an injection fluid (brine, seawater, or modified seawater) and a rock plays an important role in both oil recovery and geothermal energy production. Consequently, this PhD study is subdivided for both purposes. The subtopic of enhanced oil recovery is mainly studied in carbonates; whereas, salinity gradient energy obtained from hypersaline geothermal fluids is assessed in sandstone rocks. In terms of oil recovery, different Isothermal Titration Calorimetry (ITC) experiments were carried out to understand the effect of the injection fluid in the wettability alteration process. The next step was to determine the influence of the different ions, which are present in the brine, seawater, and modified water, on the wettability alteration process. The impact of compositional differences in the chalk material was also determined by in-



jecting two types of advanced fluids (modified seawater and diluted seawater) into the rock+brine+oil systems. Besides, a more fundamental wettability alteration study in limestone core plugs was performed.

The reinjection impact of geothermal and diluted brines coming from Thisted and Sønderborg plants were also studied in this project. The first step was to analyze different brine samples from those plants. Then, different Isothermal Titration Calorimetry (ITC) experiments were performed to elucidate the complex physicochemical processes that take place upon reinjection. Coreflooding experiments were carried out complementary to determine if the geothermal and diluted brines could reduce the rock permeability. Finally, a proposed solution for the observed injectivity loss is presented.

In conclusion, this PhD study is an attempt to address the following research objectives:

- (1) To evaluate if the Isothermal Titration Calorimetry technique could be used to obtain rock-fluid and fluid-fluid interactions.
- (2) To investigate the impact of compositional differences on advanced waterflooding
- (3) To identify the effect of single ions and mixture of ions in wettability alteration in carbonates
- (4) To assess the wettability alteration in outcrop limestone core plugs by two different aging methods (static and dynamic)
- (5) To assess if half diluted geothermal brine could be re-injected back into a geothermal reservoir without compromising its integrity
- (6) To provide a potential solution if injectivity problems (permeability reduction) are observed upon reinjection of diluted geothermal brine

## 1.1 Thesis outline

After the introduction given in this chapter, the next sections present an overview of carbonate and sandstone rocks. In this sense, the potential of advanced water flooding is evaluated in carbonate rocks; whereas, geothermal brine reinjection is assessed in sandstone rocks. The final chapter of this part corresponds to a brief description of the materials and methods applied in the PhD thesis. Part II summarizes the key findings and outcomes of the articles which are linked and brought in an overall perspective for both non-renewable (enhanced oil recovery) and renewable (SaltPower) energies. Furthermore, recommendations for future research work by using microcalorimetry will be given. Part III consists of six published and submitted journal articles that were produced during the PhD. A schematic overview of this PhD work is presented in Figure

1.2. Those articles correspond to the overall topic of this thesis, rock-fluid, and fluid-fluid interactions. Nevertheless, they are divided into two main subtopics: wettability alteration and geothermal brine reinjection. The major part of the papers is on wettability alteration, which is again divided into two categories: advanced waterflooding and fundamental studies. Within the topic of advanced waterflooding, ionic composition, rock compositional effects (Paper I and Paper II), and the effect of ionic species (Paper III) are discussed. A more fundamental wettability alteration study by two aging methods is also presented (Paper IV). The topic of geothermal brine reinjection for SaltPower purposes is divided into two papers. In the first one, the reservoir integrity upon the reinjection of geothermal and diluted geothermal brines is assessed (Paper V). The next paper presents a potential alternative to keep iron in solution by adding citric acid to diluted geothermal brines (Paper VI). This article provides a solution to the observed injectivity problems upon the reinjection of a diluted geothermal brine.

## Papers

The following published and submitted journal articles were authored by the author of this thesis.

- (I) Cobos, Jacquelin, Peter Westh, and Erik G. Søgaaard. “Isothermal Titration Calorimetry Study of Brine–Oil–Rock Interactions, Energy” *Energy&Fuels* 2018 32 (7), 7338-7346
- (II) Cobos, Jacquelin, and Erik G. Søgaaard. “ Impact of Compositional Differences in Chalk and Water Content on Advanced Waterflooding: A Microcalorimetric Assessment” *Energy&Fuels* 2020 34(10), 12291–12300
- (III) Cobos, Jacquelin, and Erik G. Søgaaard. “ Effect of individual ions on Rock-Brine-Oil Interactions: A Microcalorimetric Approach” Under review in *Fuel*, 2020
- (IV) Cobos, Jacquelin, Martine Sandnes, Marianne Steinsbø, Bergit Brattekås, Erik G. Søgaaard, and Arne Graue. “ Evaluation of Wettability Alteration in Heterogeneous Limestone at Microscopic and Macroscopic Levels” Under review in *Journal of Petroleum Science and Engineering*, 2020
- (V) Cobos, Jacquelin, and Erik G. Søgaaard. “ Study of geothermal brine reinjection by microcalorimetry and core flooding experiments” *Geothermics* 2020, 87 101863
- (VI) Cobos, Jacquelin, and Erik G. Søgaaard. “ Systematic Study of Geothermal Brine Reinjection for SaltPower Generation Purposes: Citric Acid as a Potential Iron Control Agent” Under review in *Geothermics*, 2020

## Rock-Fluid and Fluid-Fluid Interactions

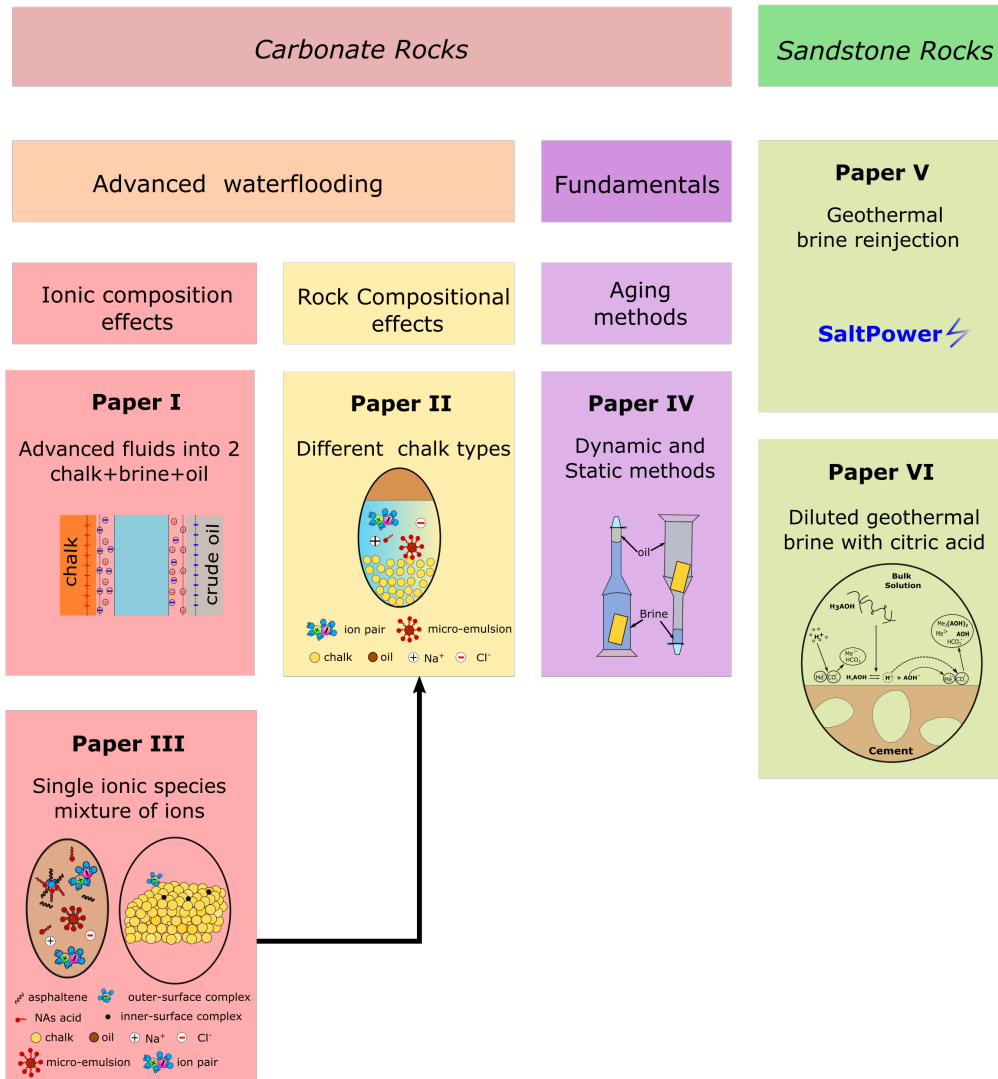


**Fig. 1.2:** Schematic overview and connection of all papers in the PhD work

## References

- [1] “Ekofisk norwegian petroleum,” <https://www.norskpetroleum.no/en/facts/field/ekofisk/>, accessed: 2020-08-18.
- [2] A. Awan, R. Teigland, and J. Kleppe, “A survey of north sea enhanced-oil-recovery projects initiated during the years 1975 to 2005,” *SPE Reservoir Evaluation & Engineering*, vol. 11, pp. 497–512, 06 2008.
- [3] S. Chandrasekhar, H. Sharma, and K. K. Mohanty, “Dependence of wettability on brine composition in high temperature carbonate rocks,” *Fuel*, vol. 225, pp. 573 – 587, 2018.
- [4] J. E. Cobos and E. G. Sjøgaard, “Study of geothermal brine reinjection by microcalorimetry and core flooding experiments,” *Geothermics*, vol. 87, p. 101863, 2020.
- [5] I. Dincer and H. Ozcan, *1.17 Geothermal Energy*, 02 2018, pp. 702–732.
- [6] H. Hermansen, G. Landa, J. Sylte, and L. Thomas, “Experiences after 10 years of water-flooding the ekofisk field, norway,” *Journal of Petroleum Science and Engineering*, vol. 26, no. 1, pp. 11 – 18, 2000.
- [7] International Energy Agency, “Global energy &  $CO_2$  status report / the latest trends in energy and emissions in 2018,” International Energy Agency, Tech. Rep., 2018.
- [8] —, “World energy outlook 2018,” International Energy Agency, Tech. Rep., 2018.
- [9] —, “World energy outlook 2019,” International Energy Agency, Tech. Rep., 2019.
- [10] H. T. Madsen, S. Søndergaard Nissen, J. Muff, and E. G. Sjøgaard, “Pressure retarded osmosis from hypersaline solutions: Investigating commercial fo membranes at high pressures,” *Desalination*, vol. 420, pp. 183 – 190, 2017.
- [11] H. T. Madsen, S. Søndergaard Nissen, and E. G. Sjøgaard, “Theoretical framework for energy analysis of hypersaline pressure retarded osmosis,” *Chemical Engineering Science*, vol. 139, pp. 211 – 220, 2016.
- [12] S. Pal, M. Mushtaq, F. Banat, and A. Al Sumaiti, “Review of surfactant-assisted chemical enhanced oil recovery for carbonate reservoirs: challenges and future perspectives,” *Petroleum Science*, vol. 15, no. 1, pp. 77–102, 2018.
- [13] H. Ritchie, “Energy,” *Our World in Data*, 2014, <https://ourworldindata.org/energy>.
- [14] S. M. Sarge, *Calorimetry : fundamentals, instrumentation and applications*, 2nd ed. Weinheim, Germany: Wiley-VCH Verlag.
- [15] J. J. Sheng, “Comparison of the effects of wettability alteration and ift reduction on oil recovery in carbonate reservoirs,” *Asia-Pacific Journal of Chemical Engineering*, vol. 8, no. 1, pp. 154–161, 2013.
- [16] A. Sohal, “Wettability modification in chalk: Systematic evaluation of salinity, brine composition and temperature effects,” Ph.D. dissertation, Aalborg University, 2016.
- [17] X. Xie, W. W. Weiss, Z. J. Tong, and N. R. Morrow, “Improved oil recovery from carbonate reservoirs by chemical stimulation,” 2005.
- [18] H. Yang and E. Wadleigh, “Dilute surfactant ior - design improvement for massive, fractured carbonate applications,” 2000.

- [19] N. Y. Yip, D. Brogioli, H. V. M. Hamelers, and K. Nijmeijer, “Salinity gradients for sustainable energy: Primer, progress, and prospects,” *Environmental Science & Technology*, vol. 50, no. 22, pp. 12 072–12 094, 2016.
- [20] N. Y. Yip and M. Elimelech, “Thermodynamic and energy efficiency analysis of power generation from natural salinity gradients by pressure retarded osmosis,” *Environmental Science & Technology*, vol. 46, no. 9, pp. 5230–5239, 2012.
- [21] H. K. Zubari and V. B. Sivakumar, “Single well tests to determine the efficiency of alkaline-surfactant injection in a highly oil-wet limestone reservoir,” 2003.



# Chapter 2

## Carbonate Rocks

### 1 Introduction

Carbonates are sedimentary rocks that contain more than 50% of carbonate minerals (e.g. calcite,  $\text{CaCO}_3$ , and/or dolomite,  $\text{CaMg}(\text{CO}_3)_2$ ). Those rocks hold more than 50% of the world's oil and gas reserves. Moreover, they are commonly used for different applications, such as cement production, building material or aggregates for road building, paint, plastic, adhesive, textile, food, and several other industries [22, 34]. Danish petroleum resources (80% of the oil and gas) are extracted from fields in chalk reservoirs of late Cretaceous (Maastrichtian) and early Paleocene (Danian) ages [3]. Thus, the study of how to enhance the oil recovery from carbonate reservoirs is of great importance.

This chapter is about the nature of carbonate reservoirs and their wettability alteration. It begins by describing the origin of carbonate sediments, followed by an account of the major minerals and classification of carbonate rocks. Some definitions of wettability come after this discussion. The chapter concludes with an advanced water flooding state of the art, which reviews the suggested recovery mechanisms at the solid-liquid and liquid-liquid interfaces.

### 2 Properties and Minerals

Carbonate sediments can be formed and accumulated in different depositional environments from oceans to hot springs but commonly those sediments are associated with shallow tropical seas [34]. Carbonate rocks exhibit higher levels of complexity than sandstones. A biological origin and extensive diagenetic changes make them more com-

plex than sandstones. The principal complexities include variations in shapes and types of pores, secondary porosity, and a broad range of pore size distributions [62].

Carbonate rocks are composed primarily of carbonate minerals. Solid calcium carbonate ( $\text{CaCO}_3$ ) exists in three different polymorphs or crystal structures, which are displayed in Figure 2.1.

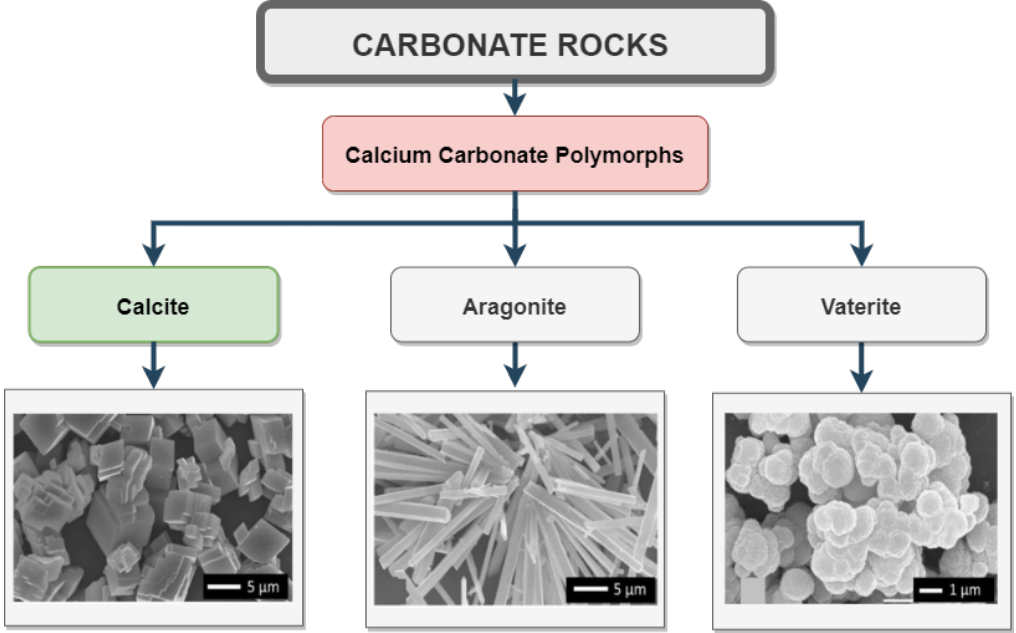
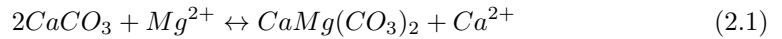


**Fig. 2.1:** Polymorphs or crystal structures of calcium carbonate. Calcite with a deformed cube shape, aragonite with needed-like facies, and vaterite with lenses facies. SEM images were reprinted with permission of American Chemical Society from Carré et al. [14]

An important subgroup of  $\text{CaCO}_3$  minerals are magnesium calcites. Those carbonate minerals contain not only calcium but also magnesium ions. Dolomite,  $\text{CaMg}(\text{CO}_3)_2$ , is part of this subgroup. It is the common component of many carbonate rocks, which could be formed from calcite (dolomitization) and vice versa (dedolomitization or calcification) by Equation 2.1 [57].



From all those minerals, calcite is the main mineral present in the rock samples used in this PhD thesis. This mineral is the most abundant and thermodynamically stable polymorph under ambient conditions. It is referred to as low-magnesium calcite (LMC)



since it contains  $<4$  mol%  $\text{MgCO}_3$  [57]. It crystallizes in the trigonal system but the shape of the crystal depends on temperature and pressure. This is because at high temperatures calcite transforms to phase IV (an orientational disorder of carbonate groups) and phase V (rotation of carbonate groups). On the other hand, at high pressures, calcite undergoes several phase transitions (i.e. high-pressure polymorphs II, III, and VI). If both pressure and temperature are high enough to overcome the kinetic barrier (phase boundary) for the phase transition, this mineral will transform into aragonite [13].

### 3 Classification of Carbonate Rocks

The carbonate rocks classification according to the mineralogy content can be found in Figure 2.2. As observed if a rock contains a significant amount (more than 50%) of calcite/aragonite and dolomite can be classified as carbonate rock. The principal carbonate rocks types are briefly described as follows. Note that from all those rocks, only limestone and chalk were used in the experimental part presented in this thesis.

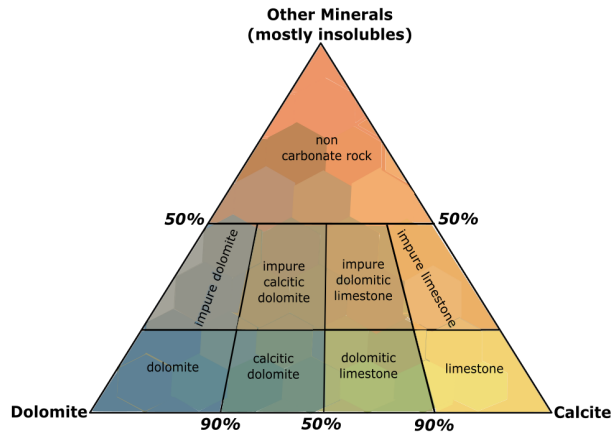


**Fig. 2.2:** Mineralogical classification of carbonate rocks. Adapted from [17]

#### 3.1 Limestone

Sedimentary rock that has a carbonate fraction that exceeds 50%, over half of which could be calcite or aragonite [24]. It constitutes approximately 10% of the earth's surface outcrops. Limestone is created from the accumulation of shells/fragments, or direct crystallization of calcium carbonate from water. The great majority of limestones have a marine origin, being formed in shallow waters with a depth of less than 20 m, and a

few from freshwater and lagoons [17].

The limestone formation is characterized by cementation, compaction, and selective dissolution [1]. The first diagenetic process corresponds to cementation that occurs soon after deposition, in which a hard compact rock is formed by the precipitation of calcium carbonate in the pore space that binds loose grains together [17]. The cementation process by calcite continues as long as the sediments are buried. It propagates from the pore walls into the pore space, which in turn reduces the pore size. Consequently, the permeability, capillary properties, and porosity are also disturbed by the cementation process [1]. The increased overburden pressure during burial causes compaction. This physical and chemical process causes a loss of porosity, reduction of pore-size, grain deformation, breaking, and fracturing [1]. However, compaction is a source of energy to displace fluids from a sediment into adjacent sediments. Therefore, it is considered as a reservoir drive mechanism to produce hydrocarbons. The last diagenetic process is dissolution by which carbonate and evaporite minerals are dissolved and removed. This in turn creates and modifies the pore space of limestone rocks. The dissolution process is fabric selective because one fabric element is dissolved in preference to others, giving as a result, moldic pores or separate vugs (cavity). The dissolution of anhydrite and gypsum is example of fabric selective dissolution since those minerals are more soluble than calcite or dolomite and therefore they are commonly dissolved first. When the dissolution is not fabric selective, touching vugs (interconnected voids) will be formed. Those interconnected vugs result from the collapse of molds due to an overburden pressure that increases with burial depth. The direct impact of those interconnected vugs is an enhancement in the rock permeability without changing the porosity significantly [1].

Limestone usually has a high primary porosity in the range 40-70% during deposition, which decreases due to the severe diagenetic changes, such as cementation, mechanical and chemical compaction, and dissolution. A porosity reduction between 5-15% is commonly observed in carbonate reservoirs [62]. The diagenetic effects also have an impact on permeability depending on the rock fabrics (e.g. grainstone, grain-dominated packstone, and mud-dominated fabrics). For instance, grainstones have the highest permeability (100 mD), whereas, mud-dominated limestone has the lowest value (1 mD) [1].

### 3.2 Chalk

A relatively pure form of limestone that consists of stable low-magnesium calcite [56]. It is a soft rock formed by the accumulation of coccoliths (microscopic shells) from micro-organisms called coccolithophores in warm waters, where the temperature and nutrient conditions favor calcareous plankton [23, 34]. Due to the low-Mg content in the calcite that forms the coccoliths, less diagenetic changes occur in chalk in comparison to

other carbonates (mixed aragonitic and high-Mg composition) [30]. Scanning electron micrographs of a chalk sample from the Ekofisk Formation are presented in Figure 2.3. As observed, coccolith plates or laths are present in the chalk since complete coccospheres with diameters between 10 and 30  $\mu\text{m}$  were broken up into their minute components called coccolith laths or plates. Each lath with a size of typically 0.5-1  $\mu\text{m}$  is a tablet-shaped crystal of low magnesium calcite [21, 30].

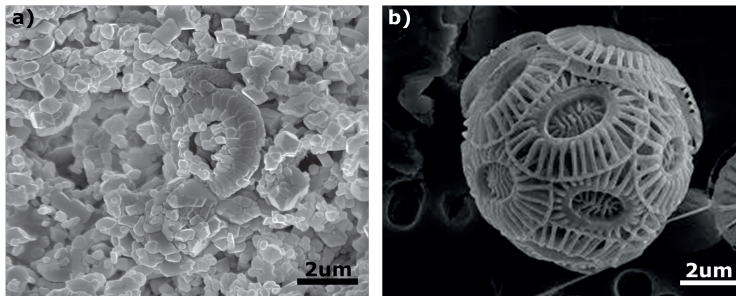


**Fig. 2.3:** a) Scanning-electron micrographs of rock surface from the Ekofisk Formation in the Ekofisk field. b) Coccolithophore species *Emiliana huxleyi*. Adapted from: Gennaro [30]

Secondary components can also be presented in this carbonate rock, where, the non-biogenic fraction is represented by detrital quartz and clay minerals. Although the content of clay minerals in chalk is low, there are some intervals in which those minerals can reach up to 20% wt of the bulk sediment [37]. Those siliciclastic materials could have been transported as erosional detritus by wind and/or rivers from the continent and coast. Volcanic ash may also have contributed to the clay material in the chalk [23].

The porosity of newly deposited calcareous ooze (shells of coccolithophores) is around 70% at the sediment-water interface, which corresponds to the interparticle porosity between sediment grains and within shells of microfossils [23]. This value decreases as a consequence of chemical compaction and pressure solution effects, which are related to the increasing overburden. In this sense at a burial of 1 km, the porosity declines to about 35%; at 2 km to about 15% [30]. The permeability also declines with increasing the effective burial stress, similarly to the change in porosity. The relationship between permeability and porosity is no constant, varying with the stratigraphic age of the chalk. An early oil migration into the reservoir, which prevented further cementation during burial, is the reason why over-pressured chalk reservoirs as the ones found in the North Sea maintain porosities up to 45-50% and matrix permeabilities between 3-10 mD at a burial depth in the range 1700-3300 m [34].

## 4 Wettability

In a petroleum reservoir system, different fluids (crude oil, natural gas, or both) are in equilibrium with the reservoir rock. As a consequence, the contact between the solid surface and the reservoir fluids causes active intermolecular forces (adhesion and cohesion). If the cohesive forces are weaker than the adhesive forces, the liquid adheres (wet) to the surface. Wettability is therefore often defined as “the ability of a fluid to spread on or adhere to a solid surface in the presence of other immiscible fluids” (Craig) [19]. When oil preferentially spreads on the rock surface, the rock is said to be oil-wet. While a surface is water-wet when water preferentially spreads on it. The porous rock may also show no preference towards either fluid (neutrally wet). Wettability controls the fluid distribution and flow (including oil recovery) within the porous medium by controlling capillary pressure and relative permeability [63, 64].

The wettability tendencies of the rock-fluid systems is a function of the level of adhesion ( $A_d$ ), which also depends on the interfacial tension. According to Abhijit [20], the adhesion between crude oil and water (immiscible fluids) which are present in the porous media can be defined by Equation 2.2. In this equation,  $\gamma_{sw}$  is the interfacial tension between the solid and the denser fluid phase (water in this case) and  $\gamma_{so}$  is the interfacial tension between the solid and the lighter fluid phase (oil in this case).

$$A_d = \gamma_{so} - \gamma_{sw} \quad (2.2)$$

The contact angle, conventionally measured through the denser liquid phase, is the angle where a fluid interface (water-oil or liquid-vapor) meets a solid interface as seen in Figure 2.4. It can be determined by rearranging the Young’s Equation, which dictates the relationship among the interfacial and surface energies, though Equation 2.3.

$$\cos\theta_{ow} = \frac{\gamma_{so} - \gamma_{sw}}{\gamma_{so}} \quad (2.3)$$

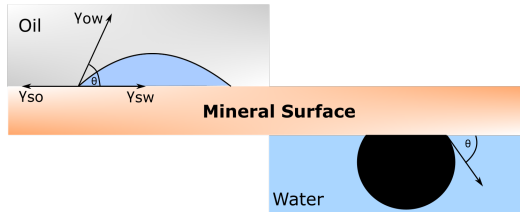


**Fig. 2.4:** Schematic representation of two immiscible fluids (water and crude oil) in contact with a mineral surface. Adapted from [20]

The adhesion ( $A_d$ ) can be obtained by Equation 2.4, which is a combination of Equations 2.2-2.3. As observed, the only parameters needed to determine  $A_d$  are the oil-water interfacial tension and contact angle. If  $A_d$  is positive, the system is water-wet ( $\theta=0^\circ$ ) and negative for an oil-wet system ( $\theta=180^\circ$ ). While if  $A_d$  is zero ( $\theta=90^\circ$ ), the affinity of both liquid phases to adhere to the solid surface is equal [20]. A graphical representation of the different wetting states are presented in Figure 2.5.

$$A_d = \gamma_{ow} \cos \theta_{ow} \quad (2.4)$$

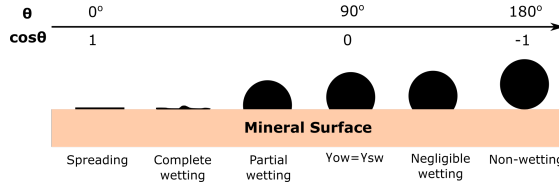


**Fig. 2.5:** Schematic representation of different wetting states based on contact angles. Adapted from [48]

## 4.1 Wettability measurement

Different methods have been used to assess the wettability. Those methods include contact angles, Amott-Harvey wettability index, USBM (U.S. Bureau of Mines), flotation, relative permeability, permeability/saturation relationships, imbibition rates, reservoir logs, nuclear magnetic resonance spectroscopy [63].

In this thesis, the Amott-Harvey index (imbibition and forced displacements) is the main quantitative method to assess the wettability. This method is briefly described as follows.

### Amott-Harvey wettability index

Amott [5] implemented a method to quantify the average wetting state of a porous medium by combining imbibition and forced displacements. This method is based on the fact that depending on the wetting state of the porous media one fluid will be spontaneously imbibed into the rock sample, displacing the non-wetting one. The Amott-Harvey method uses the ratio between spontaneous imbibition to forced imbibition to reduce the influence of other factors, such as initial water saturation, relative permeability, and viscosity [63]. As observed in Figure 2.6, one full Amott-Harvey cycle consists of the following four steps: (1) spontaneous imbibition of water, (2) forced water injection, (3) spontaneous imbibition of oil, (4) forced oil injection. The Amott-Harvey wettability

index,  $I_{AH}$  can be calculated by Equation 2.5, where,  $I_w$  is the water wettability index and  $I_o$  is the oil wettability index.

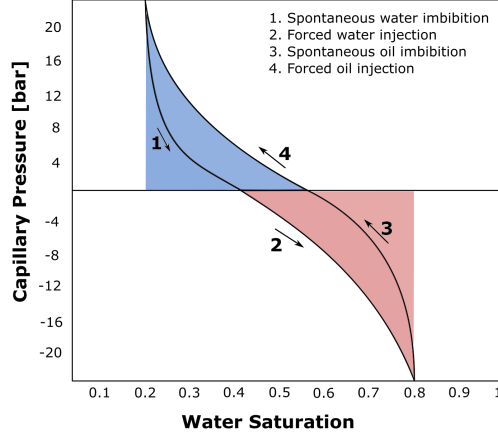


**Fig. 2.6:** The four steps of one full Amott-Harvey cycle. Adapted from [63]

$$I_{AH} = I_w - I_o \quad (2.5)$$

The water and oil wettability indices are quantified by measuring the increase in water and oil saturation during spontaneous imbibition ( $\Delta S_w$  and  $\Delta S_o$ ) and the total increase after forced displacements and imbibition ( $\Delta S_{wt}$  and  $\Delta S_{ot}$ ). Consequently, the water wettability index ( $I_w$ ) and the oil wettability index ( $I_o$ ) can be estimated by Equations (2.6-2.7).

$$I_w = \frac{\Delta S_w}{\Delta S_{wt}} \quad (2.6)$$

$$I_o = \frac{\Delta S_{os}}{\Delta S_{ot}} \quad (2.7)$$

Depending on the Amott-Harvey index, the mineral surface can be water-wet, neutrally-wet, and oil-wet. The approximate values of the Amott-Harvey indices for those wetting conditions are given in Table 2.1.

**Table 2.1:** Approximate relationship between wettability and Amott-Harvey wettability indices. Source: [63]

Amott-Harvey Index	
Water-wet	$0.3 \leq I_{AH} \leq 1.0$
Neutrally-wet	$-0.3 \leq I_{AH} \leq 0.3$
Oil-wet	$-1.0 \leq I_{AH} \leq -0.3$

## 5 Advanced Waterflooding

Different terms have been used for this recovery technique such as “smart waterflooding” [26, 51, 53, 65], “advanced ion management” [31], and “low salinity waterflooding” [2, 6, 38, 40, 46]. As mentioned in a literature review done by Bartels et al. [12], the number of publications on this topic has increased over the years with a maximum of 360 papers between 2015 and 2018. Such huge attention among the scientific community and petroleum industry is due to the following reasons: 1) novel and effective EOR method that could be applied to improve the oil recovery in carbonate reservoirs, 2) cost-effective method with low capital investment and operational costs, 3) environmentally friendly that no requires the addition of other chemicals, 4) it can be applied at any stage of a reservoir [58].

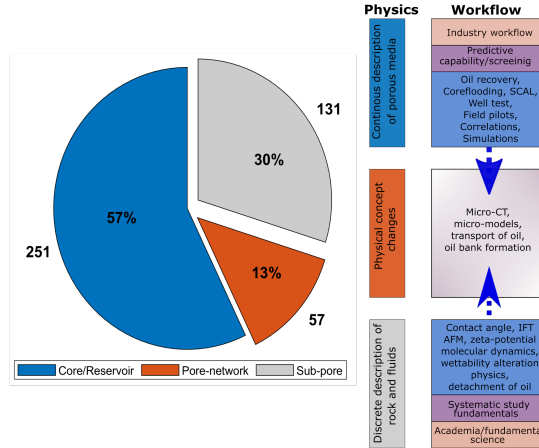


**Fig. 2.7:** Advanced waterflooding approaches used by industry and academia. Fundamental science starts from a more detailed analysis towards the application side; whereas, the industry uses the path from the application towards a detailed side. Adapted from: [12]

Despite the significant interest in this topic, knowing exactly which component of

the crude oil, brine, rock system (COBR) is responsible for the oil recovery improvement is difficult because of the complexity of the minerals, crude oil, aqueous phase, and interactions between them. In addition, it cannot be predicted the amount of additional oil that would be recovered and in what time it would be [12].

Most of the research in advanced waterflooding has been done at the core/reservoir scale with more than 57% of all publications. Fewer research reported in the literature has been done at sub-pore (30%) and pore-network scales (13%) [12], as shown in Figure 2.7. Previously, coreflooding and spontaneous imbibition experiments, conducted at the core scale, served as the main argument that advanced waterflooding actually leads to additional oil recovery. However, this scale resulted in several trends and mechanisms that explain the additional oil recovery [12]. Recently, more fundamental research has been intensified on a sub-pore and pore network scales with the aim to correlate the rock and fluid properties with the low salinity water response. The ultimate goal of this fundamental research is to increase the predictive capability of available simulators to pre-select potential candidates without running costly and intensive tests. However, it is not a straight forward task because advanced waterflooding is a cooperative process that benefits the detachment, coalescence, transport, banking, and ultimate oil recovery on different length and time scales. Energy landscapes, kinetics, and thermodynamics could be potentially useful when trying to unify different processes on different time and length scales. However, those values are difficult to obtain due to the intrinsic complexity of the COBR system [12]. As shown through this thesis, isothermal titration calorimetry provides valuable information on the rock-fluid and fluid-fluid interactions in the complex COBR system that could help to discern and unify the processes that take place when a low salinity fluid contacts an oil reservoir.

## 5.1 Suggested recovery mechanisms

Several mechanisms for the observed oil recovery increment in carbonates have been postulated in the literature from either direct measurements/observations or core and reservoir scales. Those mechanisms can be divided into processes related to solid-liquid and liquid-liquid interfaces. The proposed mechanisms in the category of a solid-liquid interface are multi-component ion exchange, surface charge, and double-layer expansion, mineral dissolution, pH change effect. The mechanisms related to the liquid-liquid interface are osmosis and diffusion, interfacial tension (IFT), micro-dispersions, and viscoelasticity.

The general consensus is that wettability alteration towards a more water-wet state is the macroscopic effect of advanced water flooding but the mechanisms that contribute to the wettability alteration are poorly understood.



### Solid-liquid interface

The mechanisms related to the solid-liquid interface are briefly described as follows:

**Multi-component ion exchange (MIE):** According to this mechanism, sulfate ( $\text{SO}_4^{2-}$ ) from seawater absorbs onto the positively charged calcite surface which reduces the electrostatic repulsion for calcium ( $\text{Ca}^{2+}$ ), which gets close to the rock lattice. Hence,  $\text{Ca}^{2+}$  ions release the negatively charged carboxylic groups ( $-\text{COO}^-$ ) bonded to the calcite surface by reacting with them. This process renders the initial wettability towards a more water wetting condition at room temperature. Magnesium ( $\text{Mg}^{2+}$ ) have the same affinity as  $\text{Ca}^{2+}$  towards the rock surface. Nevertheless,  $\text{Mg}^{2+}$  becomes more reactive at high temperatures (e.g. 100-130°C) and assist in the wettability alteration process by displacing both  $\text{Ca}^{2+}$  and calcium-carbonate complexes  $[-\text{COOCa}]^+$  [7, 25, 26, 52, 60, 61, 67, 68]. It has also been suggested that  $\text{SO}_4^{2-}$  cannot alter the wettability of the rock without the presence of  $\text{Ca}^{2+}$  and  $\text{Mg}^{2+}$  and the same occurs if only those divalent cations are present in the brine [68]. However, various laboratory studies have shown an oil improvement even though the concentration of those ions (potential determining ions, PDIs), was small. In those cases, the seawater was diluted and has a low salinity (TDS  $\sim$  1000 ppm) [2, 38, 46, 66]. As claimed by those studies diluted seawater improves the injectivity, accelerates the oil production, and reduces the risks of souring and scaling.

**Surface charge and double layer expansion:** This mechanism suggests that lowering the brine salinity leads to a more negatively charged calcite surface, which contributes to the expansion of the electrical double layer (EDL). In other words, a low salinity fluid has a thicker water film in comparison to a higher salinity fluid. The EDL expansion increases the opportunity for crude oil to be displaced by the injection fluid. This mechanism is supported by  $\zeta$ -potential measurements. The results presented by several authors [4, 38, 41, 45, 65] shows that the  $\zeta$ -potential at the brine-carbonate interface becomes increasingly negative as the brine salinity is decreased at a specific temperature. According to Mahani et al. [38], this  $\zeta$ -potential response shows a large sensitivity to the rock type and mineralogy. In this sense, chalk particles showed the most negative surface charge followed by limestone. Dolomite, on the other hand, exhibited a more positive surface charged [40].

**Mineral dissolution:** Hiort et al. [32, 33] proposed that oil can be liberated from a calcite rock (chalk) if dissolution takes place where the oil was attached, changing the wettability to a more water-wetting state. This process is temperature-dependent. At low temperatures, all the fluids are in equilibrium with calcite. This equilibrium is disrupted at high temperatures at which anhydride ( $\text{CaSO}_4$ ) is formed. During the anhydride formation, calcium is supplied from the rock because the aqueous phase loses calcium. However, Austad et al. [8], disapproved this hypothesis since it contradicts the

experimental facts in which the addition of  $\text{Ca}^{2+}$  decreases the dissolution of chalk.

In later publications Yousef et al. [65, 66] showed that a diluted version of seawater is also able to alter the rock wettability, which was attributed to mineral dissolution. According to Chen et al. [16], a selective dissolution of the mineral occurs as the fluid (saturated) in contact with a solid mineral surface is diluted. This effect restructures the carbonate surfaces, which in turn increases the water wetness by reducing the adhesion energy between the rock and crude oil. Even though this mechanism could occur at a laboratory scale, it loses its importance at the field scale since the injection fluid becomes buffered/equilibrated as it moves away from the injector [46, 47].

**pH change effects:** An increment in the concentration of hydroxide ions ( $\text{OH}^-$ ) causes a pH rise, which leads to in-situ surfactant generation similarly to alkaline flooding. This, in turn, reduces the interfacial tension (ITF) and alters the initial rock wettability towards a more water-wet condition [35]. However, this mechanism requires a pH exceeding to 10, which rarely occurs in advanced waterflooding [40].

### Liquid-liquid interface

The mechanisms related to the crude oil/brine interface which are gaining popularity are described as follows:

**Osmosis and diffusion:** Residual and capillary trapped oil could be mobilized by low salinity water injection due to the salinity gradient difference between the injection fluid and connate water in the matrix. In this case, the oil phase acts as a semi-permeable membrane that allows the diffusion of water from the low salinity fluid towards the high-saline water-in-oil emulsions (w/o) to equalize the concentrations of those two fluids [27]. Hence, the observed increased water spontaneous imbibition is not necessarily an indication of wettability alteration but an osmosis effect [55]. Osmosis and diffusion are believed to be involved in the incremental oil production in fractured reservoirs where the injection fluid mainly flows across the fracture rather than contacting the matrix. As explained by Fredriksen et al. [28], low salinity water flowing through a fracture could diffuse along the high-saline wetting-film into the matrix. This film expansion eventually displaces the surrounding oil-phase into the interconnected pore throats.

**Interfacial tension (IFT) alteration:** There is no conclusive evidence that shows that the injection of a lower salinity fluid causes a reduction in the interfacial tension of the oil/brine interface. This is because, some articles reported a lower IFT and therefore a higher oil recovery [49], whereas, other works showed an IFT increase at lower salinities [54]. Lashkarbolooki et al. [36] explained that those highly controversial IFT results are a consequence of the wt% of asphaltene and resins and also their aromaticity values. In this sense, if the asphaltene fraction of crude oil contains a lower H/C ratio

(high aromatic asphaltene), the interfacial tension will be smaller since the performance of the asphaltene fraction vs. salt concentration will be reduced. The opposite occurs if the aromaticity of crude oil decreases (higher IFT). Resin fractions, on the other hand, will decrease IFT as H/C increases.

**Micro-dispersion:** Relocation and rearrangement of active moieties in the crude are responsible for the formation of reverse micro-dispersions, which in turn induce the desorption of oil from the rock lattice [59]. This process results from the injection of a low salinity fluid, which activates natural surface-active components of the crude oil. In addition to this process, Mazani et al. [42] linked micro-dispersions with oil recovery by the expulsion of crude oil from dead-end pores due to coalescence of micro-dispersions at the crude oil/high salinity brine interfaces. It is believed that micro-dispersions will be formed immediately after the low salinity brine contacts the resident oil, being stabilized depending on the brine ionic composition. [59]. According to Perles et al. [50] the water-in-oil (w/o) emulsions are stabilized by asphaltenes adsorption at the oil/water interface and strong complexation between cations in solution and polar groups. These authors stated that emulsions are stabilized through the following steps: 1) accumulation of active components (asphaltenes and resins) at the interface; 2) restructuring of molecules at the interface which maximizes the intermolecular forces.

**Visco-elasticity of the brine-oil interface:** It is believed that the development of interfacial viscoelasticity of the brine/oil interface could also be part of the improved oil recovery. If an elastic interface is developed, the snap-off of crude oil into small droplets could be hindered. Consequently, this snap-off reduction leads to a more continuous phase that can be displaced easily from the porous media [15, 44]. According to Chavez et al. [15], the visco-elasticity of the interface could be explained through the EDL expansion. At low concentrations, the polar components in the crude oil are adsorbed and organized at the interface through electrostatic attractions since the EDL is wide (stronger screening). In the case of a higher salinity brine, the attraction of polar components towards the interface is much lower because of a compressed EDL (smaller Debye length). This causes a reduction in the screening of charge due to a high density of counterions. These authors found through rheology measurements that the optimum viscoelasticity occurs at a salt concentration of  $10^{-2}$  wt%. At this concentration, the elastic moduli ( $G'$ ) is approximately 24 mN/m and 26 mN/m for NaCl and MgCl, respectively. The viscous moduli ( $G''$ ) is also the highest with a value of 10 mN/m for those salts. Garcia-Olvera [29] mentioned that asphaltenes increase the interfacial visco-elasticity, whereas, acidic components reduce the elasticity of the interface. The effect also varies depending on the brine-oil ratio. At a low brine-to-oil ratio the interface is more viscous. The opposite occurs at a higher brine-oil ratio because the amount of asphaltenes and organic acids is much lower.

**Coalescence based oil mobilization:** Oil droplets adhering to the rock surface will be detached and released after the wettability has been altered towards more water-wet conditions. Then, drop-drop coalescence and easy mobilization of those released droplets will occur due to the destabilization of the interfacial film between water and oil with certain ions (e.g. calcium and magnesium) [10]. According to Ayirala et al. [11], less rigid interfaces promote a rapid coalescence between oil droplets. This in turn improves the connection of the oil ganglia and therefore oil recovery. These authors found through shear rheology experiments that the water-soluble ions that promote less stable films at the crude oil-water interface follows:  $\text{Mg}^{2+} > \text{Ca}^{2+} > \text{Na}^+ > \text{SO}_4^{2-}$  [11]. It was also mentioned in [10] and [11] that  $\text{SO}_4^{2-}$  ions form a more rigid film at the oil-water interface, which is hard to deform and therefore the coalescence time is much higher.

A schematic representation of the proposed mechanisms for advanced waterflooding related to the solid-liquid and liquid-liquid interfaces is presented in Figure 2.8.

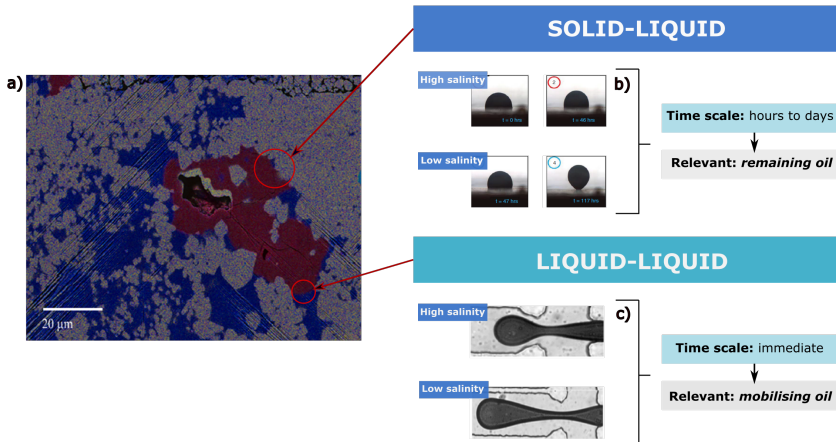


**Fig. 2.8:** Mechanisms proposed in the literature for advanced waterflooding at the solid-liquid and liquid-liquid interfaces. a) EDS (cryo-BIB SEM imaging in combination with energy dispersive X-ray) layered images showing distributions of oil (red) and brine (blue) for a carbonate reservoir rock in presence of low salinity water from [9]. b) oil droplet under high salinity fluid (HS) and low salinity (LS) brines from [39]. c) influence of salinity on interfacial elasticity from [43].

As observed, several mechanisms are involved in the oil recovery improvement by this enhanced oil recovery method (EOR). According to Bartels et al. [12], different cooperative physical and chemical processes are involved in the detachment of crude oil, efficient transport (better microscopic sweep efficiency), the formation of an oil bank, and final recovery. The processes at the solid-liquid interface that causes the detachment of crude oil (wettability change) could take hours to days due to the slow kinetics

of advanced waterflooding [39]. After the detachment of crude oil droplets, fluid-fluid mechanisms (e.g. viscoelasticity that suppress pore-level snap-off events) play a role in the creation and displacement of an efficient oil bank at the pore-network scale [43]. Those fluid-fluid events occur immediately after the injection of the low salinity fluid (advanced waterflooding).

As mentioned before microcalorimetry experiments have not been used and reported previously in the literature. Part II presents the valuable results at the rock-brine and brine-oil interfaces obtained through isothermal titration calorimetry for the complex COBR system. The adsorption energies (enthalpy change,  $\Delta H$ ), which are related to wettability changes, could be useful to discern between proposed mechanisms and increase the predictive capabilities of surface complexation models (SCMs) [18].

## References

- [1] Berlin, Heidelberg: Springer Berlin Heidelberg, 2007. [Online]. Available: [https://doi.org/10.1007/978-3-540-72742-2\\_6](https://doi.org/10.1007/978-3-540-72742-2_6)
- [2] “Low salinity waterflooding for a carbonate reservoir: Experimental evaluation and numerical interpretation,” *Journal of Petroleum Science and Engineering*, vol. 164, pp. 640 – 654, 2018.
- [3] T. Abramovitz, “Geophysical imaging of porosity variations in the danish north sea chalk,” *Geological Survey of Denmark and Greenland bulletin*, vol. 15, pp. 17–20, 2008.
- [4] M. B. Alotaibi, H. A. Nasr-El-Din, and J. J. Fletcher, “Electrokinetics of limestone and dolomite rock particles,” *SPE Reservoir Evaluation & Engineering*, vol. 14, no. 05, p. 10, 2011.
- [5] E. Amott, “Observations relating to the wettability of porous rock.” SPE/Transactions of the AIME, 1959, p. 7.
- [6] T. Austad, S. F. Shariatpanahi, S. Strand, H. Aksulu, and T. Puntervold, “Low salinity eor effects in limestone reservoir cores containing anhydrite: A discussion of the chemical mechanism,” *Energy & Fuels*, vol. 29, no. 11, pp. 6903–6911, 2015.
- [7] T. Austad, “Chapter 13 - water-based eor in carbonates and sandstones: New chemical understanding of the eor potential using “smart water”,” in *Enhanced Oil Recovery Field Case Studies*, J. J. Sheng, Ed. Boston: Gulf Professional Publishing, 2013, pp. 301 – 335.
- [8] T. Austad, S. Strand, and T. Puntervold, “Is wettability alteration of carbonates by seawater caused by rock dissolution?”
- [9] S. Ayirala, A. Alghamdi, A. Gmira, D. K. Cha, M. A. Alsaud, and A. Yousef, “Linking pore scale mechanisms with macroscopic to core scale effects in controlled ionic composition low salinity waterflooding processes,” *Fuel*, vol. 264, p. 116798, 2020.
- [10] S. C. Ayirala, S. H. Al-Saleh, and A. A. Al-Yousef, “Microscopic scale interactions of water ions at crude oil/water interface and their impact on oil mobilization in

- advanced water flooding,” *Journal of Petroleum Science and Engineering*, vol. 163, pp. 640 – 649, 2017. [Online]. Available: <http://www.sciencedirect.com/science/article/pii/S0920410517307519>
- [11] S. C. Ayirala, A. A. Yousef, Z. Li, and Z. Xu, “Coalescence of crude oil droplets in brine systems: Effect of individual electrolytes,” *Energy & Fuels*, vol. 32, no. 5, pp. 5763–5771, 2018. [Online]. Available: <https://doi.org/10.1021/acs.energyfuels.8b00309>
- [12] W.-B. Bartels, H. Mahani, S. Berg, and S. Hassanizadeh, “Literature review of low salinity waterflooding from a length and time scale perspective,” *Fuel*, vol. 236, pp. 338 – 353, 2019.
- [13] L. Bayarjargal, C.-J. Fruhner, N. Schrodte, and B. Winkler, “Caco 3 phase diagram studied with raman spectroscopy at pressures up to 50 gpa and high temperatures and dft modeling,” *Physics of the Earth and Planetary Interiors*, vol. 281, p. 16, 05 2018.
- [14] C. Carré, A. Zanibellato, M. Jeannin, R. Sabot, P. Gunkel-Grillon, and A. Serres, “Electrochemical calcareous deposition in seawater. a review,” *Environmental chemistry letters*, vol. 18, no. 4, pp. 1193–1208, 2020.
- [15] T. Chavez M., A. Firoozabadi, and G. G. Fuller, “Nonmonotonic elasticity of the crude oil–brine interface in relation to improved oil recovery,” *Langmuir*, vol. 32, no. 9, pp. 2192–2198, 2016.
- [16] S.-Y. Chen, Y. Kaufman, K. Kristiansen, D. Seo, A. M. Schrader, M. B. Alotaibi, H. A. Dobbs, N. A. Cadirov, J. R. Boles, S. C. Ayirala, J. N. Israelachvili, and A. A. Yousef, “Effects of salinity on oil recovery (the “dilution effect”): Experimental and theoretical studies of crude oil/brine/carbonate surface restructuring and associated physicochemical interactions,” *Energy & Fuels*, vol. 31, no. 9, pp. 8925–8941, 2017.
- [17] T. Christie, B. Thompson, Bob, and Brathwaite, “Mineral commodity report 21-limestone , marble and dolomite,” 2007.
- [18] J. E. Cobos, P. Westh, and E. G. Søgaaard, “Isothermal titration calorimetry study of brine oil rock interactions,” *Energy & Fuels*, vol. 32, no. 7, pp. 7338–7346, 2018.
- [19] F. Craig, “The reservoir engineering aspects of waterflooding,” Henry L. Doherty Memorial Fund of AIME., New York, 7 1971.
- [20] A. Y. Dandekar, *Petroleum reservoir rock and fluid properties.*, 2nd ed. Boca Raton, FL: CRC Press.
- [21] M. D’Heur, “Porosity and hydrocarbon distribution in the north sea chalk reservoirs,” *Marine and Petroleum Geology*, vol. 1, no. 3, pp. 211 – 238, 1984.
- [22] N. Erdogan and H. Eken, “Precipitated calcium carbonate production, synthesis and properties,” *Fizykochemiczne Problemy Mineralurgii - Physicochemical Problems of Mineral Processing*, vol. 53, pp. 57–68, 01 2017.
- [23] I. Fabricius, “Chalk: Composition, diagenesis and physical properties,” *Bulletin of the Geological Society of Denmark*, vol. 55, 12 2007.
- [24] R. W. Fairbridge, G. V. Chilingar, and H. J. Bissell, “Chapter 1 introduction,” in *Carbonate Rocks Origin, Occurrence and Classification*, ser. Developments in Sedimentology, G. V. Chilingar, H. J. Bissell, and R. W. Fairbridge, Eds. Elsevier, 1967, vol. 9, pp. 1 – 28.

- [25] S. J. Fathi, T. Austad, and S. Strand, ““smart water” as a wettability modifier in chalk: The effect of salinity and ionic composition,” *Energy & Fuels*, vol. 24, no. 4, pp. 2514–2519, 2010.
- [26] ———, “Water-based enhanced oil recovery (eor) by “smart water”: Optimal ionic composition for eor in carbonates,” *Energy & Fuels*, vol. 25, no. 11, pp. 5173–5179, 2011.
- [27] S. B. Fredriksen, A. U. Rognmo, and M. A. Fernø, “Pore-scale mechanisms during low salinity waterflooding: Water diffusion and osmosis for oil mobilization,” in *SPE Bergen One Day Seminar*. Society of Petroleum Engineers, 2016, p. 14.
- [28] ———, “Pore-scale mechanisms during low salinity waterflooding: Oil mobilization by diffusion and osmosis,” *Journal of Petroleum Science and Engineering*, vol. 163, pp. 650 – 660, 2018. [Online]. Available: <http://www.sciencedirect.com/science/article/pii/S0920410517308033>
- [29] G. Garcia-Olvera, T. M. Reilly, T. E. Lehmann, and V. Alvarado, “Effects of asphaltenes and organic acids on crude oil-brine interfacial visco-elasticity and oil recovery in low-salinity waterflooding,” *Fuel*, vol. 185, pp. 151–163, 2016.
- [30] M. Gennaro, “3d seismic stratigraphy and reservoir characterization of the chalk group in the norwegian central graben, north sea,” Ph.D. dissertation, University of Bergen, 2011.
- [31] R. Gupta, G. Smith, L. Hu, T. Willingham, M. Lo Cascio, J. J. Shyeh, and C. R. Harris, “Enhanced waterflood for carbonate reservoirs - impact of injection water composition,” in *SPE Middle East Oil and Gas Show and Conference held in Manama, Bahrain*. Society of Petroleum Engineers, 09 2011, p. 21.
- [32] A. Hiorth, L. M. Cathles, and M. V. Madland, “The impact of pore water chemistry on carbonate surface charge and oil wettability,” *Transport in porous media*, vol. 85, no. 1, pp. 1–21, 2010.
- [33] A. Hiorth, L. Cathles, J. Kolnes, O. Vikane, A. Lohne, and M. Madland, “Chemical modelling of wettability change in carbonate rocks,” 10 2008.
- [34] B. Jones, “Minerals: Carbonates,” in *Encyclopedia of Geology*, R. Selley, L. R. Cocks, and I. R. Plimer, Eds. Boston: Elsevier Academic Press, 2005, pp. 522 – 532.
- [35] A. Lager, K. Webb, C. Black, M. Singleton, and K. Sorbie, “Low salinity oil recovery - an experimental investigation1,” *Petrophysics*, vol. 49, 02 2008.
- [36] M. Lashkarbolooki and S. Ayatollahi, “Effects of asphaltene, resin and crude oil type on the interfacial tension of crude oil/brine solution,” *Fuel*, vol. 223, pp. 261 – 267, 2018. [Online]. Available: <http://www.sciencedirect.com/science/article/pii/S0016236118304204>
- [37] H. Lindgreen, V. Drits, B. Sakharov, H. Jakobsen, A. Salyn, L. Dainyak, and H. Krøyer, “The structure and diagenetic transformation of illite-smectite and chlorite-smectite from north sea cretaceous-tertiary chalk,” *Clay Minerals*, vol. 37, pp. 429–450, 09 2002.
- [38] H. Mahani, R. Menezes, S. Berg, A. Fadili, R. Nasralla, D. Voskov, and V. Joekar-Niasar, “Insights into the impact of temperature on the wettability alteration by low salinity in carbonate rocks,” *Energy & Fuels*, vol. 31, no. 8, pp. 7839–7853, 2017.
- [39] H. Mahani, S. Berg, D. Ilic, W.-B. Bartels, and V. Niasar, “Kinetics of low-salinity-flooding effect,” *SPE Journal*, vol. 20, pp. 8–20, 02 2015.



- [40] H. Mahani, A. L. Keya, S. Berg, W.-B. Bartels, R. Nasralla, and W. R. Rossen, "Insights into the mechanism of wettability alteration by low-salinity flooding (lsf) in carbonates," *Energy & Fuels*, vol. 29, no. 3, pp. 1352–1367, 2015.
- [41] —, "Insights into the mechanism of wettability alteration by low-salinity flooding (lsf) in carbonates," *Energy & Fuels*, vol. 29, no. 3, pp. 1352–1367, 2015.
- [42] P. Mahzari and M. Sohrabi, "Crude oil/brine interactions and spontaneous formation of micro-dispersions in low salinity water injection," vol. 2, 04 2014.
- [43] B. Morin, Y. Liu, V. Alvarado, and J. Oakey, "A microfluidic flow focusing platform to screen the evolution of crude oil–brine interfacial elasticity," *Lab on a chip*, vol. 16, no. 16, pp. 3074–3081, 2016.
- [44] P. Myint and A. Firoozabadi, "Thin liquid films in improved oil recovery from low-salinity brine," *Current Opinion in Colloid & Interface Science*, vol. 20, no. 2, pp. 105,114, 2015.
- [45] R. A. Nasralla and H. A. Nasr-El-Din, "Double-layer expansion: Is it a primary mechanism of improved oil recovery by low-salinity waterflooding?" *SPE Reservoir Evaluation & Engineering*, vol. 17, no. 01, p. 11, 2014.
- [46] R. Nasralla, E. Sergienko, S. Masalmeh, H. Linde, N. Brussee, H. Mahani, B. Suijkerbuijk, and I. Alqarshubi, "Potential of low-salinity waterflood to improve oil recovery in carbonates: Demonstrating the effect by qualitative coreflood (spe-172010-pa)," *SPE Journal*, vol. 21, p. 12, 10 2016.
- [47] R. Nasralla, J. Snippe, and R. Farajzadeh, "Coupled geochemical-reservoir model to understand the interaction between low salinity brines and carbonate rock," in *SPE Asia Pacific Enhanced Oil Recovery Conference held in Kuala Lumpur, Malaysia*. Society of Petroleum Engineers, 08 2015, p. 21.
- [48] D. Njobuenwu, E. Obobo, and R. Gumus, "Determination of contact angle from contact area of liquid droplet spreading on solid substrate," *Leonardo Electronic Journal of Practices and Technologies*, vol. 6, 01 2007.
- [49] T. M. Okasha and A. Alshiwaish, "Effect of brine salinity on interfacial tension in arab-d carbonate reservoir, saudi arabia," 2009.
- [50] C. Perles, V. Guersoni, and A. Bannwart, "Rheological study of crude oil/water interface – the effect of temperature and brine on interfacial film," *Journal of Petroleum Science and Engineering*, vol. 162, pp. 835 – 843, 2018. [Online]. Available: <http://www.sciencedirect.com/science/article/pii/S0920410516309834>
- [51] T. Puntervold, S. Strand, R. Ellouz, and T. Austad, "Modified seawater as a smart eor fluid in chalk," *Journal of Petroleum Science and Engineering*, vol. 133, pp. 440–443, 09 2015.
- [52] —, "Modified seawater as a smart eor fluid in chalk," *Journal of Petroleum Science and Engineering*, vol. 133, pp. 440–443, 09 2015.
- [53] A. RezaeiDoust, T. Puntervold, S. Strand, and T. Austad, "Smart water as wettability modifier in carbonate and sandstone: A discussion of similarities/differences in the chemical mechanisms," *Energy & Fuels*, vol. 23, no. 9, pp. 4479–4485, 2009.



- [54] M. Salehi, P. Omidvar, and F. Naeimi, "Salinity of injection water and its impact on oil recovery absolute permeability, residual oil saturation, interfacial tension and capillary pressure," *Egyptian Journal of Petroleum*, vol. 26, no. 2, pp. 301 – 312, 2017.
- [55] K. Sandengen, K. Melhuus, and L. Josang, "Osmosis as mechanism for low salinity eor," *SPE Journal*, p. 9, 08 2016.
- [56] P. A. Scholle, "Chalk Diagenesis and Its Relation to Petroleum Exploration: Oil from Chalks, a Modern Miracle?1," *AAPG Bulletin*, vol. 61, no. 7, pp. 982–1009, 07 1977. [Online]. Available: <https://doi.org/10.1306/C1EA43B5-16C9-11D7-8645000102C1865D>
- [57] R. C. Selley and S. A. Sonnenberg, "Chapter 6 - the reservoir," in *Elements of Petroleum Geology (Third Edition)*, third edition ed., R. C. Selley and S. A. Sonnenberg, Eds. Boston: Academic Press, 2015, pp. 255 – 320. [Online]. Available: <http://www.sciencedirect.com/science/article/pii/B9780123860316000060>
- [58] A. Sohal, "Wettability modification in chalk: Systematic evaluation of salinity, brine composition and temperature effects," Ph.D. dissertation, Aalborg University, 2016.
- [59] M. Sohrabi, P. Mahzari, S. A. Farzaneh, J. Mills, P. Tsolis, and S. Ireland, "Novel insights into mechanisms of oil recovery by low salinity water injection," in *SPE Middle East Oil & Gas Show and Conference held in Manama, Bahrain*. Society of Petroleum Engineers, 03 2015.
- [60] S. Strand, T. Austad, T. Puntervold, E. J. Høgnesen, M. Olsen, and S. M. F. Barstad, "'smart water" for oil recovery from fractured limestone: A preliminary study," *Energy & Fuels*, vol. 22, no. 5, pp. 3126–3133, 2008.
- [61] S. Strand, E. J. Høgnesen, and T. Austad, "Wettability alteration of carbonates—effects of potential determining ions ( $\text{Ca}^{2+}$  and  $\text{SO}_4^{2-}$ ) and temperature," *Colloids and Surfaces A: Physicochemical and Engineering Aspects*, vol. 275, no. 1, pp. 1 – 10, 2006. [Online]. Available: <http://www.sciencedirect.com/science/article/pii/S092777570500796X>
- [62] H. Tie, "Oil recovery by spontaneous imbibition and viscous displacement from mixed-wet carbonates," Ph.D. dissertation, University of Wyoming, Laramie, Wyoming, 2006.
- [63] A. W.G., "Wettability literature survey—part 1: Rock/oil/brine interactions and the effects of core handling on wettability," *Journal of Petroleum Technology*, vol. 38, no. 10, 1986.
- [64] —, "Wettability literature survey- part 4: Effects of wettability on capillary pressure," *Journal of Petroleum Technology*, vol. 39, no. 10, 1987.
- [65] A. Yousef, J. Liu, G. Blanchard, S. Al-Saleh, T. Al-Zahrani, R. Al-Zahrani, H. Al-Tammar, and N. Al-Mulhim, "Smartwater flooding: Industry's first field test in carbonate reservoirs," in *Proceedings - SPE Annual Technical Conference and Exhibition*, vol. 3, 01 2012, pp. 2469–2494.
- [66] A. Yousef, S. Al-Saleh, A. Ubaid Al-Kaabi, and M. Saleh Al-Jawfi, "Laboratory investigation of novel oil recovery method for carbonate reservoirs," *Society of Petroleum Engineers - Canadian Unconventional Resources and International Petroleum Conference*, vol. 3, 01 2010.

- [67] P. Zhang and T. Austad, “Wettability and oil recovery from carbonates: Effects of temperature and potential determining ions,” *Colloids and Surfaces A-physicochemical and Engineering Aspects*, vol. 279, pp. 179–187, 05 2006.
- [68] P. Zhang, M. T. Tweheyo, and T. Austad, “Wettability alteration and improved oil recovery by spontaneous imbibition of seawater into chalk: Impact of the potential determining ions  $\text{Ca}^{2+}$ ,  $\text{Mg}^{2+}$ , and  $\text{SO}_4^{2-}$ ,” vol. 301, pp. 199–208, 07 2007.

# Chapter 3

## Sandstone Rocks

### 1 Introduction

Sandstones are an important group of sedimentary rocks, approximately nearly one-quarter in the geologic record [5]. Those sedimentary rocks are economically important since they hold the major water reservoirs and some petroleum reserves. Moreover, they are used as a building material, as flagstone, as road filler if crushed, and as valuable sources of metallic ores (sediment that contains one or more valuable minerals) [1]. Danish geothermal resources are widely distributed in the Lower Triassic Bunter Sandstone Formation and the Upper Triassic–Lower Jurassic Gassum Formation [22]. Therefore, the study of the main characteristics of sandstone reservoirs is of great importance for this study.

This chapter is about the nature of geothermal reservoirs. It begins by describing porosity and permeability. Those definitions are followed by an account of how sandstone rocks are made up, with a special emphasis on the major minerals. This discussion is thereafter followed by a description of the mechanisms that cause a permeability reduction, which diminishes the reservoir performance. The chapter concludes with a general explanation of geothermal energy in Denmark and SaltPower electricity generation.

### 2 Porosity and Permeability

Sandstone rocks are made of particles with an average size of between 2 and 0.0625 mm in diameter [25]. The major components of sandstone rocks are grains, matrix, and cement. In this sense, the framework of sandstone rocks is made of sand-sized particles. The finer-grained material that was deposited at the same time as the framework grains corresponds to the matrix of the rock. Cement, on the other hand, describes the minerals that have been precipitated in the pore space after the sediment deposition [25]. Those components can be seen in the

schematic diagram presented in Figure 3.1.

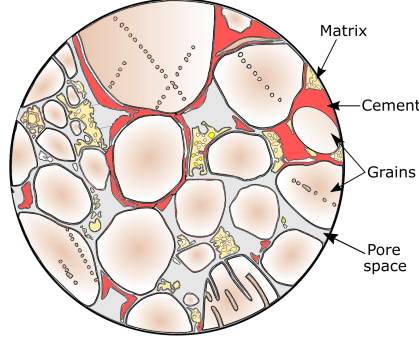


**Fig. 3.1:** Schematic diagram of a thin section of a sandstone rock showing the principal components, grains, matrix, cement, and pore space. Based on [25]

The portion of the rock not occupied by its solid components is called void space, which can store fluids (e.g. groundwater, oil, and gas). Porosity (represented by  $\phi$ ) is the measurement of that void space in the rock, is being defined by Equation 3.1 as “ratio of the volume of the voids or pore space divided by the total volume” Pettijhon [21]. In this equation,  $V_b$  is the bulk volume,  $V_s$  is volume of solids, and  $V_p$  is the pore space or volume of voids. The porosity can be absolute or effective. The absolute porosity takes into account the percentage of all void space, connected or not. The effective porosity, on the other hand, only includes the pores that are connected and therefore it is the percentage of interconnected pore space.

$$\phi = \frac{V_b - V_s}{V_b} = \frac{V_p}{V_b} \quad (3.1)$$

The ability of sandstone to transmit fluids is called permeability or hydraulic conductivity,  $k$ . It is defined by Darcy’s equation 3.2. In this equation,  $Q$  is volume of transmitted flow per unit time,  $A$  is the cross-sectional area,  $k$  is permeability,  $\mu$  is viscosity,  $L$  is length, and  $\Delta P$  is the pressure gradient [21].

$$Q = \frac{kA}{\mu L} \Delta P \quad (3.2)$$

Porosity and permeability thereby influence the storage and displacement of fluids within the pore space. Therefore, those properties will be used to evaluate the reinjection of geothermal brines and half diluted brines into a sandstone reservoir.

### 3 Minerals and Properties

Sandstones are made of mixtures of rock fragments and mineral grains coming from rocks of all kinds that have been eroded and disaggregated naturally. Consequently, a large number of mineral species can be found in this type of sedimentary rock [21]. As mentioned before (Section 1), sandstone rocks are made of grains, matrix, and cement.

The framework grains are composed predominantly (commonly > 90 percent) of quartz, feldspars, and rock fragments. Moreover, a few percent of the framework grains of many sandstones are made of coarse micas, especially muscovite. Heavy minerals, such as zircon, tourmaline, and rutile, can also constitute a small percentage of the detrital constituents of sandstones [5, 25]. The matrix that occupies some of the space between the grains could consist of silt, clay, and organic matter. [25]. A schematic illustration of the common minerals and rock fragments is presented in Figure 3.2.

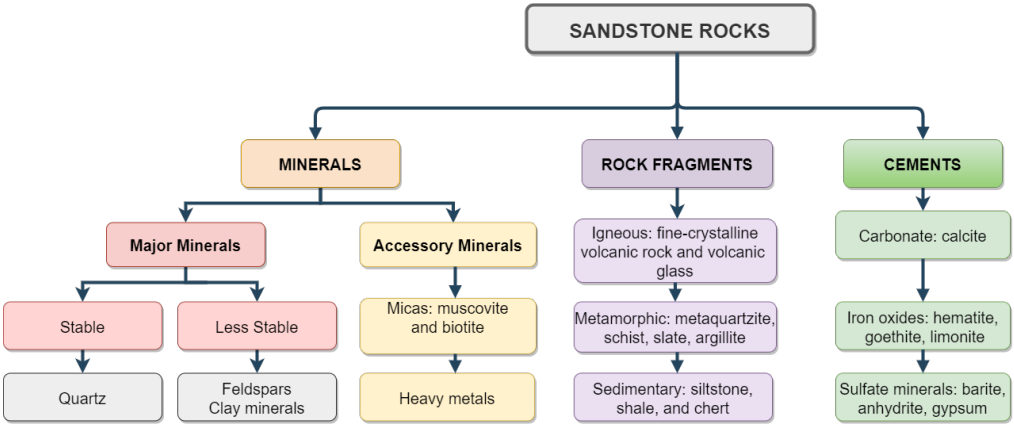


**Fig. 3.2:** Common minerals and rock fragments in sandstone rocks. Based on [5]

The typical mineralogical composition of a sandstone rock can be described as follows. **Framework grains:** 45% quartz, 10% feldspar, 5% rock fragments, 5% mafics, 5% mica, 2% heavy metals; **Matrix:** 7% clay; **Cement:** 5% calcite; **Pore space:** 16% [25]. Many sandstones can also present authigenic minerals that replace some framework grains, matrix, or cement [5].

### 4 Formation Damage

Formation damage is the general terminology implying the alteration of the original characteristics of a producing formation due to the negative interaction between the producing formation and injection fluids [7]. Normally, it is associated with petroleum bearing formations but it can

also occur in geothermal reservoirs, where its economic viability depends on the production of tremendous amounts of heated water and/or steam. Consequently, formation damage is an undesirable operational and economic problem that should be understood, controlled, and minimized [4]. The main formation damage indicators include permeability impairment and a decrease of well performance [7].

#### 4.1 Mechanisms

From the perspective of oil/gas production, physicochemical, chemical, biological, hydrodynamic, and thermal interactions of porous formation, particles, and fluids could cause formation damage [7]. However, the main mechanism associated with formation damage in geothermal reservoirs is fine particle migration, straining, and blocking during the exploitation of heated water and/or steam. Pore plugging in geothermal reservoirs is severer than in oil and gas reservoirs. This is because, at high temperatures, the electrostatic forces which attach the clay particles to the grain surfaces are reduced, which in turn enhances the particle-grain repulsion [23].

As mentioned in the previous section, the matrix of sandstone rocks is composed of clay minerals. Non-swelling clays, such as kaolinites and illites, can be released from the pore walls, migrate with the fluid, and strain in thinner pore throats, as observed in Figure 3.3. This process causes that those particles get stuck within the porous media [8].

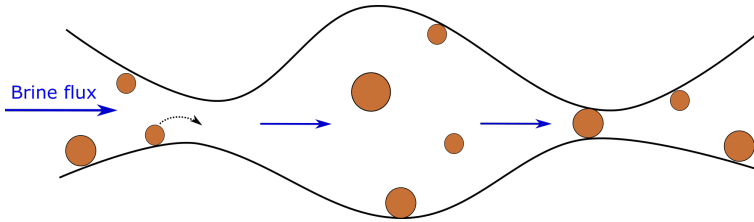


**Fig. 3.3:** Sketch of fines attachment, detachment, and straining in thinner pore throats. Based on [3]

Electrostatic force ( $F_e$ ), drag force ( $F_d$ ), lifting force ( $F_l$ ) and gravitational force ( $F_g$ ) stabilizes the fine particles on the pore wall, as observed in Figure 3.4. In this sense, the electrostatic and gravitational forces attach the fine particles on the grain surface while the drag and lifting forces detach them. High velocities and/or reduced ionic strength of geothermal fluids cause a disturbance in those forces, which gradually releases particles from the pore wall [3].

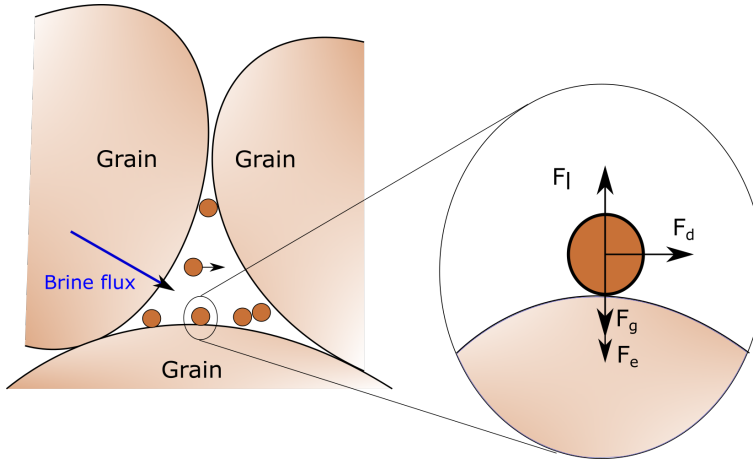


**Fig. 3.4:** Schematic diagram of a pore throat and forces acting on the attached particles. Based on [3]

When the fluid velocity is higher than a threshold flow rate, a function of ionic strength, wettability, pore geometry, and interfacial tension [2], the wall shear stresses are in excess. Those hydrodynamic forces mobilize fines inside of the porous medium [6, 19, 20]. According to Ochi and Vernoux [19] the critical velocity for fines migration in Berea sandstone core plugs is between 0.6 to 1.4 cm/s.

The migration and straining of non-swelling clays in thinner pore throats could also occur when the ionic strength of the geothermal fluid has been decreased. This is because the clay minerals do not have enough time to equilibrate on ion exchange with the injection fluid. For instance, if the brine injection is followed by freshwater, an instantaneous permeability reduction occurs [18]. Khilar and Fogler [6, 13] found that the colloiddally induced mobilization of clay particles occurs when the NaCl concentration is decreased below 0.071 M [12]. Those authors attributed that mobilization to a double-layer expansion, which in turn causes a net repulsion between the clay particles (kaolinite and illite) and quartz surfaces. The clay minerals can be stabilized and resist dispersion if the fluid has an adequate amount of divalent cations, which are mainly adsorbed on the clay crystal edges where the valence bonds are not filled [11, 24, 26]. According to the adsorption capacity, the most common exchangeable cations in geothermal brines can be distributed as follows:  $\text{Fe}^{3+} > \text{Al}^{3+} > \text{Ba}^{2+} > \text{Sr}^{2+} > \text{Ca}^{2+} > \text{Mg}^{2+} > \text{K}^+ > \text{Na}^+$  [27, 28].

## 5 Geothermal Energy

Geothermal energy is considered as clean and cost-competitive renewable energy that can be used to achieve a long-term and sustainable solution to the global energy demand. It is recognized as one of the most abundant resources for heating-power production applications [9]. This

resource can be utilized in two ways: direct utilization and electricity production. In direct use, heat is produced directly from the resource without further conversion into other types of energy. Electricity generation, on the other hand, uses steam to rotate a turbine that activates a generator. In this way, electricity is produced with a low carbon footprint (minimum levels of greenhouse gas emissions) [17]. If the geothermal resource has a very low temperature ( $< 100^{\circ}\text{C}$ ), the groundwater is used to produce heat by adsorption pumps. After extracting heat from the groundwater, this liquid is returned to the aquifer via an injection well [10].

The Danish geothermal resources have a temperature gradient between  $40\text{--}70^{\circ}\text{C}$ . Thus, the heated saline fluids ( $> 15\%$  saline water) are used directly to produce heat by adsorption pumps, which is distributed to the district heating system [22]. Thereafter, the cooled brines are returned to the same sandstone aquifer through injection well(s) as a disposal solution and also for reservoir pressure maintenance [22]. Three geothermal plants, which are located in Thisted, Copenhagen, and Sønderborg are used to extract heat from those shallow reservoirs and re-inject afterwards the heat depleted brines [16]. Instead of re-injecting the heat depleted geothermal fluids (hypersaline water) back into the same reservoir, they could be mixed with freshwater to produce electricity through osmosis. This is because the salinity difference between those fluids is quite considerable.

Madsen, et al. [15] demonstrated that hypersaline fluids could be used to harness energy through pressure retarded osmosis (PRO). The salinity difference between those fluids produces an osmotic pressure that drives water molecules to move from the diluted fluid (LS) or feed to the concentrated brine (HS) or draw, as observed in Figure 3.5. If hydraulic pressure is applied to the draw solution, the water flux across the membrane will increase the volume of the pressurized draw solution. With the help of a hydro-turbine, this pressurized fluid can be converted into electricity [15, 29].

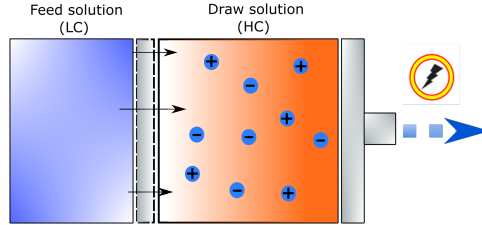


**Fig. 3.5:** Schematic diagram of a pressure retarded osmosis (PRO). Based on [29]

In a later work, Madsen et al. [14] showed that the hypersaline PRO process is economically viable since it can be operated at pressures up to 70 bar with power densities above  $5 \text{ W/m}^2$ . These authors called this electricity generation obtained by mixing a hypersaline fluid (geothermal brine) with freshwater as “SaltPower”. Reinjection is the best disposal option to handle large amounts of diluted brine coming from SaltPower energy generation most environmentally. However, questions regarding the overall reservoir assurance arise due to the complex



fluid-fluid and rock-fluid interactions that are taking place upon reinjection [8].

The second part of this PhD study concerns the study of the complex fluid-fluid and rock-fluid interactions upon reinjection of geothermal brines and half diluted geothermal brines and their implication in the overall reservoir performance.

## References

- [1] “Sedimentary rock encyclopedia britannica,” <https://www.britannica.com/science/sedimentary-rock/Sandstones>, note = Accessed: 2020-09-15,.
- [2] J. O. Amaefule, A. Ajufo, E. Peterson, and K. Durst, “Understanding formation damage processes: an essential ingredient for improved measurement and interpretation of relative permeability data,” *Society of Petroleum Engineers Journal-SPE Production Operations Symposium*, vol. SPE-16232-MS, 1987.
- [3] P. Bedrikovetsky, Z. You, A. Badalyan, M. Hand, C. Matthews, and D. Jenson, “Formation damage in geothermal wells (salamander field case),” 2012.
- [4] G. L. Bergosh and D. O. Ennis, “Mechanisms of formation damage in matrix permeability geothermal wells,” 1981.
- [5] S. Boggs, “Sandstones,” in *Petrology of Sedimentary Rocks*, 2nd ed. Cambridge: Cambridge University Press, 2009, p. 111–164.
- [6] K. C. Khilar and H. S. Fogler, “Water sensitivity of sandstones,” *Society of Petroleum Engineers Journal*, vol. 23, pp. 55–64, 02 1983.
- [7] F. Civan, “Chapter 1 - overview of formation damage,” in *Reservoir Formation Damage (Second Edition)*, second edition ed., F. Civan, Ed. Burlington: Gulf Professional Publishing, 2007, pp. 1 – 9. [Online]. Available: <http://www.sciencedirect.com/science/article/pii/B9780750677387500026>
- [8] J. E. Cobos and E. G. Sogaard, “Study of geothermal brine reinjection by microcalorimetry and core flooding experiments,” *Geothermics*, vol. 87, p. 101863, 2020.
- [9] I. Dincer and H. Ozcan, *1.17 Geothermal Energy*, 02 2018, pp. 702–732.
- [10] C. Ditlefsen and A. Højberg, “Shallow geothermal energy in denmark,” *Geological Survey of Denmark and Greenland Bulletin*, vol. 26, p. 4, 01 2012.
- [11] F. O. Jones, “Influence of chemical composition of water on clay blocking of permeability,” *Journal of Petroleum Technology*, p. 6, 04 1964.
- [12] K. Khilar, H. Fogler, and J. Ahluwalia, “Sandstone water sensitivity: Existence of a critical rate of salinity decrease for particle capture,” *Chemical Engineering Science*, vol. 38, no. 5, pp. 789 – 800, 1983.
- [13] S. Kia, H. S. Fogler, and M. Reed, “Effect of salt composition on clay release in berea sandstones,” *Society of Petroleum Engineers*, p. 11, 02 1987.

- [14] H. T. Madsen, S. Søndergaard Nissen, J. Muff, and E. G. Søgaaard, "Pressure retarded osmosis from hypersaline solutions: Investigating commercial fo membranes at high pressures," *Desalination*, vol. 420, pp. 183 – 190, 2017.
- [15] H. T. Madsen, S. Søndergaard Nissen, and E. G. Søgaaard, "Theoretical framework for energy analysis of hypersaline pressure retarded osmosis," *Chemical Engineering Science*, vol. 139, pp. 211 – 220, 2016.
- [16] A. Mahler, B. Røgen, C. Ditlefsen, L. Nielsen, and T. Vangkilde-Pedersen, "Geothermal energy use, country update for denmark," in *European Geothermal Congress 2013*, 2013, p. 12.
- [17] A. Manzella, "Geothermal energy," *EPJ Web of Conferences*, vol. 148, p. 12, 01 2017.
- [18] N. Mungan, "Permeability reduction through changes in ph and salinity," *Journal of Petroleum Technology*, p. 5, 12 1965.
- [19] J. Ochi and J.-F. Vernoux, "Permeability decrease in sandstone reservoirs by fluid injection: Hydrodynamic and chemical effects," *Journal of Hydrology*, vol. 208, no. 3, pp. 237 – 248, 1998.
- [20] M. A. Oliveira, A. S. Vaz, F. D. Siqueira, Y. Yang, Z. You, and P. Bedrikovetsky, "Slow migration of mobilised fines during flow in reservoir rocks: Laboratory study," *Journal of Petroleum Science and Engineering*, vol. 122, pp. 534 – 541, 2014.
- [21] F. J. F. J. Pettijohn. New York: Springer-Verlag, 1972.
- [22] S. Poulsen, H. Bjørn, A. Mathiesen, L. Nielsen, H. Vosgerau, T. Vangkilde-Pedersen, and B. Ditlefsen, C. Røgen, "Geothermal energy use, country update for denmark," in *European Geothermal Congress 2019*, 2019, p. 9.
- [23] E. Rosenbrand, C. Kjølner, J. F. Riis, F. Kets, and I. L. Fabricius, "Different effects of temperature and salinity on permeability reduction by fines migration in berea sandstone," *Geothermics*, vol. 53, pp. 225 – 235, 2015.
- [24] R. K. Schofield and H. R. Samson, "Flocculation of kaolinite due to the attraction of oppositely charged crystal faces," *Discuss. Faraday Soc.*, vol. 18, pp. 135–145, 1954.
- [25] R. Selley, "Sedimentary rocks | mineralogy and classification," in *Encyclopedia of Geology*, R. C. Selley, L. R. M. Cocks, and I. R. Plimer, Eds. Oxford: Elsevier, 2005, pp. 25 – 37. [Online]. Available: <http://www.sciencedirect.com/science/article/pii/B012369396900304X>
- [26] F. Smith, "Ion-exchange conditioning of sandstones for chemical flooding," *Journal of Petroleum Technology*, vol. SPE-6598-PA, 1978.
- [27] W. Stumm and J. Morgan, *Aquatic chemistry*. Jhon Wiley & Sons, Inc., 1991.
- [28] A. Tchistiakov, "Physico-chemical aspects of clay migration and injectivity decrease of geothermal clastic reservoirs," *Proceedings World Geothermal Congress*, 01 2000.
- [29] N. Y. Yip and M. Elimelech, "Thermodynamic and energy efficiency analysis of power generation from natural salinity gradients by pressure retarded osmosis," *Environmental Science & Technology*, vol. 46, no. 9, pp. 5230–5239, 2012.

# Chapter 4

## Methodology

This chapter introduces the materials and methods used in the PhD study. First, the rock samples (carbonates, and sandstones) are described, followed by an account of the fluids used for wettability alteration and geothermal brine reinjection experiments. The chapter is concluded with a description of the microcalorimetric method that was used to quantify the complex rock-fluid and fluid-fluid interactions for both purposes. Additional methods can be found in Part III, which presents all the published and submitted journal articles that were produced during this PhD study.

### 1 Rock Samples

As mentioned in Chapter 1, carbonate and sandstone rocks were used for wettability alteration and geothermal brine reinjection studies, respectively.

#### 1.1 Carbonate rocks

The main type of carbonates used for wettability alteration studies were chalk and limestone. Those rock samples are briefly described as follows:

- (i) **Dan chalk.** Outcrop chalk material provided by Dankalk A/S from a quarry in Aggersund, Denmark [4]. This outcrop corresponds to a Maastrichtian coccolith zone that has a bioturbated ichnofabric [3, 6].
- (ii) **Stevns Klint chalk.** Material from Stevns Klint in Copenhagen, Denmark. It corresponds to the uppermost Maastrichtian chalk with a matrix with more than 96% fine graded coccoliths. However, clay minerals ( smectite and mica) can also be present in the matrix as larger flakes [3, 7, 9, 12].

- (iii) **Austin chalk.** “Impure” depositional chalk provided by Kocurek industries from outcrops near Austin, Texas. Fossiliferous chalk which is relatively shallow-marine [3, 5, 10].
- (iv) **Synthetic chalk.** Artificial  $\text{CaCO}_3$  material with a purity of 99%. This analytical grade material (ACS reagent) was provided by Acros Organics. It is produced by the decomposition of limestone to  $\text{CaO}$  followed by a recarbonization process [3].
- (v) **Edwards limestone.** Outcrop limestone that can be found in numerous locations across Texas, United States. It contains well-sorted fossil shells that are cemented by calcite. The pore space is vugular, which includes both separate and touching vugs. This outcrop rock has a very small micro-porosity due to the presence of fossil shells and calcite crystals [13].

As discussed in Chapter 2, the wettability of carbonate reservoirs depends on the individual components of the crude oil, brine, rock system (COBR). Consequently, knowing the chemical composition of those rock samples is relevant. The elemental composition of those carbonate samples was determined by the X-ray fluorescence (XRF) technique. The details of the XRF method can be found in Cobos et al. [3, 4] and the composition is given in Table 4.1. As explained by Sohal et al. [11], grain sizes between 50-100  $\mu\text{m}$  produce the best wettability alteration results. Thus, the rock samples were grounded with a ceramic ball mill and sieved to mesh between 50-100  $\mu\text{m}$  for the microcalorimetry experiments.

**Table 4.1:** X-ray Fluorescence (XRF) Analysis of Different Chalk Materials and Edwards Limestone. Source: [3]

Component	Dan Chalk %	Stevens Klint Chalk %	Austin Chalk %	Synthetic Chalk %	Edwards Limestone %
MgO	0.5	1.8	1.2	-	-
$\text{Al}_2\text{O}_3$	-	11.4	0.4	-	-
$\text{SiO}_2$	4.9	3.2	1.6	1.2	1.6
$\text{P}_2\text{O}_5$	0.3	0.2	0.2	1.0	0.2
$\text{SO}_3$	-	0.1	0.1	-	-
Cl	-	0.1	0.02	-	-
$\text{K}_2\text{O}$	0.1	0.2	0.1	0.1	0.1
$\text{CaO}$	93.7	82.7	95.9	98.5	97.6
$\text{Fe}_2\text{O}_3$	0.3	0.3	0.3	-	0.4
$\text{As}_2\text{O}_3$	-	0.1	0.2	0.1	0.1
$\text{SrO}$	0.4	0.1	0.1	-	0.1

## 1.2 Sandstone rocks

Berea sandstone was used in this PhD thesis to evaluate the reinjection of heat depleted geothermal and half diluted brines. As mentioned in Cobos et al. [2], Berea sandstone is relatively homogeneous, inexpensive, and readily available. Thus, it is widely used as a reference rock for coreflooding experiments. In a similar manner to the carbonate rocks, the elemental composition was also determined by XRF and the results are given in Table 4.2. More details about

the XRF method can be found in Cobos et al. [2].

**Table 4.2:** X-ray Fluorescence (XRF) Analysis of Berea Sandstone. Source: Cobos et al. [2]

Compound	%
MgO	0.70
Al <sub>2</sub> O <sub>3</sub>	13.8
SiO <sub>2</sub>	81.4
Cl	0.11
K <sub>2</sub> O	2.00
CaO	0.32
TiO <sub>2</sub>	0.55
Fe <sub>2</sub> O <sub>3</sub>	0.98

An X-ray Power Diffraction instrument (XRD) provided by PANalytical Instruments was used to determine the mineral composition of Berea sandstone. It was found that the available Berea sandstone is made up of quartz and kaolinite. More information about the XRD method and results can be found in Cobos et al. [2].

## 2 Fluids

The fluids used for the experiments presented in this PhD thesis are divided according to their purpose into wettability alteration and geothermal brine reinjection. Moreover, a short description of the crude oil samples is included.

### 2.1 Wettability alteration brines

The wettability alteration studies account principally 10 times diluted seawater (10\*DSW) and seawater spiked with sulfate, which is called smart water or modified seawater (AW). Furthermore, synthetic formation water similar to the Ekofisk and Valhall fields were used for the microcalorimetry experiments and static/dynamic aging methods that were used to alter the wettability of Edwards limestone core plugs. In order to get an improved understanding of the physicochemical processes associated with low salinity waterflooding (LSWF) in carbonates, solutions 0.001 M of the main ionic species present in seawater, MgCl<sub>2</sub>, CaCl<sub>2</sub>, Na<sub>2</sub>SO<sub>4</sub>, NaCl, were further studied in paper III. The ionic composition and the main characteristics of the advanced fluids and synthetic reservoir fluids are summarized in Table 4.3. The details of all the methods used to prepare those advanced fluids from seawater and how the properties were measured are explained in Cobos et al. [3]. Note that synthetic advanced fluids (diluted seawater and modified seawater) were used for the first publication. More details of those fluids can be found in Cobos et al. [4]

**Table 4.3:** Ionic Composition, ionic strength ( $I_c$ ), and pH for artificial Valhall brine (VB), artificial Ekofisk brine (EFB), 10 times diluted seawater (10D\*SW) and advanced water or smart water (AW). Source: [3, 4]

ions (mmol/L)	VB	EFB	10D*SW	AW
$\text{Ca}^{2+}$	29.25	99.92	1.1	3.1
$\text{Mg}^{2+}$	7.87	21.89	4.4	12.6
$\text{SO}_4^{2-}$	0.7	0	2.2	5.7
$\text{Na}^+$	996	1156	39	127
$\text{Cl}^-$	1065	1423	48	91
$I_c$ (mmol/l)	1113	1559	59	151
pH	7.85	7.93	7.46	7.50

## 2.2 Geothermal brine

Geothermal fluids from Thisted and Sønderborg plants were used to evaluate the impact of re-injecting a half diluted geothermal fluid in the same reservoir and the remedial fluids to avoid injectivity problems (permeability reduction). Information about the methods used to measure the properties of those geothermal brines is explained in Cobos et al. [2] and paper VI.

**Table 4.4:** Ionic composition in mmol/l, ionic strength  $I_c$  in mmol/l, electrical conductivity (EC) in mS, total dissolved solids (TDS) in ppt, density ( $\rho$ ) in  $\text{g/cm}^3$ , pH, and viscosity ( $\mu$ ) in cP of all used brines in the microcalorimetry and core flooding experiments for this PhD thesis. Source: [2]

	Ionic Composition									Intrinsic Properties					
	$\text{K}^+$	$\text{Mg}^{2+}$	$\text{Na}^+$	$\text{Sr}^{2+}$	$\text{Ca}^{2+}$	$\text{SO}_4^{2-}$	$\text{Cl}^-$	$\text{HCO}_3^-$	$Fe(II)$	$I_c$	EC	TDS	$\rho$	pH	$\mu$
TB	17.8	64.0	1999	3.6	143	1.2	2728	0.5	1.6	2.8	190	176	1.11	6.71	1.05
2D*TB	10.4	33.1	1245	1.9	88	0.6	1621	0.5	0.9	1.7	110	103	1.05	6.69	0.87
TB <sub>air</sub>	9.1	27.6	1145	1.6	72	0.6	1509	0.4	0.1	1.5	111	103	1.05	6.91	0.87
SB	16.2	48.3	1966	2.2	90.7	9.4	2893	0.9	2.1	2.7	182	169	1.10	6.57	1.01
2D*SB	10.7	23.9	1179	1.1	47.1	5.3	1437	0.5	0.8	1.5	109	101	1.05	6.70	0.87
SB <sub>citric</sub>	9.9	21.0	1219	1.0	48.8	4.8	1525	-	0.1	1.5	74	102	1.05	2.44	0.87

## 2.3 Crude oil

Crude oil from North Sea carbonate reservoirs was used for the microcalorimetry and wettability alteration experiments. The properties of those samples are shown in Table 4.5. Crude oil A was used for the experiments done in papers I-III, whereas, crude oil B was used in paper IV. More details about the measuring equipment and the properties of those oil samples can be found in Cobos et al [3, 4] and paper IV.

**Table 4.5:** Crude oil properties. Source: [3, 4]

sample	AN (mg KOH)/g	BN (mg KOH)/g	viscosity mPa.s	density g/cm <sup>3</sup>
A	0.52	1.60	11.94	0.86
B	0.41	1.40	14.30	0.89

### 3 Microcalorimeter Apparatus

TAM IV is a completely modular system that combines both heat flow sensitivity and long term temperature stability for measuring many processes accurately and efficiently. The 4 channel version can accommodate a single microcalorimeter in one of the four available positions in the TAM IV thermostat with an accuracy of  $\pm 0.1^\circ\text{C}$  and precision of  $\pm 100$  nW. [4]. Each microcalorimeter has two accessible positions: sample and reference. The latter is used to reduce the short-term noise in the experiments. Advanced hardware and electronics control accurately the set temperature for the thermostat that can range between  $4\text{-}150^\circ\text{C}$  for real-world applications. The best stability, signal-to-noise ratio, and reproducibility in the measurements are obtained due to the precise temperature control and incomparable sensitivity of the TAM IV apparatus. Moreover, the heat flow can be measured precisely in experiments that last anywhere from a few hours to days and weeks [1].

The TAM IV equipment used for this PhD study has two microcalorimeters, which operate simultaneously and independently. A photograph of the TAM IV available at the Chemical Engineering and Biotechnology Section at Aalborg University, Esbjerg is presented in Figure 4.1. As observed, the available microcalorimeters are located in positions 1 and 2. Those microcalorimeters were used for the Isothermal Titration Calorimetry (ITC) experiments presented in this PhD thesis. This calorimetric technique was used for all the experiments because it gives a realistic overview of the rock-fluid and fluid-fluid interactions that occur in both sandstone and carbonate reservoirs [3]. More information about sample preparation, initial equilibration time, number of injections, and general procedures for the ITC experiments can be found in papers I-VI

### 4 Core Flooding Systems

Two different experimental setups were used in this thesis for the flooding experiments, which are briefly described as follows:

The first flooding system is composed of an ISCO pump, three stainless steel pistons, a Hassler-type core holder, a syringe pump, pressure transducers, a manometer, an oven, and a computer. This setup was mainly used to inject hypersaline geothermal brines into Berea sandstone core plugs. A schematic diagram is shown in Cobos et al. [2] and presented in Figure 4.2. More information about the flooding experiments performed using this setup can be found

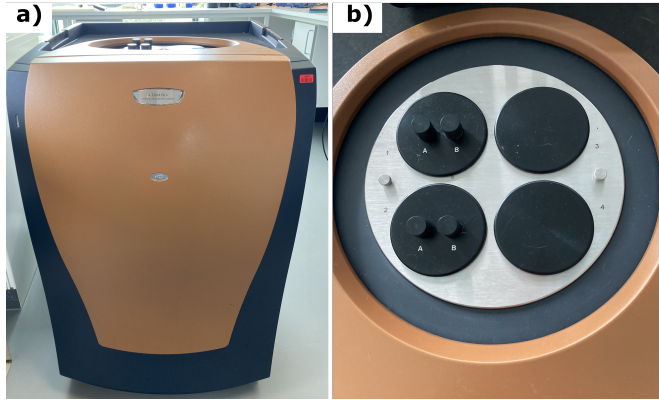


**Fig. 4.1:** Ultra-sensitive TAM IV isothermal microcalorimeter. a) TAM IV apparatus, b) microcalorimeters in position 1 and 2

in Cobos et al. [2] and paper VI.

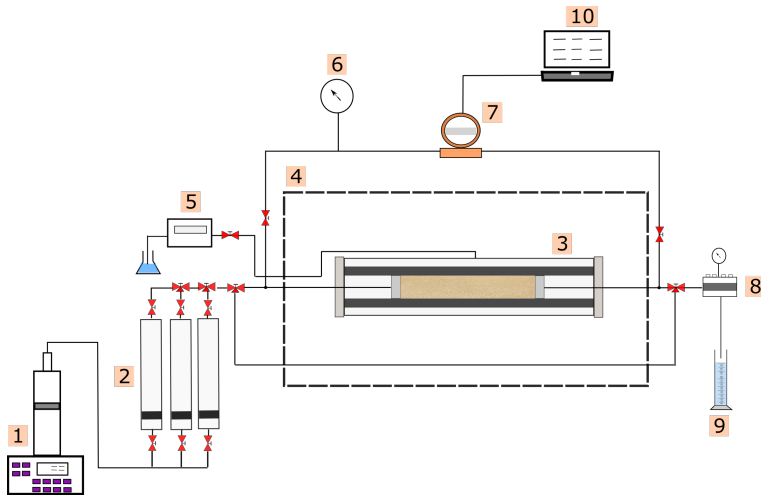


**Fig. 4.2:** Experimental set-up at Aalborg University: 1 - ISCO pump, 2 - stainless steel pistons, Hassler-type core holder with core, 4 - oven, 5 - pump, 6 - manometer, 7 - pressure transmitter, 8 - effluent collector, 9 - computer. Source: [2]

As observed in Figure 4.3, the second flooding experimental system consists of Quizix pumps, crude oil accumulator, Hassler-type core holder, heating cabinet (oven), and a measuring cylinder. This setup was used to filter crude oil following the procedure presented by



Fernø et al. [8]. Moreover, it was employed for the dynamic and static aging procedures, in which crude oil was injected in both directions through Edwards limestone core plugs. The explanation of both aging methods is presented in paper IV.

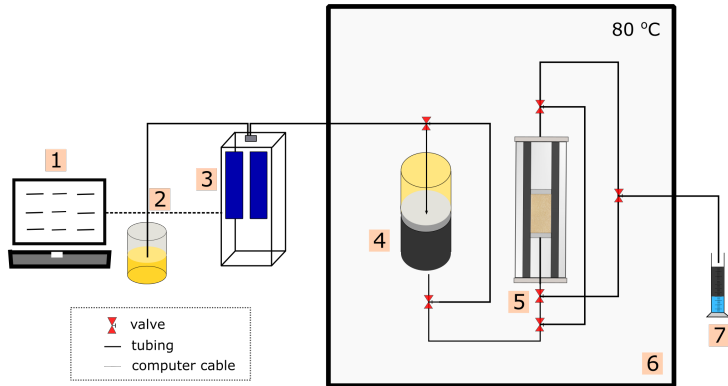


**Fig. 4.3:** Experimental set-up at University of Bergen: 1 - computer, 2 - pump oil, 3 - Quizix pump, 4 - crude oil accumulator, 5 - Hassler-type core holder with core, 6 - heating cabinet, 7 - measuring cylinder

## References

- [1] “Tam iv isothermal microcalorimeter,” 2020. [Online]. Available: <https://www.tainstruments.com/wp-content/uploads/BROCH-TAM-IV.pdf,howpublished=>
- [2] J. E. Cobos and E. G. Søgaaard, “Study of geothermal brine reinjection by microcalorimetry and core flooding experiments,” *Geothermics*, vol. 87, p. 101863, 2020.
- [3] J. E. Cobos and E. G. Søgaaard, “Impact of compositional differences in chalk and water content on advanced water flooding: A microcalorimetric assessment,” *Energy & Fuels*, vol. 34, no. 10, pp. 12 291–12 300, 2020. [Online]. Available: <https://doi.org/10.1021/acs.energyfuels.0c02108>
- [4] J. E. Cobos, P. Westh, and E. G. Søgaaard, “Isothermal titration calorimetry study of brine oil rock interactions,” *Energy & Fuels*, vol. 32, no. 7, pp. 7338–7346, 2018.
- [5] W. Dawson, B. Katz, and V. Robison, “Austin chalk, petroleum system: Upper cretaceous, southeastern texas,” *AAPG Bulletin - AAPG BULL*, vol. 79, 01 1995.
- [6] A. Ekdale and R. BROMLEY, “Trace fossils and ichnofabric in the kjølby gaard marl, uppermost cretaceous, denmark,” *Bulletin - Geological Society of Denmark*, vol. 31, 01 1983.
- [7] M. A. Fernø, R. Grønsdal, J. Åsheim, A. Nyheim, M. Berge, and A. Graue, “Use of sulfate for water based enhanced oil recovery during spontaneous imbibition in chalk,” *Energy & Fuels*, vol. 25, no. 4, pp. 1697–1706, 2011.
- [8] M. A. Fernø, M. Torsvik, S. Haugland, and A. Graue, “Dynamic laboratory wettability alteration,” *Energy & Fuels*, vol. 24, no. 7, pp. 3950–3958, 2010.
- [9] M. Hjuler, “Diagenesis of upper cretaceous onshore and offshore chalk from the north sea area,” Ph.D. dissertation, 11 2007.
- [10] K. Pearson, “Geologic models and evaluation of undiscovered conventional and continuous oil and gas resources: Upper Cretaceous Austin Chalk,” USGS, Tech. Rep., 2012.
- [11] M. A. Sohal, S. Kucheryavskiy, G. Thyne, and E. G. Søgaaard, “Study of ionically modified water performance in the carbonate reservoir system by multivariate data analysis,” *Energy & Fuels*, vol. 31, no. 3, pp. 2414–2429, 2017. [Online]. Available: <http://dx.doi.org/10.1021/acs.energyfuels.6b02292>
- [12] F. Surlyk, T. Damholt, and M. Bjerager, “Stevns klint , denmark : Uppermost maastrichtian chalk , cretaceous – tertiary boundary , and lower danian bryozoan mound complex,” 2007.
- [13] H. Tie, “Oil recovery by spontaneous imbibition and viscous displacement from mixed-wet carbonates,” Ph.D. dissertation, University of Wyoming, Laramie, Wyoming, 2006.

## Part II

### Main Findings

In this part, the main findings in wettability alteration by advanced waterflooding and reinjection of diluted geothermal brine for SaltPower electricity generation are presented. The conclusion section summarizes the obtained results from a larger perspective.



## Chapter 5

# Wettability Alteration

This chapter presents the main results related to the papers I-IV. Those studies were aiming at investigating the complex rock-fluid and fluid-fluid interactions in carbonate rocks. In particular, the following research questions were investigated:

- (1) How applicable is Isothermal Titration Calorimetry technique to evaluate rock-fluid and fluid-fluid interactions in complex chalk+brine+oil systems?
- (2) How is advanced waterflooding affected by compositional differences in the rock material and ionic composition of the injection fluid?
- (3) What is the contribution of single ions and mixture of ions to Adhesion Energies?
- (4) Is there any difference between static and dynamic aging methods for wettability alteration?

## 1 Isothermal Titration Calorimetry for Wettability Studies

The great potential of Isothermal Titration Calorimetry (ITC) in the characterization of rock-fluid and fluid-fluid interactions that occur in carbonate reservoirs has been proved throughout this PhD study.

Paper I is the first attempt at using ITC for geosciences research purposes that have been reported in the literature so far. Normally, this ultra-sensitive calorimetric technique is used in physical and bio-chemical research areas because it measures directly the heat absorbed or released during a binding interaction [20]. The robustness and flexibility of this calorimetric technique were tested by adding synthetic North Sea formation brines with a different ionic composition and ionic strength to Dan chalk particles. Then, crude oil was brought to the chalk+brine systems. 100 times diluted seawater (100D\*SW) or modified seawater (SW\*0NaCl\*4S), which was spiked with 4 times sulfate, were thereafter added separately to

resulting rock+brine+oil systems.

The thermograms (heat flow vs time signals) for different COBR systems are completely different from each other depending on which fluid contacts the rock particles. As observed in Figure 5.1, formation brines with different ionic strengths attain a unique heat response. The darker colors indicate a system in which Dan chalk particles were contacted with a synthetic formation brine similar to the Valhall oil field (VB). The light colors, on the other hand, show a system made up of synthetic formation brine similar to the Ekofisk oil field (EFB).

Different complexes are formed at a calcite lattice as soon as it is contacted by an aqueous fluid [19, 40, 42]. As expected, the microcalorimeter was able to detect those complexes at the water-mineral interface. It can be observed from Figure 5.1a that positive deflections from the baseline were obtained for the Dan chalk+VB system. According to the data acquisition of the microcalorimeter, those deflections (peaks up) indicate an exothermic event, which indicates different complexation reactions between the VB and the chalk mineral surface. On the other hand, the thermogram for the EFB system shows a negative deflection (endothermic) and only small positive peaks in the following titrations. The difference between both systems was attributed to the ionic composition of those brines (see Table 4.3). EFB has a high concentration of  $\text{Cl}^-$  but low concentration of  $\text{HCO}_3^-$  and  $\text{SO}_4^{2-}$ , which has an impact on the pair creation processes. It is harder for the unpaired  $\text{Ca}^{2+}$  ions to reach and interact with the rock surface sites (e.g.  $>\text{CaH}_2\text{O}^+$  and  $>\text{CO}_3^-$ ). Nevertheless, VB has less concentration of  $\text{Cl}^-$  and high concentration of  $\text{HCO}_3^-$  and  $\text{SO}_4^{2-}$ , which enhances the formation of calcium-hydrogen carbonate and calcium-sulphate pairs in the brine. It is much easier for those ions to reach and interact with the surface sites of the rock than the EFB unpaired ions.

As observed in Figure 5.1b, the heat flow signal recorded by the microcalorimeter shows negative deflections (endothermic peaks) for the addition of crude oil into the two chalk+formation brine systems. This means that crude oil picks energy from the surroundings to interact with those systems. One part of the crude oil makes a kind of micro-emulsion, which has more entropy than the two separated liquids and reach the rock surface. The other part will form a layer on top of the brine, creating a new interface with a second diffuse layer. The thermograms for both systems are similar but the peaks for the chalk+EFB+oil system are higher than the ones for the chalk+VB+oil system. This difference was ascribed to the chemical composition of the formation brine that contacts the rock before the oil invasion. EFB has a higher ionic strength than VB (see Table 4.3). Consequently, more energy is needed for a similar amount of oil to penetrate the EFB interface and become physisorbed to the surface due to the number of counterions in the double layer.

The sensitivity and robustness of the isothermal titration calorimetry technique give a realistic overview of the interactions that take place when an advanced fluid (seawater spiked with sulfate or diluted seawater) contacts a COBR system. For instance, when seawater spiked with four times sulfate and depleted in  $\text{Na}^+$  and  $\text{Cl}^-$  contacts the chalk+VB+oil system, an exothermic event takes place. On the other hand, the addition of 100 times diluted seawater (100\*DSW) in the same system is both exothermic and endothermic. The exothermic peaks in both advanced fluids could be attributed to the adsorption of  $\text{SO}_4^{2-}$  onto the chalk surface.

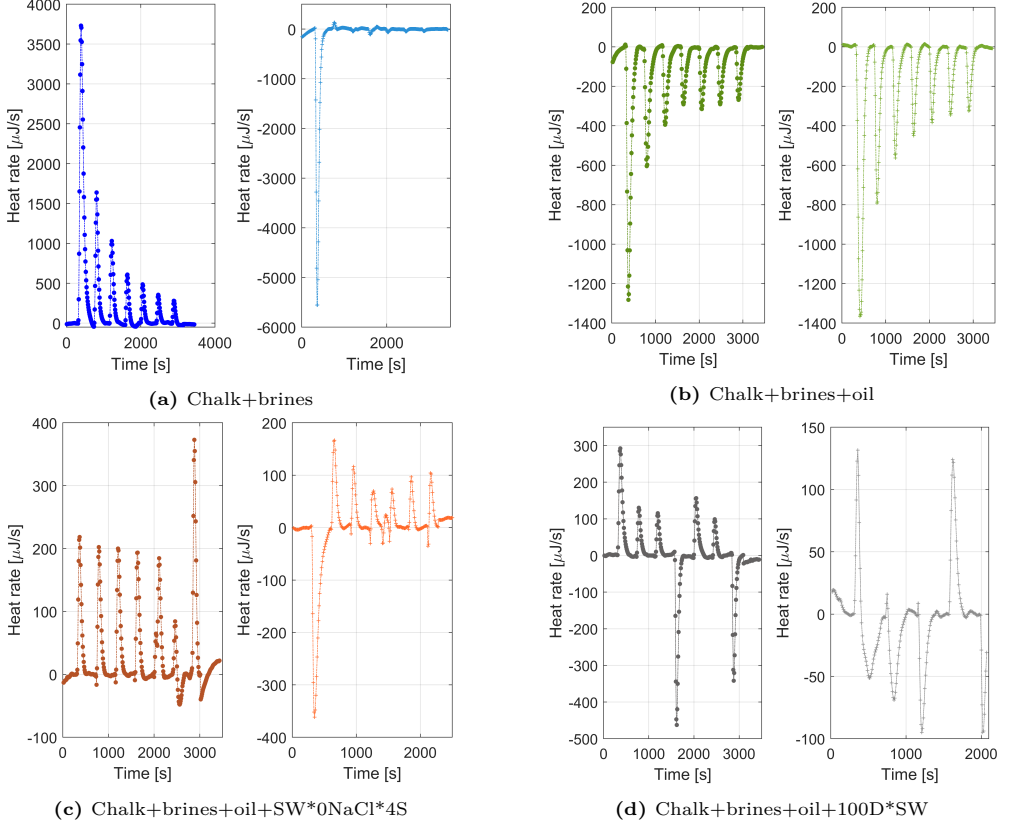


**Fig. 5.1:** Heat flow vs time signals for different systems: darker colors correspond to Valhall brine system and light colors indicate Ekofisk brine system

The endothermic peaks may indicate the displacement of  $\text{Ca}^{2+}$  and  $\text{Ca}^{2+}$ -carboxylate complexes from the surface due to a less suppressive force exerted by the ions in the bulk solution (EDL expansion). In other words, it is much easier for the physisorbed oil components to escape from the surface since not so many counter ions are present very close to the chalk surface.

The integration of the area between peaks and the baseline that can be seen in Figure 5.1 gives the heat developed ( $Q_{\text{injection}}$ ) by each injection of SW\*0NaCl\*4S and 100D\*SW into the Dan chalk+formation brines+oil systems. Those heat vales are used to calculate the enthalpy change ( $\Delta H$ ) by Equation (5.1) since the system is at isobaric and isothermal conditions. Those  $\Delta H$  values are useful in the wettability evaluation of a rock. As mentioned by Korobkov et al. [11], calorimetry has great potential in the characterization of rock-fluid interactions, which are related to wettability. These authors could only measure the heat released when gases

adsorb onto a surface since the mainly calorimetric technique was adsorption calorimetry. The possibility of measuring the heat absorbed or released when a fluid (oil or brine) contacts a rock surface, makes isothermal titration calorimetry an optimum technique to evaluate wettability alteration changes.

$$Q_{inj} = \left( \Delta H \times [C] \times V_{injection} \right) \quad (5.1)$$

## 2 Compositional Differences in Chalk and Water Content on Advanced Waterflooding

Once the potential of Isothermal Titration Calorimetry (ITC) for geosciences research has been proved, the next step was to investigate the impact compositional differences that could occur in an oil reservoir. This was done in Paper II, in which the performance of advanced water flooding was tested by using diverse chalk materials (see Table 4.1). The two advanced fluids (diluted seawater and low salinity seawater spiked with sulfate) were produced in the lab using a portion of seawater collected from Esbjerg Harbor. In the case of diluted seawater, the fluid was only filtered. Additional nanofiltration (NF) and reverse osmosis (RO) processes were used to obtain a fluid with optimum conditions, which as claimed in the literature [14, 30] could alter the wettability towards less oil-wet conditions in carbonate reservoirs.

In order to diminish some calorimetric artifacts, blank experiments were carried out under the same experimental conditions (e.g. injection time, number of injections, temperature) as the injection of advanced fluids into different chalk samples. The first blank experiment corresponds to the injection of crude oil into an empty cylinder to determine the vaporization of light crude oil compounds at 75 °C. Figure 5.2a shows that effectively an endothermic process took place when crude oil was injected into an empty cylinder. A large amount of volatile liquid hydrocarbons passed to the vapor phase at the beginning of the experiment. As observed, the accumulation of crude oil in the empty cylinder reduces this vaporization effect (smaller endothermic peaks) since a new vapor-liquid equilibrium is established inside of the reaction vessel [8].

The next blank experiments correspond to the injection of crude oil into artificial Valhall brine. Then, advanced fluids (modified seawater or 10 times diluted seawater) were added separately into the resulting Vb+oil system. As observed in Figure 5.2b-5.2d, the heat response of those fluids is dominantly endothermic (net reaction). As expected, the thermograms for those two systems differ from each other since different physicochemical alterations occur when an advanced fluid displaces the original formation brine (high salinity and low sulfate content) in the porous media. The heat flow for 10D\*SW into Vb+oil is higher than for AW into the same crude oil+brine system. This difference is ascribed to a disruption of the second and third hydration shells around the single ionic species [23] and different competitive processes at the brine-oil interface. For instance, reorientation of polar components in crude oil [2], diffusion and accumulation of naphthenic acids at the brine-oil interface [25], creation [26] and stabilization of micro-emulsions [13].



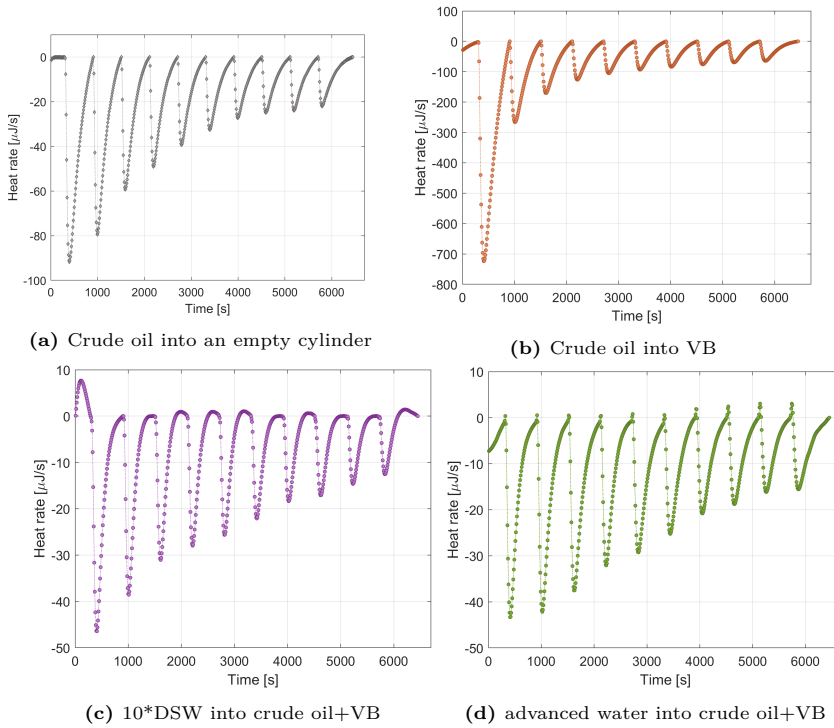


**Fig. 5.2:** Heat flow vs time signals for different blank experiments

“Smart water” or modified seawater (AW) and 10 times diluted seawater (10D\*SW) were injected separately into different chalk+brine+oil systems. As observed in Figure 5.3, the heat response varies greatly with the injection fluid and changes slightly between chalk+VB+oil systems [8]. Figure 5.3a shows that the heat response for 10D\*SW added to the Dan chalk+VB+oil system is much higher than for AW added to the same system. The same occurs in system 2 (Stevn chalk+VB+oil), system 3 (Austin chalk+VB+oil), and system 4 (synthetic chalk+VB+oil).

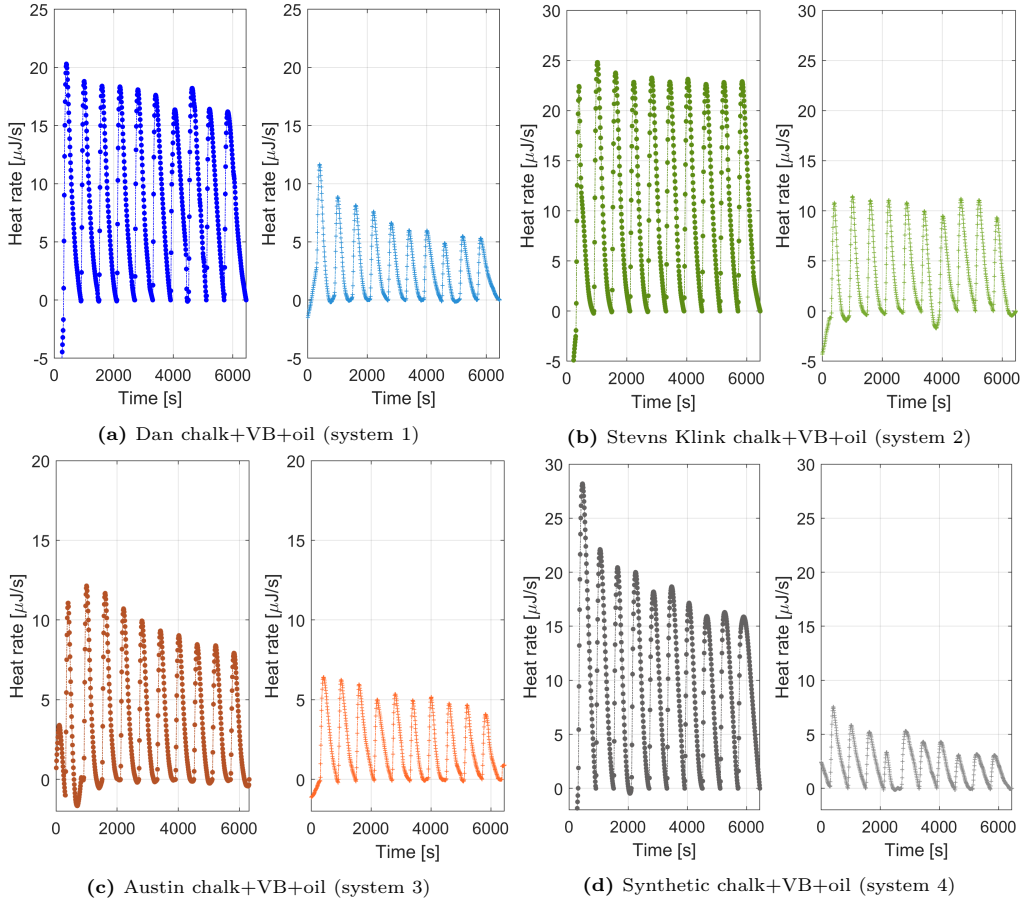


**Fig. 5.3:** Heat flow vs time signals for advanced fluids into different chalk+VB+oil systems: darker colors correspond to 10\*DSW and light colors to AW

As mentioned in Cobos et al. [9], the heat needed ( $Q_{\text{injection}}$ ) for the interaction between advanced fluids and the chalk+VB+oil systems can be obtained by integrating the area between peaks and the baseline of a thermogram (e.g. Figure 5.3). Since the microcalorimeter system is at isobaric and isothermal conditions, those heat values can be used to determine the enthalpy change ( $\Delta H$ ) of interaction between advanced fluids and the chalk+VB+oil systems through Equation 5.1. In this equation,  $[C]$  is the molar concentration of the ligand (advanced fluids) titrated into the calorimeter cell, and  $V_{\text{injection}}$  represents the volume of each injection (9.948  $\mu\text{l}$ ). Notice that  $[C]$  indicates the ionic strength of each advanced fluid (diluted seawater or modified seawater).

The enthalpy change ( $\Delta H$ ) for each chalk+Vb+oil+advanced fluid systems calculated through Equation 5.1 are shown in Figure 5.4. As observed the highest  $\Delta H$  values correspond to 10D\*SW in all the systems, whereas, the lowest values are for AW. Note that those enthalpies do not include the dilution effect from the addition of a brine with a lower ionic strength or other calorimetric contributions.

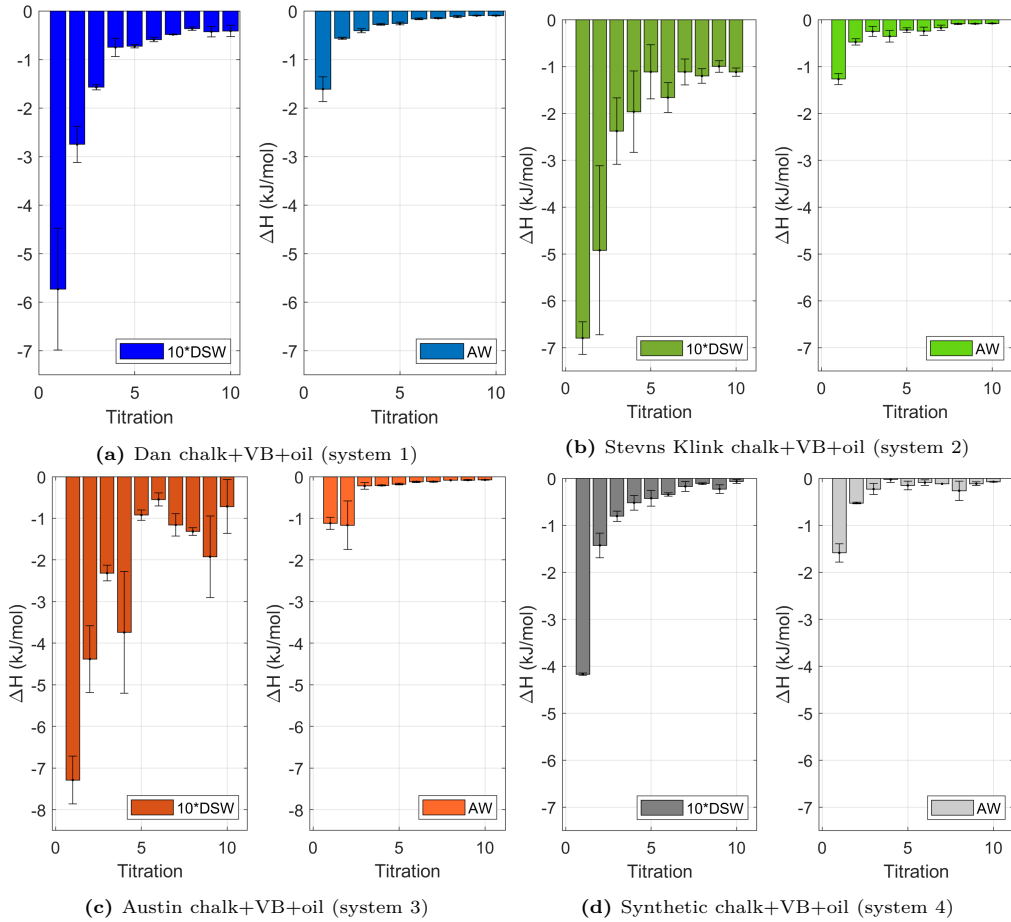
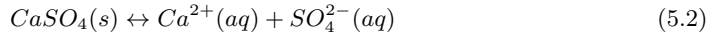


**Fig. 5.4:** Enthalpy change ( $\Delta H$ ) values for titration of advanced water (AW) and 10 times diluted seawater (10D\*SW) into different systems

By subtracting the blank experiments (fluid-fluid interactions) from the chalk + VB + oil + Aw and chalk + VB + oil + 10D\*SW heat responses, the isolated rock-fluid interactions can be found [8]. Those enthalpy change values without other calorimetric contributions (e.g. vaporization of light crude oil fractions) are presented in Table 5.1. When either AW or 10D\*SW

is injected into a carbonate oil reservoir, a set of composition variation changes “waves” rise as a result of salinity difference between the formation brine and those fluids (see Table 4.3).

As expected, the enthalpy change ( $\Delta H$ ) for 10\*DSW is much higher than AW. In this sense,  $\Delta H_{10D*SW}$  is 50% more than  $\Delta H_{AW}$  for all the chalk+Vb+oil systems. For instance, the total enthalpy change value for 10D\*SW injected into system 1 is -44.9 kJ/mol, whereas, the enthalpy value for the injection of AW into the same system is -16.9 kJ/mol. Diluted seawater is much more exothermic and therefore also more reactive than modified seawater, as shown in the preliminary calorimetry studies. Therefore, diluted seawater can also alter the wettability, and having large quantities of potential determining ions (PDIs) is not necessary to observe the low salinity effect, as mentioned by Mahani et al. [22]. The enthalpy change for the systems contacted by modified seawater varies slightly between them. This is because the average enthalpy change for system 1 is -16.86 kJ/mol, system 2 -16.37 kJ/mol, system 3 -16.50 kJ/mol, and system 4 -16.30 kJ/mol. The enthalpy change for diluted seawater also changes to some extent between chalk+Vb+oil systems. The total enthalpy change for 10\*DSW added to system 1 is -44.9 kJ/mol, systems 2 -54.3 kJ/mol, system 3 -55.4 kJ/mol, and system 4 -39.3 kJ/mol. System 2 and 3 have the highest enthalpy change and therefore wettability alteration. This better performance on a small scale could be associated with the presence of anhydrite in Stevns Klint and Austin chalk samples, which provides an extra supply of  $SO_4^{2-}$  as shown in Equation (5.2), where,  $CaSO_4$  is anhydrite,  $Ca^{2+}$  and  $SO_4^{2-}$  are ions dissolved in the pore water [3].



Nonetheless, that dissolution process loses its importance at field scale as the injection fluid becomes buffered/equilibrated as it moves away from the injector [27, 28].

inj	system 1		system 2		system 3		system 4	
	$\Delta H_{AW}$ [kJ/mol]	$\Delta H_{10D*SW}$ [kJ/mol]	$\Delta H_{AW}$ [kJ/mol]	$\Delta H_{10D*SW}$ [kJ/mol]	$\Delta H_{AW}$ [kJ/mol]	$\Delta H_{10D*SW}$ [kJ/mol]	$\Delta H_{AW}$ [kJ/mol]	$\Delta H_{10D*SW}$ [kJ/mol]
1	-7.33±0.25	-21.25±1.26	-6.99±0.12	-22.32±0.35	-6.84±0.15	-22.81±0.58	-7.31±0.19	-19.69±0.02
2	-2.93±0.02	-8.57±0.37	-2.84±0.07	-10.75±1.80	-3.53±0.58	-10.21±0.80	-2.89±0.02	-7.25±0.26
3	-1.87±0.04	-4.47±0.05	-1.71±0.10	-5.27±0.71	-1.68±0.08	-5.21±0.19	-1.69±0.12	-3.70±0.11
4	-1.37±0.02	-2.73±0.19	-1.45±0.12	-3.94±0.87	-1.30±0.01	-5.72±1.46	-1.12±0.06	-2.50±0.16
5	-1.04±0.03	-2.14±0.03	-1.00±0.05	-2.53±0.58	-0.96±0.02	-2.33±0.13	-0.94±0.09	-1.84±0.17
6	-0.70±0.02	-1.73±0.05	-0.78±0.09	-2.80±0.32	-0.66±0.01	-1.69±0.16	-0.63±0.06	-1.48±0.04
7	-0.58±0.01	-1.25±0.01	-0.61±0.06	-1.88±0.27	-0.55±0.01	-1.92±0.27	-0.55±0.01	-0.93±0.10
8	-0.40±0.02	-1.05±0.03	-0.38±0.01	-1.89±0.16	-0.37±0.01	-2.00±0.09	-0.55±0.21	-0.80±0.01
9	-0.31±0.01	-0.95±0.11	-0.30±0.01	-1.52±0.13	-0.30±0.01	-2.44±0.98	-0.33±0.04	-0.75±0.09
10	-0.32±0.01	-0.73±0.12	-0.31±0.01	-1.43±0.09	-0.31±0.01	-1.03±0.65	-0.30±0.01	-0.38±0.04

**Table 5.1:** Enthalpy change values for titration of modified seawater (AW) and 10 times diluted seawater (10D\*SW) into different systems. System 1: Dan chalk+Vb+oil, System 2: Stevns Klint chalk+Vb+oil, System 3: Austin chalk+Vb+oil and System 4: Synthetic chalk+Vb+oil. Source: [8]

### 3 Contribution of Individual Ions and Mixtures of Ions to Adhesion Energies

As presented in the previous sections, the adhesion energies which are related to changes in wetting properties vary significantly with the ionic composition of the injection fluid. Therefore, the next research step, which is presented in Paper III, is to determine the contribution of the most common ionic species to those adhesion energies. Similar ITC experiments as in the previous sections were performed. The only difference is that the liquid phase is mainly composed by individual ionic species ( $\text{Na}^+$ ,  $\text{Ca}^{2+}$ ,  $\text{Mg}^{2+}$ ,  $\text{SO}_4^{2-}$  and  $\text{HCO}_3^-$ ) or mixtures of ions ( $\text{Ca}^{2+}$ - $\text{SO}_4^{2-}$ , and  $\text{Mg}^{2+}$ - $\text{SO}_4^{2-}$ ) at a low concentration (0.001 M) in order to resemble 10\*DSW.

The heat flow signal registered in the microcalorimeter for the titration of crude oil into those individual ionic species and mixture of ions also indicates an endothermic process. The heat of interaction between crude oil and those species was found by integrating the area between the endothermic peaks and the respective baseline. Table 5.2 shows the energy that crude oil picked up from the surroundings to interact with 0.001 M  $\text{CaCl}_2$ ,  $\text{MgCl}_2$ ,  $\text{Na}_2\text{SO}_4$ ,  $\text{NaHCO}_3$ , and  $\text{NaCl}$  ions. This energy cost could be related to specific ion effects at the brine-oil interface.

**Table 5.2:** Heat values for crude oil interaction with most common ionic species of low salinity water system

	$\text{Ca}^{2+}$ [mJ]	$\text{Mg}^{2+}$ [mJ]	$\text{Na}^+$ [mJ]	$\text{SO}_4^{2-}$ [mJ]	$\text{HCO}_3^-$ [mJ]
1	137.9± 6.1	135.9±2.0	109.3±4.5	119.2±11.5	111.9±11.2
2	33.8± 5.1	40.9±1.5	22.2±1.3	21.1±4.4	32.4±1.9
3	17.1± 5.8	26.6±0.8	15.3±2.2	13.7±3.7	17.5±1.4
4	11.1±3.4	17.8±1.6	8.4±0.4	11.9±3.2	15.8±5.3
5	9.8±0.3	14.1±0.1	9.8±1.8	9.6±1.3	11.9±5.1
6	6.6±1.3	10.8±0.6	7.7±0.2	6.4±0.8	11.5±4.1
7	5.8±1.6	10.1±0.3	7.5±0.2	8.8±0.6	10.0±3.4
8	5.5±1.5	9.7±1.3	7.1±0.2	5.1±1.2	8.1±3.2
9	3.7±2.6	8.5±0.5	6.8±0.2	7.7±1.5	10.8±2.4
10	1.3±5.5	9.6±0.5	7.3±0.9	4.8±1.2	7.5±1.7

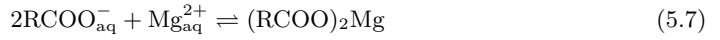
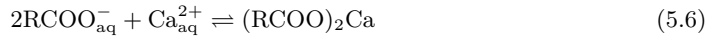
#### 3.1 Adhesion energies for oil-individual ions

When crude oil is in contact with an ionic solution, self-assemblage oil components (resins and asphaltenes) orient themselves in the plane of the interface. On the contrary, alkyl chains align perpendicular to the interface [2]. Besides, the crude oil used for the ITC experiments (sample A) has a total acid number (TAN) of 0.52 mg KOH/g, indicating a high concentration of naphthenic acids ( $\text{R-COOH}$ ). Compounds containing oxygen, such as carboxylic acids, alcohols, phenols, ketones are known as naphthenic acids (NAs). Those compounds can be accumulated at the oil-water interface due to its hydrophilicity. As mentioned by Mokhtari et al. [25],

decreasing the ionic strength of a brine (e.g. seawater) induces the dissociation of NAs. This process is explained by Equations (5.3-5.4), where the subscripts “o” and “aq” indicate the oil and aqueous phases, respectively [26].



According to those Equations, NAs dissociate into a carboxylic type anion ( $\text{RCOO}^-$ ) and a proton ( $\text{H}^+$ ). If cations are present in the liquid phase, the carboxylic anions would react with them to form naphthenates, according with the following equations:



Another important process that occur when a low salinity fluid contacts crude oils with higher interfacial activity is the formation of micro-dispersions [15, 33, 34]. The formation of micro-dispersions can be expressed by the subdivision of the dispersed phase into very small droplets. This in turn gives a configurational entropy change ( $\Delta S_{\text{conf}}$ ) that can be expressed by Equation 5.8, where,  $n$  is the number of droplets,  $k_B$  is Boltzmann’s constant, and  $\phi$  is the dispersed phase volume fraction [12].

$$\Delta S_{\text{conf}} = -nk_B[\ln\phi + \{(1-\phi)/\phi\}\ln(1-\phi)] \quad (5.8)$$

The sum of the free energy require for creating a new interface ( $\Delta A\gamma_{wo}$ ) and the configurational entropy change give the associated Gibbs free energy change ( $\Delta G_{\text{form}}$ ) for the formation of micro-dispersions, expressed by Equation 5.9, where,  $\Delta A$  is the change in interfacial area and  $\gamma_{wo}$  is the interfacial tension between water and oil at given temperature [12].

$$\Delta G_{\text{form}} = \Delta A\gamma_{wo} - T\Delta S_{\text{conf}} \quad (5.9)$$

Since  $\phi$  is always less than 1, the configurational entropy ( $\Delta S_{\text{conf}}$ ) is positive independent of the dispersed phase volume fraction. The crude oil used in all the microcalorimetric experiments has a high interfacial activity (surface active components) that may lower the interfacial tension. A relatively small and positive  $\Delta A\gamma_{wo}$  term allows a spontaneous microemulsification (negative Gibbs free energy) due to the overall IFT reduction. Once the micro-dispersions are formed, naphthenates soaps will stabilize them. This is because the naphthenates soaps, represented by Equations (5.5-5.7), accumulates at the brine-oil interface [13]. Therefore, the heat values presented in Table 5.2 could be associated with the formation and stabilization of micro-dispersions. Even though energy in the form of heat will be released from the saponification reactions (exothermic process), much more energy is needed for the formation and stabilization of micro-dispersions.

A graphical representation of the microcalorimeter and the endothermic processes at the water-oil interface are presented in Figure 5.5. When crude oil is in contact with an ionic

solution different competitive processes take place at the interface. For instance, reorientation of self-assemblage oil components (resins and asphaltenes) and naphthenic acids in the crude oil, diffusion of naphthenic acids towards the water-oil interface, creation (saponification), and stabilization of micro-dispersions.

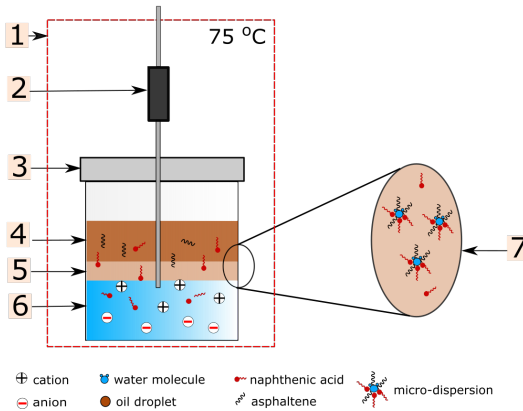


**Fig. 5.5:** Microcalorimeter description and graphical representation of oil+individual ions interaction. 1-TAM IV microcalorimeter at 75 °C, 2-titration ampule, 3-reaction vessel, 4-crude oil, 5-interface, 6-solution and 7-micro-dispersions.

In order to understand the trend of fluid-fluid interactions, the cumulative heat of adsorption,  $\Sigma Q$  (mJ), was plotted vs. the amount of crude oil added to the individual ion systems. Figure 5.6a shows that the total energy required to create and stabilize a micro-dispersion is in the following order:  $Mg^{2+} > Ca^{2+} > Na^+$ . In this sense, 233 mJ, 284, and 202 mJ is the total energy required to create and stabilize micro-dispersions when  $Ca^{2+}$ ,  $Mg^{2+}$  and  $Na^+$  ions are present in the liquid phase, respectively.  $Cl^-$  anions in those solutions are present principally as co-ions in the diffuse layer and therefore they do not participate in micro-dispersion formation. The heat response of  $Na^+$  is 13 and 29% lower than  $Ca^{2+}$  and  $Mg^{2+}$ , respectively. Those results indicate that the kinetics of partitioning and dissociation of NAs is much slower with  $Na^+$  than with the other cations, as suggested by Moradi et al. [26]. It can be observed in Figure 5.6 that the interaction of crude oil with anions follows:  $HCO_3^- > SO_4^{2-}$ . The total energy picked up from the surroundings was 237 mJ, 208 mJ for  $HCO_3^-$  and  $SO_4^{2-}$ , respectively. These results point out that  $HCO_3^-$  is more active than  $SO_4^{2-}$ .

There are several contradictory results in the existing literature regarding fluid-fluid interactions, which inhibits the understanding of the underlying mechanisms behind low salinity flooding. For instance, Chakravarty et al. [7] reported that the emulsion formation follows the Hofmeister series:  $Ca^{2+} > Mg^{2+} > Na^+ > K^+$ , which is different to the results presented in this thesis. As explained before,  $Mg^{2+}$  is more active than  $Ca^{2+}$ , which is in accordance with the findings of Ayirala et al. [5]. Those authors reported that the efficiency of different ions to promote a less rigid interfacial film and therefore a faster coalescence time follows:  $Mg^{2+} >$

$\text{Ca}^{2+} > \text{Na}^+$ . In other words,  $\text{Mg}^{2+}$  promotes the coalescence between oil droplets resulting in a faster oil mobilization by the waterflooding. However, Liu et al. [21] claims that at low salinity conditions,  $\text{Na}^+$  facilitates the formation of an elastic interface that prevents snap-off events. Since isothermal titration calorimetry (ITC) measures directly the heat absorbed or released during a binding interaction, it gives a more accurate overview of the physico-chemical processes associated with low salinity waterflooding (LSWF). Consequently, ITC may help to discern the real processes that take place when a low salinity fluid contacts an oil reservoir, filling major gaps in the literature.

A non-linear relationship was found for the interaction between crude oil and all the individual ionic species that are commonly present in seawater. This indicates that the heat adsorbed by those systems is not directly proportional to the amount of oil added to the reaction vessel.

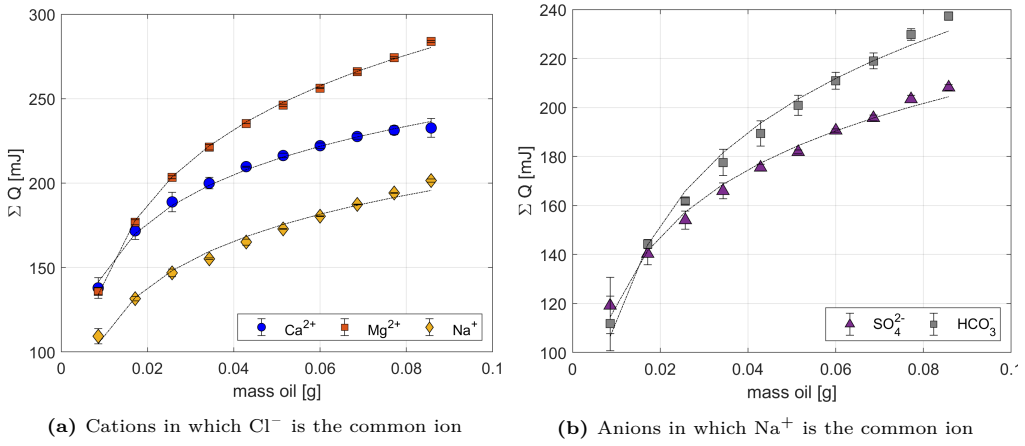


**Fig. 5.6:** Cumulative heat of adsorption of individual ionic species per gram of oil. The fitted data is shown by dash lines

A logarithmic function expressed by equation (5.10) was used to fit the data presented in Figure 5.6. In this equation,  $x$  is the cumulative mass oil and  $y$  is the cumulative heat of adsorption. The results from the non-linear regression are presented in Table 5.3. It can be seen that among all the salts in which  $\text{Cl}^-$  is the common ion,  $\text{Na}^+$  has the lowest  $\beta_1$  coefficient. On the other hand,  $\text{SO}_4^{2-}$  has the lowest  $\beta_1$  coefficient among the salts that contain  $\text{Na}^+$ . The  $\beta_1$  coefficient numbers indicate that the entropy production (which ensures the spontaneity of the endothermic reactions by the creation of micro-dispersions) increases by least a factor of 0.39 in the case of  $\text{Na}^+$  and  $\text{SO}_4^{2-}$ . On the contrary as observed in Table 5.3, this entropy production is much higher for  $\text{Mg}^{2+}$  and  $\text{HCO}_3^-$ .

$$y = \beta_1 \ln(x) + \beta_0 \quad (5.10)$$



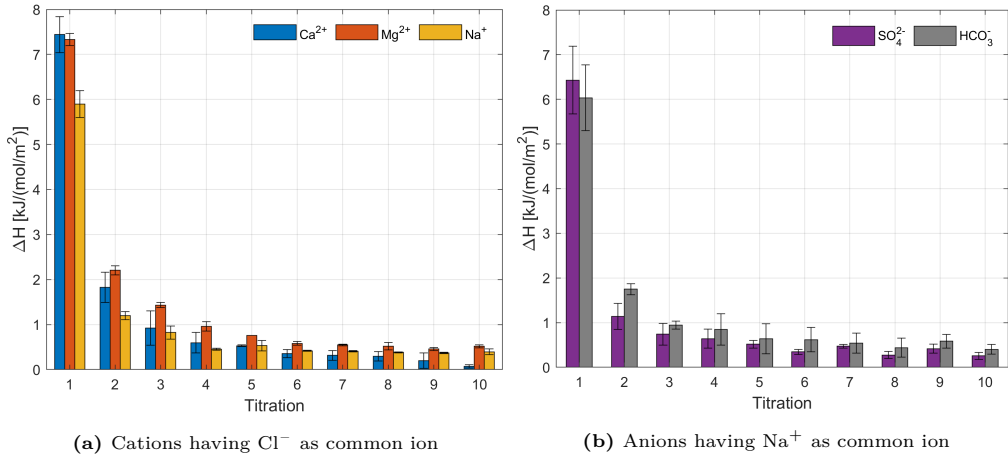
**Table 5.3:** Non-linear regression model for single ions-crude oil system interaction

Ion	Equation	R <sup>2</sup>
Ca <sup>2+</sup>	$y = 41.3\ln(x) + 338$	0.995
Mg <sup>2+</sup>	$y = 63.6\ln(x) + 437$	0.999
Na <sup>+</sup>	$y = 39.4\ln(x) + 293$	0.987
SO <sub>4</sub> <sup>2-</sup>	$y = 39.0\ln(x) + 300$	0.989
HCO <sub>3</sub> <sup>-</sup>	$y = 54.2\ln(x) + 364$	0.989

Considering that only the acid group of the oil components interacts with the ionic species, the enthalpy can be expressed in terms of carboxylic sites in [kJ/ (mol/m<sup>2</sup>)] according to Equation 5.11. In this equation, AN is the acid number,  $a_{oil} = 0.5$  [m<sup>2</sup>/g] is the specific area of oil [39], and  $MW_{KOH} = 56.1$  [g/mol] is the molecular weight of potassium hydroxide.

$$\Delta H_{COOH} = \frac{Q}{\frac{AN}{1000 \times a_{oil} \times MW_{KOH}}} \quad (5.11)$$

As revealed in Figure 5.7, the obtained  $\Delta H$  values calculated through Equation 5.11 are positive. The meaning of those values is that different competitive processes, such as redistribution of oil components, formation, and stabilization of micro-dispersions are taking place at the oil-brine interface, as indicated previously. The highest  $\Delta H$  occurs at the first crude oil injection in all the cases (cations, and anions). A lower enthalpy change is obtained in further crude oil additions since an oil layer is being formed on top of the ionic solutions. Consequently, less entropy production will occur in those subsequent injections.

**Fig. 5.7:** Enthalpy change ( $\Delta H$ ) values for crude oil titrated into single 0.001 M ionic species

### 3.2 Adhesion energies for oil-mixture of ions

It is believed that  $\text{Ca}^{2+}$ ,  $\text{Mg}^{2+}$ , and  $\text{SO}_4^{2-}$  play an important role in the wettability alteration of carbonate rock towards a less oil wetness condition [4, 31, 37]. However, the behaviour of those ions at the oil-brine interface in presence of other ions (mixtures) has not been evaluated at the microscopic level. Thus, the interaction of crude oil with different mixtures, mixture 1 (0.001M  $\text{CaCl}_2$ +0.001 M  $\text{Na}_2\text{SO}_4$ ), mixture 2 (0.001M  $\text{MgCl}_2$ +0.001  $\text{Na}_2\text{SO}_4$ ), was evaluated as well. The heat values obtained for the crude oil interaction with those mixtures are presented in Table 5.4. As observed previously, each mixture attains a different heat response, being the first crude oil injection the highest in all the cases.

**Table 5.4:** Heat response of crude oil interaction with different mixtures of ions

	1	2	3	4	5	6	7	8	9	10
mixture 1 [mJ]	134.4±0.4	31.7±0.7	18.5±0.6	11.3±0.5	8.4±0.3	6.8±0.2	5.7±0.2	4.8±0.2	3.7±0.1	4.4±0.7
mixture 2 [mJ]	86.4±9.5	26.9±0.1	18.6±0.2	13.1±1.4	9.0±0.8	7.1±0.7	7.4±0.8	5.8±0.1	6.7±0.7	6.6±0.9

The cumulative heat of adsorption,  $\Sigma Q$  (mJ), was also plotted vs. the amount of crude oil added to the mixture systems. Figure 5.8 shows that the interaction between crude oil and mixture 1 and mixture 2 follows a non-linear relationship. Similarly to the individual ions - oil interaction, the heat data can be fitted by a logarithmic function; obtaining a regression coefficient ( $R^2$ ) close to 1.

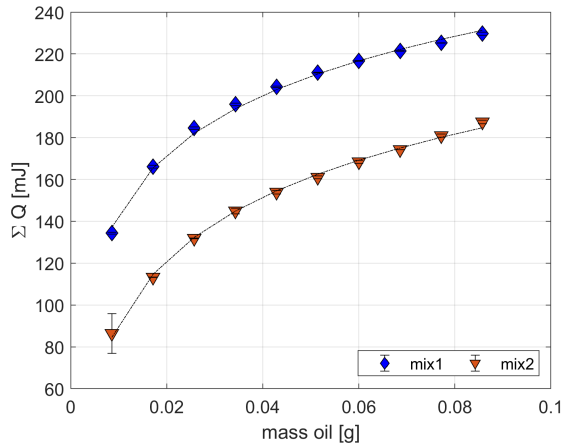


**Fig. 5.8:** Cumulative heat of adsorption of mixture 1 and mixture 2 per gram of oil. The fitted data is shown by dash lines

As observed in Table 5.5, the  $\beta_1$  coefficient is analogous for both mixtures. 25% less energy

is adsorbed from the surroundings when  $\text{SO}_4^{2-}$  is added to either  $\text{Ca}^{2+}$  or  $\text{Mg}^{2+}$ . This could be because  $\text{SO}_4^{2-}$  is forming ion pairs with those ions, which interact with crude oil.

**Table 5.5:** Non-linear regression model for oil-mixture of ions interaction

Ion	Equation	$R^2$
Mixture <sub>1</sub>	$y = 40.9\ln(x) + 332$	0.997
Mixture <sub>2</sub>	$y = 43.5\ln(x) + 292$	0.998

The interaction between crude oil and ion-pairs could explain the results presented by Fernø et al. [16]. These authors observed a color change in n-decane when the imbibition fluid was spiked in sulfate. Figure 5.9 shows a graphical representation of this complex process, in which  $\text{SO}_4^{2-}$  -  $\text{Ca}^{2+}$  or  $\text{Mg}^{2+}$  ion pairs are moving from solution towards the interface due to the strong attraction of water for itself (hydrophobic effect) [38].

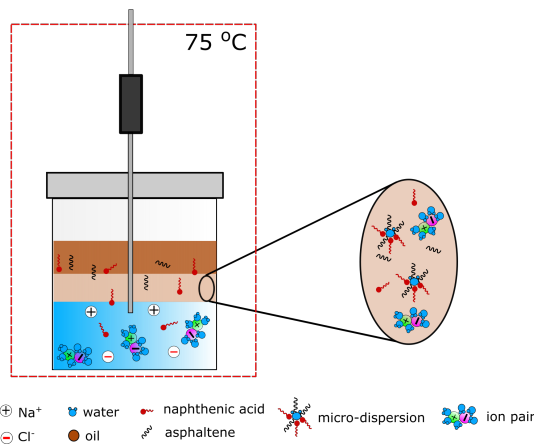


**Fig. 5.9:** Graphical representation of mixture of ions and crude oil interaction

The enthalpy values for crude oil-mixtures can be estimated by using Equation 5.11.  $\Delta H$  values for each mixture of  $\text{Ca}^{2+}$  -  $\text{SO}_4^{2-}$  and  $\text{Mg}^{2+}$  -  $\text{SO}_4^{2-}$  ions together with  $\text{Na}^+$  and  $\text{Cl}^-$  are presented in Figure 5.10. Higher endothermic enthalpy creation after the first crude oil addition resulted for mixture 1 than for mixture 2, both at 0.001 M. The reason could be that  $\text{Mg}^{2+}$  boost the pair creation process with  $\text{SO}_4^{2-}$ .

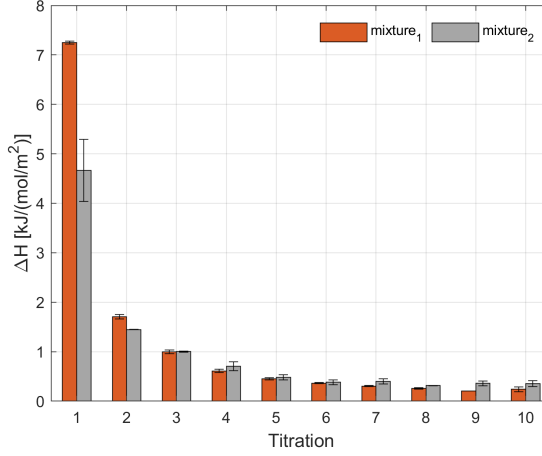


**Fig. 5.10:** Enthalpy change ( $\Delta H$ ) values for crude oil titrated into mixtures of  $\text{Ca}^{2+}$  -  $\text{SO}_4^{2-}$  (orange bars) and  $\text{Mg}^{2+}$  -  $\text{SO}_4^{2-}$  (gray bars)

### 3.3 Adhesion energies for chalk-individual ions/mixtures

The interaction heat between the rock-liquid phases could not be measured directly since the evaporation of the tested solutions masked the real effect at 75°C. Thus, another strategy was followed to determine the individual ions/mixtures and chalk interaction. It consisted of subtracting all the heat contributions from the total heat as shown in Equation 5.12. In this equation,  $\Delta H_{r-f}$  is Dan chalk + ionic species or mixtures interaction heat,  $\Delta H_T$  is the total heat (chalk, oil, and liquid solutions),  $\Delta H_{o-f}$  is the oil+ionic species or mixtures interaction heat,  $\Delta H_{o-r}$  is the oil+chalk interaction heat.

$$\Delta H_{r-f} = \Delta H_T - \Delta H_{o-f} - \Delta H_{o-r} \quad (5.12)$$

The adsorption heats for chalk-individual ions is presented in Figure 5.11. As observed, the chemisorption of those species onto the chalk lattice is effectively an exothermic process.  $\text{Mg}^{2+}$  and  $\text{Na}^+$  are common substitutes for  $\text{Ca}^{2+}$  in the atomic structure or in the interstitial positions. Thus, those cations can be incorporated into the calcite lattice [29].  $\text{SO}_4^{2-}$  ions, on the other hand, can be adsorbed as an outer-sphere surface complex, being attracted mainly to the hydrolysis layer of calcite [24]. It can also be seen that  $\text{Ca}^{2+}$  and  $\text{HCO}_3^-$  interact more strongly with the rock surface than  $\text{Mg}^{2+}$ ,  $\text{SO}_4^{2-}$  and  $\text{Na}^+$  for the first injection. It is also observed that in further injections  $\text{Mg}^{2+}$  attains a higher heat response than for the other cations. This could indicate that the incorporation of  $\text{Mg}^{2+}$  into the calcite structure is kinetically hindered at the first injections due to hydration effects [1].

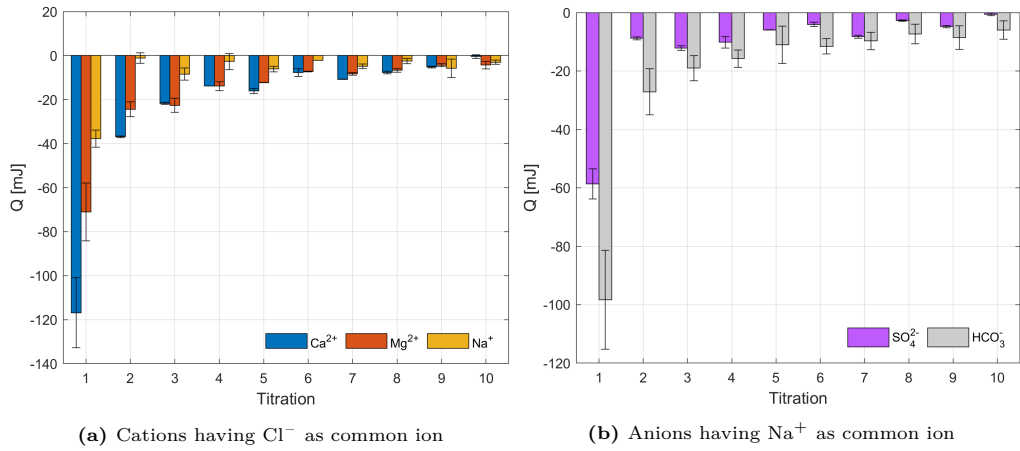


**Fig. 5.11:** Interaction between individual ions and the chalk lattice

Figure 5.12 shows that if  $\text{SO}_4^{2-}$  is added to an aqueous phase containing either  $\text{Ca}^{2+}$  or  $\text{Mg}^{2+}$ , the heat response is lower. A heat reduction of 13% and 80% in comparison with  $\text{Ca}^{2+}$  and  $\text{Mg}^{2+}$  ions was obtained for mixture 1 and mixture 2, respectively. Thus, the presence of  $\text{SO}_4^{2-}$  diminishes the incorporation of  $\text{Mg}^{2+}$  or  $\text{Ca}^{2+}$  into the calcite lattice, which is less energetically favored due to pair creation.

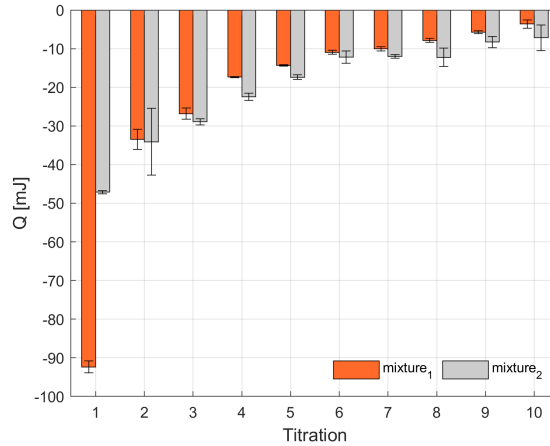


**Fig. 5.12:** Interaction between mixture of ions and the chalk lattice

## 4 Wettability Alteration of Strongly Water-Wet Edwards Limestone

Restored-state cores for special core analysis (SCAL) must have wettabilities similar to undisturbed reservoir rock, as the reservoir behavior depends on the rock preference for oil and water. Different techniques can be used to obtain a spectrum of wettability conditions. Those techniques use crude oil to alter the rock surface towards a more oil-wet state. The first technique consists in submerging rocks in crude oil at elevated temperatures to boost the adsorption of active components (carboxylic acids) for 1000h [6, 10, 35, 36, 41]. The second technique comprises the continuous injection of crude oil at low flow rates during the entire aging process (144h) [17, 18]. In Paper IV, both aging techniques were used to alter the wettability of Edwards limestone core plugs. Thereafter, microcalorimetry was used to understand the rock-fluid and fluid-fluid interactions that take place inside the porous media.

After aging 2 Edwards limestone core plugs in crude oil for 1000h, they were submitted to an Amott-Harvey cycle but none of those cores imbibed neither water nor oil after 600 hours; obtaining Amott-Harvey indices of  $I = 0$ . All the dynamically aged core plugs obtained a negative Amott-Harvey index, indicating slightly oil-wet conditions. More information about those indices can be found in Paper IV. Note that none of the dynamically aged core plugs imbibed water, being the oleic phase the only one that was imbibed spontaneously. Figure 5.13 shows the spontaneous oil imbibition for dynamically aged core plugs submitted to the first Amott-Harvey cycle. As observed, the time from which the core plugs were submerged until they start expelling water (induction time), was less than 1 hour. This relatively short induction time may indicate that the wettability of the core plugs was altered during aging because of the presence of active crude oil components.

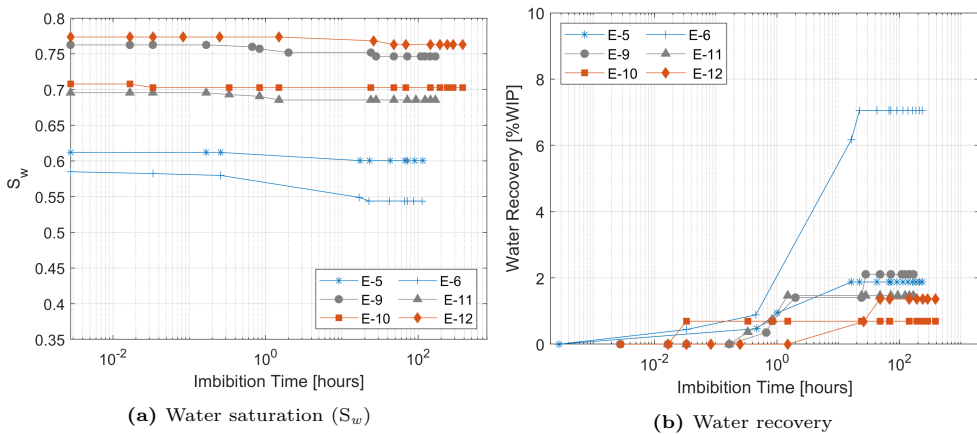


**Fig. 5.13:** Spontaneous oil imbibition characteristics for duplicate set of dynamically aged limestone whole cores with n-decane during first Amott-Harvey cycle

The ITC experiments were carried out in the same manner as the chalk experiments to get an improved understanding of the wettability process. Firstly, formation brine was injected into limestone particles in a reaction vessel. Then, crude oil was added to the resulting rock+brine system. The thermogram displaced in Figure 5.14a shows two endothermic peaks at the beginning of the reaction. The first two values could suggest the endothermic processes (see section 3) that occurs when crude oil contacts an ionic fluid, initial water saturation. The positive peaks (exothermic) may indicate that the acid/base interactions bond strongly carboxylic groups to the limestone lattice. This is because the limestone and oil interfaces become charged and therefore are attracted to each other due to the water adsorbed on the rock surface [6]. In order to confirm this hypothesis a blank experiment, in which n-decane was used as the oleic phase, was also performed. It is observed in Figure 5.14b that no major changes were registered by the microcalorimeter when n-decane was added to the rock+brine system. The first endothermic peak could be because of the evaporation of n-decane at the experimental temperature (80°C).

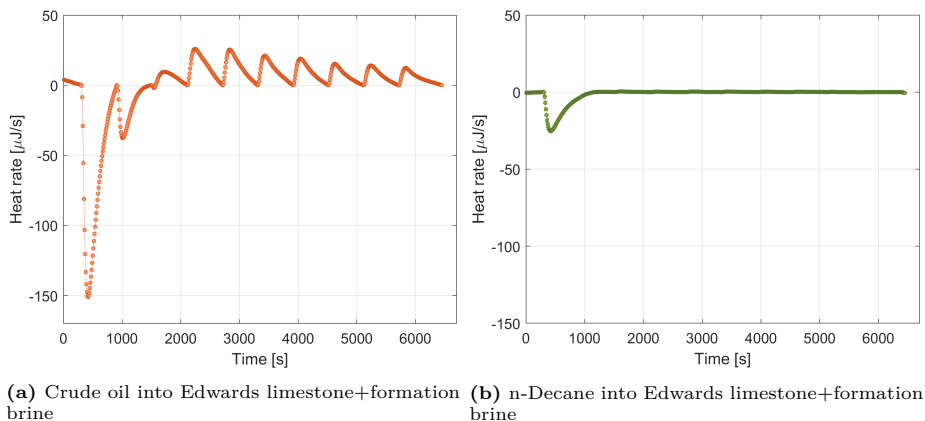


**Fig. 5.14:** Heat flow vs time for Edwards limestone+formation brine+oleic phases

Additionally to the rock-fluid interactions, fluid-fluid interactions were also carried out. In those experiments, it was measured the heat absorbed or released when crude oil contacts a formation brine. Similarly to the limestone+formation brine+crude oil system, the negative peaks observed in Figure 5.15a indicate an endothermic process related to competitive processes at the interface, as mentioned in section 3. For instance, reorientation of active components in the crude oil, diffusion of naphthenic acids towards the water-oil interface, creation, and stabilization of micro-emulsions. [2, 13, 26]. As expected the blank experiment, n-decane injected into formation brine, does not show an important heat response. Figure 5.15b indicates that n-decane (model oil) does not interact with the ionic species of the formation brine. Thus, it confirms the hypothesis that different processes take place when crude oil contacts an ionic fluid at the liquid-oil interface.

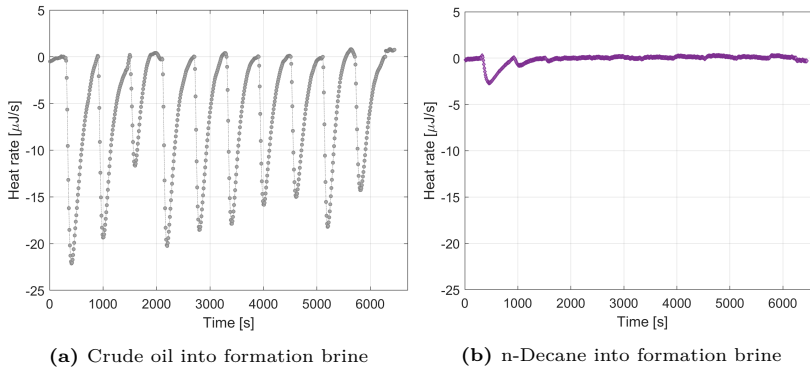


**Fig. 5.15:** Heat flow vs time for formation brine and oleic phases

#### 4.1 Change in boundary conditions for imbibition experiments

It was observed that statically aged core plugs did not imbibe any kind of fluid (brine or oil), whereas, dynamically aged cores only imbibed oil. Those findings make us think about what would happen if those statically and dynamically aged core plugs are split and submitted to imbibition as half cores. Figure 5.16 shows that effectively formation brine is not being spontaneously imbibed for any of the core plugs even after 144 hours, which was also observed in whole cores.

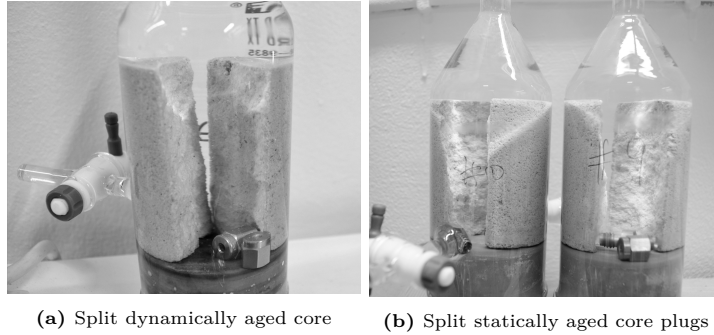


**Fig. 5.16:** Spontaneous water imbibition for Edwards limestone

After spontaneous water imbibition, the split core plugs were flooded with water (formation brine) and submitted to spontaneous oil imbibition. Note that n-decane was used in the imbibition cells since the cores (dynamically and statically aged) were flooded with 5 PV of decaline followed by 5 PV of decane in order to improve reproducibility [18]. Thus, the oleic phase in both dynamically and statically aged cores was n-decane after aging. It is observed in Figure 5.17 that the wetting fluid (oil) is displacing the non-wetting fluid (water) out of



the core plugs. Figure 5.17b shows that statically aged core plugs are slightly oil-wet in the interior, which was not observed with an all faces open (AFO) boundary condition.

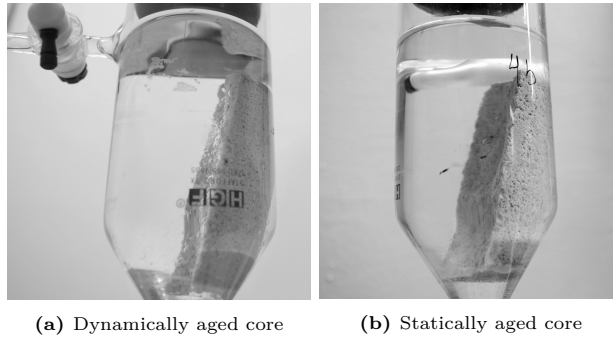


**Fig. 5.17:** Spontaneous oil imbibition for split Edwards limestone

The spontaneous oil imbibition for duplicate core plugs (dynamically and statically aged) that were split is presented in Figure 5.18. As observed, dynamic aging gives more oil-wet conditions than submerging the core plugs in crude oil for a longer period time (1000h). The statically aged core plugs only imbibed oil when the inner part was in direct contact with the wetting fluid. Consequently, the spontaneous imbibition with an AFO boundary is less reliable for statically aged cores than dynamically aged core plugs. In this thesis, the wettability alteration in the interior of statically aged core plugs is attributed to the drainage procedure, in which the core plugs were flooded bidirectionally with crude oil until  $Sw_i$  was reached. While the outermost surface of the core plugs was altered not only due to the adsorption of active crude oil components but also precipitation of heavy fractions that clogged all the open surfaces during aging.

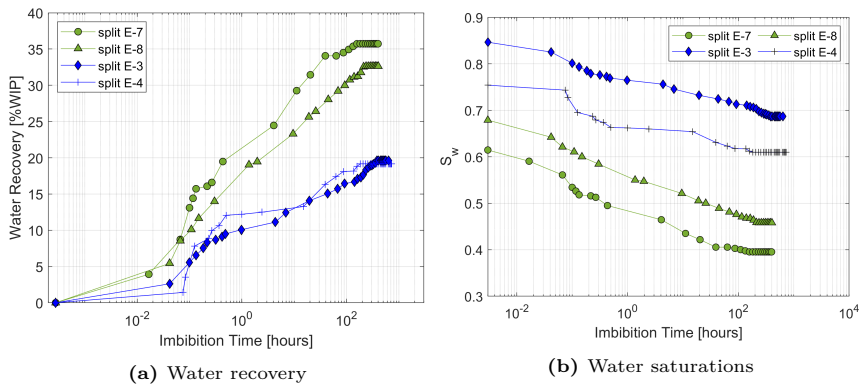


**Fig. 5.18:** Spontaneous oil imbibition for dynamically aged cores (E-7 and E-8) and statically cores (E-3 and E-4)

## 4.2 Wettability alteration towards less oil-wet conditions

Several Amott-Harvey cycles were performed on four dynamically aged core plugs aiming to alter the oil wetness condition. E-9 and E-11 core plugs started imbibing water spontaneously for the first time after the 4th Amott-Harvey cycle, whereas, E-10 and E-12 on the fifth Amott-Harvey cycle. The wettability alteration can be observed in Figure 5.19. The neutral wetting conditions of those core plugs are slightly changed towards more water-wet conditions. As mentioned in the previous sections, a wettability alteration occurs due to rock-fluid and fluid-fluid interactions inside the porous media. The reason for the slow wettability alteration could be because the injection fluid (formation brine) has a high salinity (83.091 g/l). Thus, it was not so efficient to cause the desired wettability alteration. Moreover, the limestone surface has a low reactivity towards potential determining ions (PDIs). Ravari [32] found that Edwards limestone is not able to substitute  $\text{Ca}^{2+}$  by  $\text{Mg}^{2+}$  at the rock surface in a 1:1 reaction. This author attributed the observed oil production (less than 10% ) to thermal expansion since the spontaneous imbibition tests were performed at high temperature (130 °C).

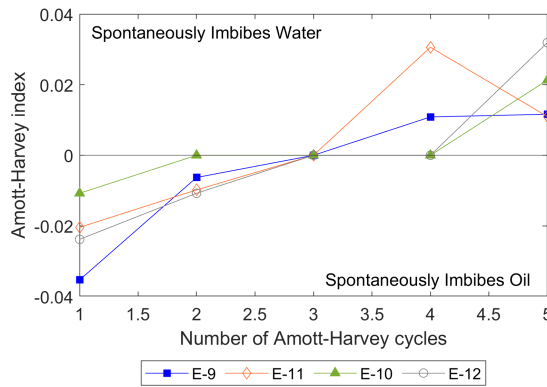


**Fig. 5.19:** Amott-Harvey indices for each cycle performed on E-9, E-10, E-11, and E-12

## References

- [1] M. Andersson, K. Dideriksen, H. Sakuma, and S. Stipp, “Modelling how incorporation of divalent cations affects calcite wettability—implications for biomineralisation and oil recovery,” *Scientific Reports*, vol. 6, 06 2016.
- [2] A. B. Andrews, A. McClelland, O. Korkeila, A. Demidov, A. Krummel, O. C. Mullins, and Z. Chen, “Molecular orientation of asphaltenes and pah model compounds in langmuir–blodgett films using sum frequency generation spectroscopy,” *Langmuir*, vol. 27, no. 10, pp. 6049–6058, 2011.
- [3] T. Austad, S. F. Shariatpanahi, S. Strand, H. Aksulu, and T. Puntervold, “Low salinity eor effects in limestone reservoir cores containing anhydrite: A discussion of the chemical mechanism,” *Energy & Fuels*, vol. 29, no. 11, pp. 6903–6911, 2015.

- [4] T. Austad, "Chapter 13 - water-based eor in carbonates and sandstones: New chemical understanding of the eor potential using "smart water"," in *Enhanced Oil Recovery Field Case Studies*, J. J. Sheng, Ed. Boston: Gulf Professional Publishing, 2013, pp. 301 – 335.
- [5] S. C. Ayirala, A. A. Yousef, Z. Li, and Z. Xu, "Coalescence of crude oil droplets in brine systems: Effect of individual electrolytes," *Energy & Fuels*, vol. 32, no. 5, pp. 5763–5771, 2018. [Online]. Available: <https://doi.org/10.1021/acs.energyfuels.8b00309>
- [6] J. Buckley and Y. Liu, "Some mechanisms of crude oil/brine/solid interactions," *Journal of Petroleum Science and Engineering*, vol. 20, no. 3, pp. 155 – 160, 1998.
- [7] K. Chakravarty, P. Fosbøl, and K. Thomsen, "Brine crude oil interactions at the oil-water interface," in *Proceedings of the SPE Asia Pacific Enhanced Oil Recovery Conference*. Society of Petroleum Engineers, 2015, pp. 817–836.
- [8] J. E. Cobos and E. G. Søgaaard, "Impact of compositional differences in chalk and water content on advanced water flooding: A microcalorimetric assessment," *Energy & Fuels*, vol. 34, no. 10, pp. 12 291–12 300, 2020. [Online]. Available: <https://doi.org/10.1021/acs.energyfuels.0c02108>
- [9] J. E. Cobos, P. Westh, and E. G. Søgaaard, "Isothermal titration calorimetry study of brine oil rock interactions," *Energy & Fuels*, vol. 32, no. 7, pp. 7338–7346, 2018.
- [10] L. Cuiec, "Rock/crude-oil interactions and wettability: An attempt to understand their interrelation." SPE Annual Technical Conference and Exhibition, Houston, Texas, September 1984, p. 14.
- [11] E. Dyshlyuk, D. Korobkov, and V. Pletneva, "Characterization of fluid-rock interaction by adsorption calorimetry," in *International Symposium of the Society of Core Analysts held in Trondheim, Norway*. Society of Core Analysts, 08 2018, p. 8.
- [12] J. Eastoe, *Microemulsions*. John Wiley & Sons, Ltd, 2010, ch. 5, pp. 77–97.
- [13] M. Ese and P. K. Kilpatrick, "Stabilization of water-in-oil emulsions by naphthenic acids and their salts: Model compounds, role of ph, and soap:acid ratio," *Journal of Dispersion Science and Technology*, vol. 25, no. 3, pp. 253–261, 2004.
- [14] S. J. Fathi, T. Austad, and S. Strand, "Water-based enhanced oil recovery (eor) by "smart water": Optimal ionic composition for eor in carbonates," *Energy & Fuels*, vol. 25, no. 11, pp. 5173–5179, 2011.
- [15] M. Fattahi Mehraban, S. A. Farzaneh, M. Sohrabi, and A. Sisson, "Novel insights into the pore-scale mechanism of low salinity water injection and the improvements on oil recovery," *Energy & Fuels*, vol. 0, no. 0, p. null, 0.
- [16] M. A. Fernø, R. Grønndal, J. Åsheim, A. Nyheim, M. Berge, and A. Graue, "Use of sulfate for water based enhanced oil recovery during spontaneous imbibition in chalk," *Energy & Fuels*, vol. 25, no. 4, pp. 1697–1706, 2011.
- [17] M. A. Fernø, M. Torsvik, S. Haugland, and A. Graue, "Dynamic laboratory wettability alteration," *Energy & Fuels*, vol. 24, no. 7, pp. 3950–3958, 2010.
- [18] A. Graue, E. Aspenes, T. Bognø, R. Moe, and J. Ramsdal, "Alteration of wettability and wettability heterogeneity," *Journal of Petroleum Science and Engineering*, vol. 33, pp. 3–17, 04 2002.

- [19] A. Hiorth, L. Cathles, and M. Madland, “The impact of pore water chemistry on carbonate surface charge and oil wettability,” *Transp Porous Med*, p. 21, 2010.
- [20] Y. Huang and A. A. Keller, “Isothermal titration microcalorimetry to determine the thermodynamics of metal ion removal by magnetic nanoparticle sorbents,” *Environ. Sci.: Nano*, vol. 3, pp. 1206–1214, 2016. [Online]. Available: <http://dx.doi.org/10.1039/C6EN00227G>
- [21] Y. Liu, J. Kaszuba, and J. Oakey, “Microfluidic investigations of crude oil-brine interface elasticity modifications via brine chemistry to enhance oil recovery,” *Fuel*, vol. 239, pp. 338 – 346, 2019. [Online]. Available: <http://www.sciencedirect.com/science/article/pii/S0016236118319276>
- [22] H. Mahani, R. Menezes, S. Berg, A. Fadili, R. Nasralla, D. Voskov, and V. Joeekar-Niasar, “Insights into the impact of temperature on the wettability alteration by low salinity in carbonate rocks,” *Energy & Fuels*, vol. 31, no. 8, pp. 7839–7853, 2017.
- [23] R. Mancinelli, A. Botti, F. Bruni, M. A. Ricci, and A. K. Soper, “Perturbation of water structure due to monovalent ions in solution,” *Phys. Chem. Chem. Phys.*, vol. 9, pp. 2959–2967, 2007.
- [24] M. Megawati, A. Hiorth, and M. Madland, “The impact of surface charge on the mechanical behavior of high-porosity chalk,” *Rock Mechanics and Rock Engineering*, vol. 46, pp. 1073–1090, 09 2013.
- [25] R. Mokhtari and S. Ayatollahi, “Dissociation of polar oil components in low salinity water and its impact on crude oil–brine interfacial interactions and physical properties,” *Petroleum Science*, vol. 16, 11 2018.
- [26] M. Moradi, E. Topchiy, T. E. Lehmann, and V. Alvarado, “Impact of ionic strength on partitioning of naphthenic acids in water–crude oil systems – determination through high-field nmr spectroscopy,” *Fuel*, vol. 112, pp. 236–248, 2013.
- [27] R. Nasralla, E. Sergienko, S. Masalmeh, H. Linde, N. Brussee, H. Mahani, B. Suijkerbuijk, and I. Alqarshubi, “Potential of low-salinity waterflood to improve oil recovery in carbonates: Demonstrating the effect by qualitative coreflood (spe-172010-pa),” *SPE Journal*, vol. 21, p. 12, 10 2016.
- [28] R. Nasralla, J. Snippe, and R. Farajzadeh, “Coupled geochemical-reservoir model to understand the interaction between low salinity brines and carbonate rock,” in *SPE Asia Pacific Enhanced Oil Recovery Conference held in Kuala Lumpur, Malaysia*. Society of Petroleum Engineers, 08 2015, p. 21.
- [29] J. Olsson, S. Stipp, E. Makovicky, and S. Gislason, “Metal scavenging by calcium carbonate at the eyjafjallajökull volcano: A carbon capture and storage analogue,” *Chemical Geology*, vol. 384, pp. 135 – 148, 2014.
- [30] T. Puntervold, S. Strand, R. Ellouz, and T. Austad, “Modified seawater as a smart eor fluid in chalk,” *Journal of Petroleum Science and Engineering*, vol. 133, pp. 440–443, 09 2015.
- [31] —, “Modified seawater as a smart eor fluid in chalk,” *Journal of Petroleum Science and Engineering*, vol. 133, pp. 440–443, 09 2015.

- [32] R. Reza, “Water-based eor in limestone by smart water,” Ph.D. dissertation, University of Stavanger, Stavanger, Norway, 2011.
- [33] M. Sohrabi, P. Mahzari, S. A. Farzaneh, J. R. Mills, P. Tsois, and S. Ireland, “Novel insights into mechanisms of oil recovery by use of low-salinity-water injection,” *Society of Petroleum Engineers*, vol. 22, p. 10, 2017.
- [34] J. Song, S. Rezaee, W. Guo, B. Hernandez, M. Puerto, F. M. Vargas, G. J. Hirasaki, and S. L. Biswal, “Evaluating physicochemical properties of crude oil as indicators of low-salinity-induced wettability alteration in carbonate minerals,” *Scientific reports*, vol. 10, no. 1, pp. 1–16, 2020.
- [35] E. Spinler, B. A. Baldwin, and A. Graue, “Simultaneous measurement of multiple capillary pressure curves from wettability and rock property variations within single rock plugs.” Symposium of the Society of Core Analysts, Golden, October 2002.
- [36] D. C. Standnes and T. Austad, “Wettability alteration in chalk: 1. preparation of core material and oil properties,” *Journal of Petroleum Science and Engineering*, vol. 28, no. 3, pp. 111 – 121, 2000.
- [37] S. Strand, T. Austad, T. Puntervold, E. J. Høgnesen, M. Olsen, and S. M. F. Barstad, ““smart water” for oil recovery from fractured limestone: A preliminary study,” *Energy & Fuels*, vol. 22, no. 5, pp. 3126–3133, 2008.
- [38] W. Stumm, *Chemistry of the solid-water interface: Processes at the mineral-water and particle-water interface in natural systems*. Jhon Wiley & Sons, 1992.
- [39] M. Takeya, M. Shimokawara, Y. Elakneswaran, T. Nawa, and S. Takahashi, “Predicting the electrokinetic properties of the crude oil/brine interface for enhanced oil recovery in low salinity water flooding,” *Fuel*, vol. 235, pp. 822 – 831, 2019.
- [40] P. Van Cappellen, L. Charlet, W. Stumm, and P. Wersin, “A surface complexation model of the carbonate mineral aqueous solution interface,” *Geochimica et Cosmochimica Acta*, vol. 57, no. 15, pp. 3505 – 3518, 1993.
- [41] A. W.G., “Wettability literature survey—part 1: Rock/oil/brine interactions and the effects of core handling on wettability,” *Journal of Petroleum Technology*, vol. 38, no. 10, 1986.
- [42] M. Wolthers, L. Charlett, and P. Cappellen, “The surface chemistry of divalent metal carbonate minerals; a critical assessment of surface charge and potential data using the charge distribution multi-site ion complexation model,” *American Journal of Science*, p. 37, 2008.



## Chapter 6

# Geothermal Brine Reinjection

This chapter presents the main results related to the papers V-VI. Those studies were aiming at investigating the reinjection of geothermal brines in sandstone rocks. In particular, the following research questions were investigated:

- (1) How safe is the re-injection of a half diluted geothermal brine from SaltPower electricity generation back in the same reservoir?. Is it possible to determine fluid-fluid and rock-fluid interactions upon geothermal brine reinjection by microcalorimetry?
- (2) How feasible is it to use citric acid to keep iron in solution?

### 1 Half Diluted Geothermal Brine Reinjection Feasibility

A synergy between microcalorimetry and core flooding experiments was used to determine the reinjection feasibility of half diluted geothermal brine coming from SaltPower Electricity Generation back in the same geothermal reservoir. The main findings presented in Paper V will be summarized. The first experiments correspond to Isothermal Titration Calorimetry (ITC) followed by coreflooding tests.

#### 1.1 Microcalorimetric evaluation of rock-fluid and fluid-fluid interactions

The addition of Thisted brine (TB) to Berea sandstone powder wetted with the same brine corresponds to a baseline experiment. It was done to gain further insights into the interactions that normally take place in a geothermal reservoir upon the reinjection of heat depleted brines. The thermogram obtained for this rock+fluid interaction is presented in Figure 6.1. Each exothermic peak represents a single titration of 9.947  $\mu\text{L}$  of TB onto the sandstone particles

saturated with TB. Those exothermic peaks were ascribed to the preferential adsorption of divalent cations ( $\text{Ca}^{2+}$ ,  $\text{Mg}^{2+}$ ) onto kaolinite clay minerals in Berea sandstone and the desorption of the monovalent cations ( $\text{K}^+$  and  $\text{Na}^+$ ) [10].

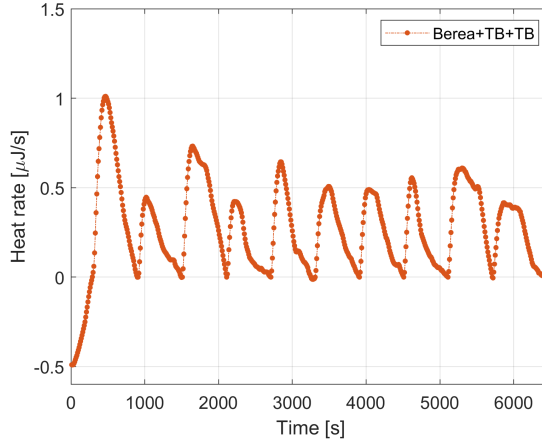


**Fig. 6.1:** Heat flow vs time for TB added to Berea sandstone wetted with TB

As presented for the ITC experiments performed on carbonate rocks, the interaction heat can be found by integrating the heat rate (each peak) over time [3–5]. Those heat values are useful because they are equal to the enthalpy change ( $\Delta H$ ) per unit ionic strength, as it was explained in Cobos et al. [5]. The  $\Delta H$  values can be calculated through Equation 5.1, where  $[\text{IS}]$  is the ionic strength of TB in mmol/L and  $V_i$  is the volume of each titration.

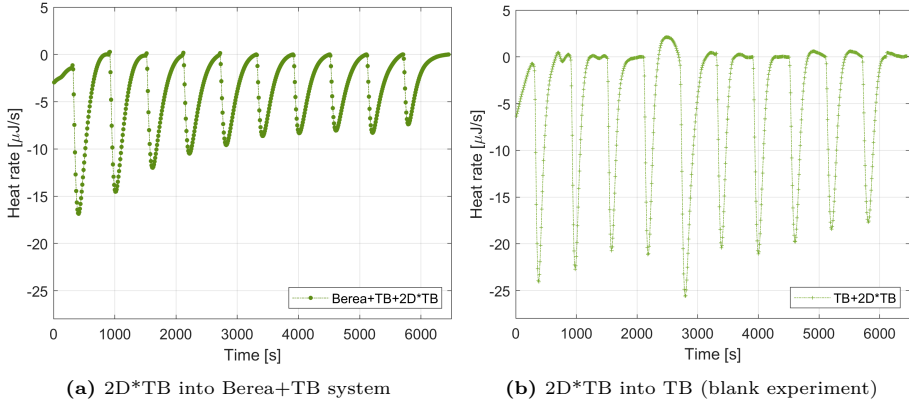
The  $\Delta H$  values for each injection of TB into berea+TB is shown in Table 6.1. The first titration of TB into the Berea+TB system is a fast exotherm. As the TB active species saturated the sandstone powder that was already impregnated with TB, the maximum enthalpy becomes less exothermic. This was ascribed to the saturation of kaolinite minerals with divalent cations; whereas,  $\text{K}^+$  and  $\text{Na}^+$  are being released from the surface. Thus, the cation exchange process, in which divalent cations take an important role, stabilizes the clay minerals inside the porous medium by reducing the particle-grain repulsion [3].

Figure 6.2 shows the heat flow signal registered by the microcalorimeter when half diluted Thisted brine ( $2\text{D}^*\text{TB}$ ) was injected into sandstone powder saturated with 100% concentrated TB (rock+brine system) and to TB. The negative peaks shown in Figure 6.2a indicates that the interaction between  $2\text{D}^*\text{TB}$  and the sandstone+TB system is dominantly endothermic (net reaction). This interaction was ascribed to a perturbation of the second and third hydration shells around the single ionic species caused by dilution of the geothermal brine [8]. When  $2\text{D}^*\text{TB}$  was injected into TB without the sandstone particles (blank experiment) at the same experimental, a higher heat flow was obtained as observed in Figure 6.2b.



**Table 6.1:** Heat, enthalpy change and cumulative enthalpy change (J/mol ionic strength) for Thisted brine (TB) and Berea sandstone interaction. Source: [3]

heat (mJ)	$\Delta H$ (J/mol)	Cum $\Delta H$ (J/mol)
$-0.29 \pm 0.05$	$-10.4 \pm 2.6$	-10.4
$-0.11 \pm 0.01$	$-1.8 \pm 0.3$	-12.3
$-0.17 \pm 0.06$	$-2.0 \pm 0.8$	-14.3
$-0.11 \pm 0.01$	$-1.0 \pm 0.1$	-15.3
$-0.12 \pm 0.02$	$-0.9 \pm 0.1$	-16.2
$-0.10 \pm 0.03$	$-0.6 \pm 0.2$	-16.8
$-0.16 \pm 0.03$	$-0.8 \pm 0.1$	-17.6
$-0.09 \pm 0.02$	$-0.4 \pm 0.1$	-17.9
$-0.16 \pm 0.05$	$-0.6 \pm 0.2$	-18.5
$-0.16 \pm 0.02$	$-0.7 \pm 0.1$	-19.1

**Fig. 6.2:** Heat flow vs time for half diluted Thisted Brine (2D\*TB)

The interaction heat for Berea+TB+2D\*TB and TB+2D\*TB found by integrating the endothermic peaks presented in Figure 6.2 is displayed in Table 6.2. The rock-fluid interactions were found by subtracting the heat response of the blank experiment (2D\*TB into TB) from the main experiment (sandstone+TB+2D\*TB). This interaction is exothermic since a set of composition variation "waves" rose as a result of salinity difference between the injected fluid and the formation brine (See Table 4.4).  $\text{Na}^+$  ions may have been desorbed from the clay particles to maintain the equilibrium in the solution as the ionic strength of the mixture decreases with every addition of 2D\*TB. The equilibration process creates a vacant site at the clay mineral lattice to be occupied by a divalent ion (e.g.  $\text{Ca}^{2+}$ ). Thus, the ITC experiments suggest that loosely attached particles (clay minerals) in the porous media will remain stabilized due to relatively high fractions of calcium ions in both TB and 2D\*TB [3], which in turn won't cause any formation damage by fines migration inside the porous media.

**Table 6.2:** Heat and enthalpy change (J/mol ionic strength) values for 2D\*TB added to sandstone aged with TB

$IS_{\text{mixture}}$ (mol/L)	$Q_{\text{exp}}$ (mJ)	$Q_{\text{blank}}$ (mJ)	$\Delta H_{\text{interaction}}$ (J/mol)
2.45	$2.76 \pm 0.7$	3.2	-19.8
2.43	$2.74 \pm 0.3$	2.9	-6.0
2.40	$2.46 \pm 0.3$	2.7	-11.0
2.38	$2.23 \pm 0.3$	2.2	1.9
2.35	$2.06 \pm 0.2$	5.4	-140.8
2.33	$1.87 \pm 0.1$	2.3	-17.5
2.31	$1.76 \pm 0.1$	3.0	-55.1
2.28	$1.69 \pm 0.2$	2.7	-46.6
2.26	$1.65 \pm 0.2$	2.7	-46.8
2.24	$1.48 \pm 0.1$	2.8	-59.0

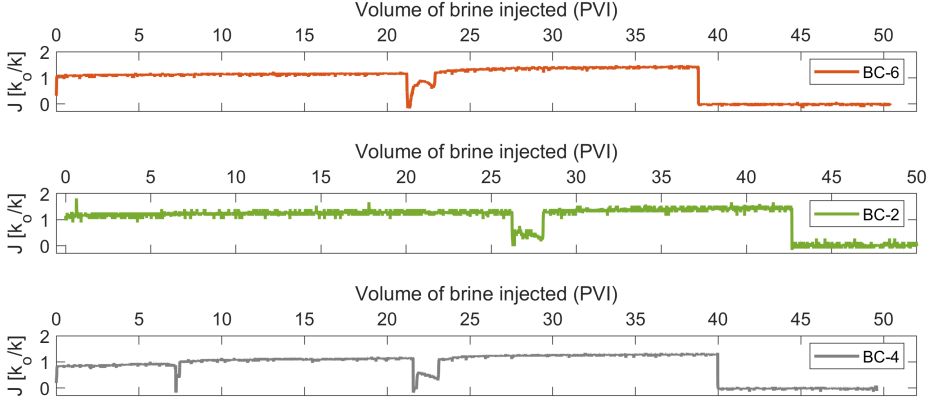
## 1.2 Brine permeability flow test

In order to confirm the observations from the ITC experiments, half diluted Thisted brines (2D\*TB and 2D\*TB<sub>air</sub>) and 100% concentrated Thisted brine (TB) were each injected in forward and backward direction into 2 Berea sandstone cores for duplication purposes [3]. Note that half diluted Thisted brine was also bubbled with air to precipitate iron, Fe(II), in solution. It is expected that clay particles should not be mobilized by the injection of diluted Thisted brines. This is because the NaCl concentration (1.4 M) of those diluted brines is well above the critical salt concentration, CSC, (0.070 M) at which the permeability of a rock sample begins to decrease [2, 6, 7]. The flooding scheme for Berea core plugs was: **BC-1 and BC-2** flooded with 2D\*TB, **BC-3 and BC-4** flooded with 2D\*TB<sub>air</sub>, **BC-5 and BC-6** flooded with TB.

The results from the pressure measurements are expressed in terms of the dimensionless impedance function, which is shown in Equation 6.1. This function relates the initial brine permeability,  $k_0$ , with the permeability values over time,  $k(t_D)$ . Where,  $J(t_D)$  is the impedance value,  $q$  is the flow rate and  $\Delta P(t_d)$  corresponds to the differential pressure over time [9].

$$J(t_D) = \frac{\Delta P(t_D)q(0)}{q(t_D)\Delta P(0)} = \frac{k_0}{k(t_D)} \quad (6.1)$$

Figure 6.3 shows the impedance values for BC-2, BC-4 and BC-6. There are 3 distinguishable sections since the ISCO D-Series pump was refilled at about 23 (PVI). In the last section, the flow was reversed after about 40 pore volumes injected (PVI). As observed, BC-2 which was flooded with 2D\*TB shows a similar impedance as BC-6 flooded with TB. BC-4 flooded with 2D\*TB<sub>air</sub> has a slightly lower impedance than BC-2 and BC-6 for the first 20 PVI.



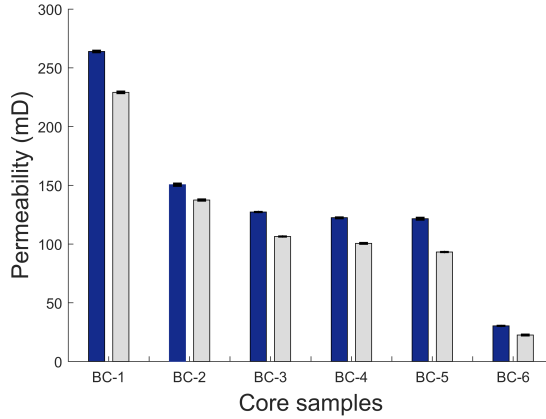
**Fig. 6.3:** Impedance change for: 2D\*TB into BC-2, 2D\*TB<sub>air</sub> into BC-4 and TB into BC-6

Table 6.5 shows the brine permeability for each core that was calculated at the zones where the pressure is stable. The term  $k_0$  is the initial brine permeability,  $k_B$  is the brine permeability either in section 1 or 2, and PRF is a permeability reduction factor [3]. It is observed that approximately 23% of the rock permeability was reduced when 2D\*TB was injected into BC-1 and BC-2. The permeability reduction for concentrated TB is about 15% due to less oxygen present in the water. It was expected that bubbling the half diluted geothermal brine with air precipitate iron, avoiding its precipitation inside the porous media. However, this solution was not the optimum since 2D\*TB<sub>air</sub> caused 13% permeability reduction, which could be ascribed to iron precipitation with the in-situ formation brine. It is also observed that a pause in the fluid injection created a higher permeability reduction in all cores samples, with an average permeability reduction of 30% for cores flooded with 2D\*TB, 29 % for 2D\*TB<sub>air</sub> and 19% for TB. Those permeabilities reductions could be associated with iron colloidal particles deposited during the forward injection. When Danish geothermal plants are shut down during summer or for other issues, similar permeability reductions have been observed.

**Table 6.3:** Brine permeabilities and damage factor for berea sandstone cores flooded with half diluted Thisted brine (BC-1 and BC-2), half diluted Thisted brine bubbled with air, (BC-3 and BC-4), and Thisted brine (BC-5 and BC-6). Source: [3]

sample	$k_0$ (mD)	$k_B$ (mD)		PRF (%)	
		$k_{B1}$	$k_{B2}$	PRF <sub>1</sub>	PRF <sub>2</sub>
BC-1	102	85.2	72.2	23	29
BC-2	186	147.9	131.3	21	30
BC-3	82	68.9	51.5	16	37
BC-4	69	62.4	55	10	21
BC-5	7	5.7	5.6	18	19
BC-6	72	63.5	51.7	12	28

The air permeability measurements before and after the core flooding experiments are displayed in Figure 6.4. The air permeability was decreased by about 15% for the core plugs flooded with  $2D*TB$  and  $2D*TB_{air}$ . A higher air permeability reduction was observed for the core plugs (BC-5 and BC-6) flooded with TB. This is because TB is a highly saline fluid and therefore more crystals salts precipitate inside the porous media when the fluid dries out before the permeability measurements [3].



**Fig. 6.4:** Measured air permeability of the cores before and after the core flooding experiments. Blue bars show the measurements prior the experiments and the grey bars indicate the measurements after the core flooding experiments

The formation damage due to iron precipitation can be observed in Figure 6.5. The first core plug was flooded with concentrated Thisted brine, the next two cores with  $2D*TB$ , and the last ones with  $2D*TB_{air}$ . Iron precipitation at the injection face for the core plugs flooded with  $2D*TB$  is remarkable. The cores flooded with  $2D*TB_{air}$  do not have visible iron precipitation in the outermost face but the air reacted with the in-situ brine causing similar formation damage than the other brines.



**Fig. 6.5:** Core plugs flooded with TB,  $2D*TB$  and  $2D*TB_{air}$

As presented in the previous sections, the main problem with the reinjection of half diluted

geothermal brine coming from SaltPower electricity generation is not a reduction of salinity that causes migration and straining of non-swelling clay minerals in the thinner pore throats but the precipitation of iron oxides inside the porous media. In this sense, the original iron concentration (1 mg/l) in 2D\*TB was reduced drastically to 0.18 and 0.33 mg/l during the forward and reverse brine injection, respectively. Since the iron concentration in 2D\*TB<sub>air</sub> was relatively low (0.09 mg/l), only a small amount of Fe(II) was oxidized and precipitated during the forward and reverse injections. However, this fluid caused similar formation damage due to impairment with the reservoir fluid.

## 2 Citric Acid as a Potential Iron Control Agent

As presented in Section 1, half diluted geothermal brine coming from SaltPower electricity generation will not cause migration and staining of fines in the narrow pore throats but the precipitation of iron oxides inside the porous media. Paper VI presents a solution for this problem by the addition of citric acid to the half diluted geothermal brines. The experiments were carried out with in-situ brine from Sønderborg geothermal brine. The ionic composition of this brine can be found in Table 4.4. Similarly to Cobos et al. [3], both microcalorimetry and core flood tests were carried out using Berea sandstone.

The microcalorimetry experiments for concentrated (SB) and half diluted Sønderborg (2D\*SB) brines into Berea particles saturated with Sønderborg (Berea+SB system) shows a similar trend as the results presented in Cobos et al. [3]. The heat flow registered in the microcalorimeter apparatus for those injections is presented in Figure 6.6. Effectively as observed in Figure 6.6a the addition of SB into a system that contains the same geothermal brine is exothermic. Consequently, fines migration is not expected to occur due to an ion exchange process that stabilizes loosely attached particles inside the porous media. As shown in Cobos et al [3], the injection of a half diluted brine into a rock+concentrated brine system is endothermic. This is also reflected in Figure 6.6b, in which 2D\*SB was added to the Berea+SB system.

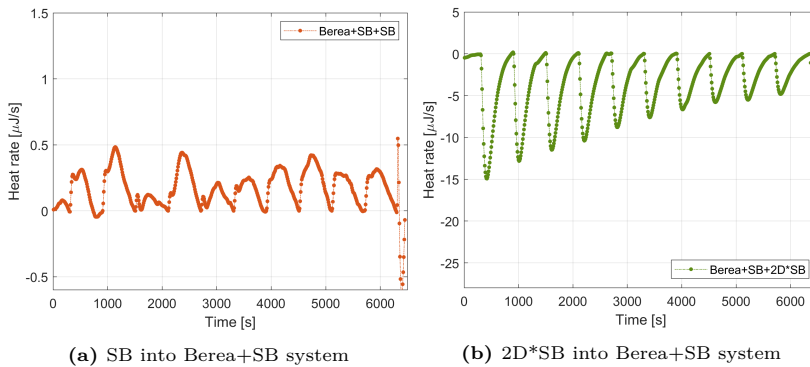


**Fig. 6.6:** Heat flow vs time for concentrated and half diluted Sønderborg Brines

Citric acid, which normally is used in oil field treatments to stabilize iron, was added to half diluted S nderborg ( $2D*SB_{citric}$ ) and injected into the Berea+SB system. As observed in Figure 6.7, the interaction of  $2D*SB_{citric}$  with Berea+SB is partially endothermic and partially exothermic. The exothermic peaks can be attributed to the reaction of citric acid with iron to form soluble complexes. On the other hand, the endothermic peaks, as assumed previously, could be associated with a disturbance in the hydrogen bonding (HB) beyond the first hydration shell.

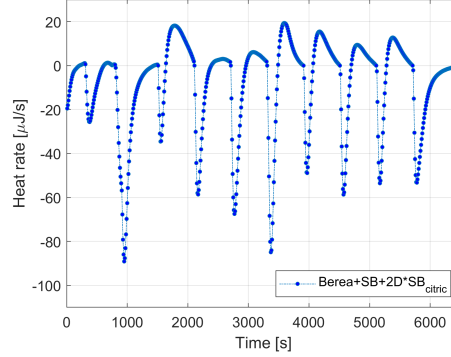


**Fig. 6.7:** Heat flow vs time for  $2D*SB_{citric}$ + Berea sandstone system aged with SB

The heat values obtained by the integration of those partially exothermic and endothermic peaks over time are presented in Table 6.4. The estimated enthalpy values ( $\Delta H$ ) for the interaction of  $2D*SB_{citric}$  with the sandstone particles impregnated with formation brine (SB) are also presented in the same table. Those values take into account both competitive processes (disturbance of hydration shells and the reaction of citric acid with iron).

**Table 6.4:** Ionic strength of the mixture ( $I_{c_{mix}}$  in mol/l, heat in mJ, enthalpy change per mole of ionic strength ( $\Delta H$ ) in J/mol for the interaction of  $2D*SB_{citric}$  and Berea+SB system

inj	1	2	3	4	5	6	7	8	9	10
$I_{c_{mix}}$	2.63	2.54	2.46	2.40	2.33	2.27	2.21	2.15	2.09	2.03
heat	$5.1 \pm 1.7$	$14.0 \pm 1.4$	$-2.8 \pm 0.4$	$6.3 \pm 0.2$	$6.9 \pm 0.2$	$4.3 \pm 0.1$	$0.7 \pm 0.1$	$3.6 \pm 0.1$	$2.0 \pm 0.1$	$9.8 \pm 0.1$
$\Delta H$	196	555	-114	263	296	190	30	169	94	483

The heat flow of  $2D*SB_{citric}$  into SB (blank experiment) is presented in Figure 6.8. It can be noticed that both endothermic and exothermic peaks in the blank experiment are much smaller than the ones presented in Figure 6.7. This difference could be attributed to the dissolution of iron-bearing carbonate cement, which might have increased the exothermic response registered in the microcalorimeter apparatus.

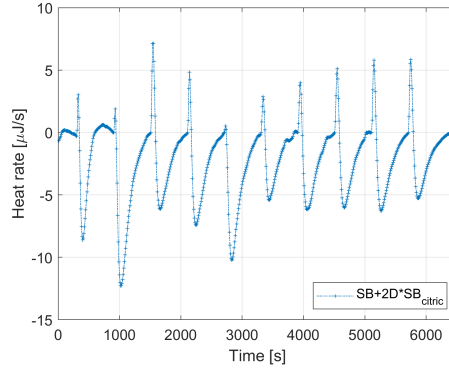


**Fig. 6.8:** Heat flow vs time for  $2D*SB_{citric} + SB$  system

Citric acid is a weak organic acid that ionizes in water stepwise. In each ionization step,  $H^+$  ions are being released, which could react with iron bearing carbonate cements, such as siderite ( $FeCO_3$ ) and ankerite [ $Ca(Fe, Mg)(CO_3)_2$ ]. The dissolution of those carbonate cements due to  $H^+$  attack can be represented by Equation 6.2, where, Me represents a metal ion, such as  $Ca^{2+}$ ,  $Mg^{2+}$  or  $Fe^{2+}$ .



The dissolution of iron-bearing carbonate cement (siderite and ankerite) in the presence of citric acid occurs in three steps: 1) transport of citric acid ( $H_3AOH$ ) to the rock surface, 2) ionization of citric acid and reaction with the rock cement, and 3) transport of the dissolved aqueous species away from the mineral surface into the bulk solution [1]. A schematic representation of this dissolution process is presented in Figure 6.9. It is assumed that a dissolution process could have taken place inside the reaction vessel. This hypothesis will be confirmed in the core flood tests.

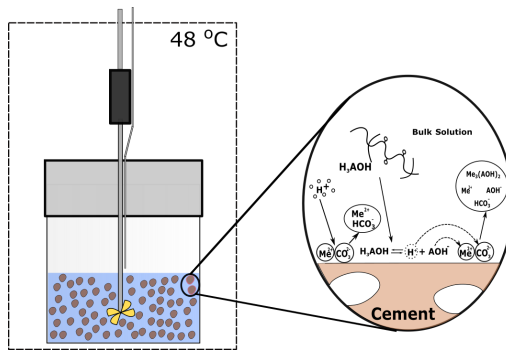


**Fig. 6.9:** Mechanism of iron bearing carbonate cements dissolution in  $2D*SB$  with citric acid

## 2.1 Brine permeability flow test

Similarly to Cobos et al. [3], 100% concentrated Sønderborg brine (SB) and half diluted Sønderborg brines (2D\*SB and 2D\*SB<sub>citric</sub>) were each injected into Berea sandstone core plugs in forward and backward directions. The flooding scheme for Berea core plugs was: **BC-7 and BC-8** flooded with SB, **BC-9 and BC-10** flooded with 2D\*SB, **BC-15 and BC-16** flooded with 2D\*SB<sub>citric</sub>.

The so-called dimensionless impedance function (see Equation 6.1) was also used to describe the medium permeability of the cores flooded with SB, 2D\*SB, and 2D\*SB<sub>citric</sub>. Figure 6.10 presents the impedance history for BC-8, BC-10, and BC-15 core plugs. As observed, 3 distinguishable sections are also shown in the impedance history because the injection could not be continuous in the forward direction and the flow was reversed at around 43 PVI. A similar impedance value ( $J > 1$ ) can be observed for BC-8 and BC-10, whereas, BC-15 has a much lower impedance ( $J < 1$ ). Consequently, the injectivity of 2D\*SB<sub>citric</sub> is much better than for SB and 2D\*SB geothermal brines. This injectivity improvement is independent of the injection continuity since the permeability is the same or a little bit better than in the first section.

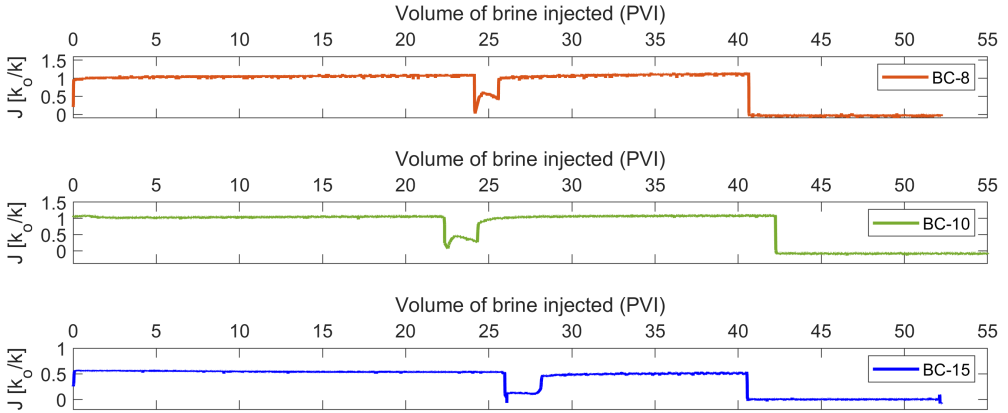


**Fig. 6.10:** Impedance change for: SB into BC-8, 2D\*SB into BC-10, and 2D\*SB<sub>citric</sub> into BC-15

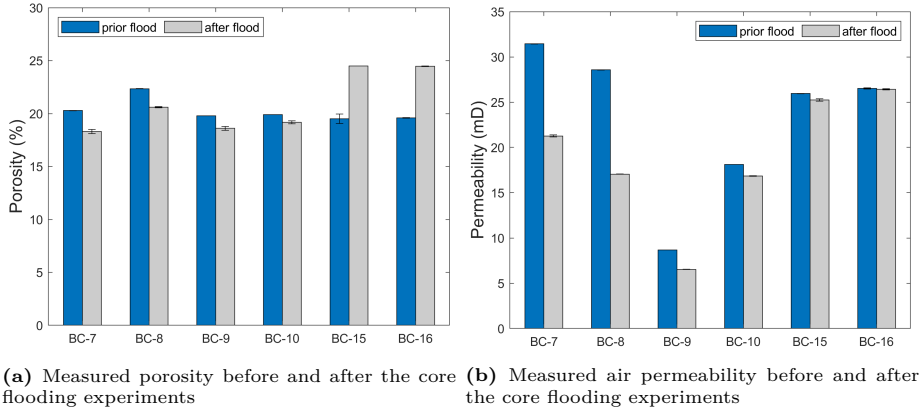
The permeability to the brine for each core plug is presented in Table 6.5. It is observed that half diluted brine with citric acid increased the rock permeability, which is the opposite of the results obtained with SB and 2D\*SB brines. As suggested by the microcalorimetry experiments, 2D\*SB<sub>citric</sub> not only keeps iron in solution but dissolves iron-bearing carbonate cement, which in turn increases the injectivity independently if the injection is continuous or not. This could solve injectivity problems when the geothermal plants are shut down during summer or for other technical issues.



**Table 6.5:** Brine permeabilities for berea plugs flooded with two times diluted S nderborg brine (2D\*SB), S nderborg brine (SB) and two times diluted S nderborg brine with citric acid (2D\*SB<sub>citric</sub>)

sample	$k_0$ (mD)	$k_{B1}$ (mD)	$k_{B2}$ (mD)
BC-7	91.7	80.4	68.9
BC-8	62.0	58.3	56.9
BC-9	11.8	11.8	11.3
BC-10	34.7	33.4	32.7
BC-15	27.1	49.2	53.3
BC-16	29.9	54.1	50.9

The porosity and air permeability measurements before and after the core flooding experiments are presented in Figure 6.11. As observed, both porosity and air permeability increased for BC-15 and BC-16, whereas, the cores flooded with SB and 2D\*SB show a porosity and permeability reduction. Consequently, the injection of half diluted brine with citric acid improves the rock quality.

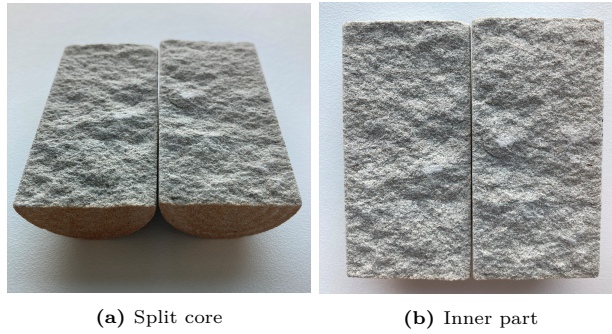
**Fig. 6.11:** Rock properties of core plugs flooded with SB (BC-7 and BC-8), 2D\*SB (BC-9 and BC-10), and 2D\*SB<sub>citric</sub> (BC-11 and BC-12) brines

Formation damage due to iron precipitation can be observed in Figure 6.12, in which the core plugs were arranged as the flooding scheme (SB, 2D\*SB, and 2D\*SB<sub>citric</sub>). The difference between those core plugs is remarkable since the first four sample shows iron precipitation at the injection face, whereas, the cores flooded with citric acid do not present any visible iron precipitation.



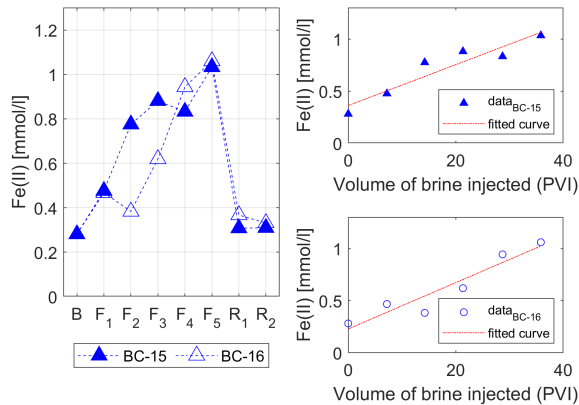
**Fig. 6.12:** Core plugs flood with SB, 2D\*SB, and 2D\*TB<sub>air</sub>

Figure 6.13 shows how the inner part of a core plug flooded with 2D\*SB looks like. It is observed that Fe (II) has been oxidized and precipitated as Fe(III) near the zone close to the injection face but not so much in the inner part. The original 2D\*SB had an iron concentration of 92.3 mg/l, which was reduced remarkably to 6.6 mg/l and 38 mg/l during the forward and reverse injections. A pre-treatment to keep iron in solution and reduce the amount of oxygen should be implemented before the injection of a half diluted geothermal brine (e.g. 2D\*SB). The addition of citric acid ( $C_6H_8O_7$ ), an iron control agent, to the diluted geothermal brine could be a possible solution to the injectivity problems due to iron precipitation.



**Fig. 6.13:** Split core plug flooded 2D\*SB

The variation of Fe(II) concentration by the injection of 2D\*SB<sub>citric</sub> through BC-15 and BC-16 core plugs is presented in Figure 6.14. As observed, the Fe(II) concentration increases as 2D\*SB<sub>citric</sub> is injected in the forward direction, whereas, it is almost the same during the reverse injection. Consequently, it confirms the dissolution of iron-bearing carbonate cement (siderite and ankerite) in the Berea sandstone core plugs.



**Fig. 6.14:** Fe(II) concentration in core plugs flooded with 2D\*SB<sub>citric</sub> and trend lines

The dissolution of iron-bearing carbonate cement can be described by a linear regression in both direct and reverse directions. The results from the linear regression are displayed in Table 6.6. Those equations indicate that the dissolution of iron-bearing carbonate cement is directly proportional to the pore volumes (PV) of 2D\*SB<sub>citric</sub> injected into the core plugs.

**Table 6.6:** Linear regression model for core plugs flooded with 2D\*SB<sub>citric</sub>

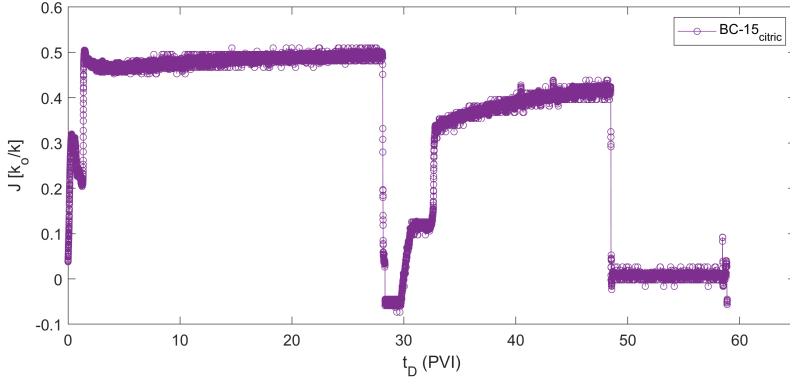
Ion	Equation	R <sup>2</sup>
BC-15	$y = 0.020 + 0.36x$	0.89
BC-16	$y = 0.022 + 0.23x$	0.90

Figure 6.15 shows the effluents collected for BC-16. As observed, the injection fluid (2D\*SB<sub>citric</sub>) is completely clear at the beginning. But as soon as citric acid contacts the rock more and more iron is being dissolved and therefore the effluents turn brownish. The effluents collected in the reverse injection, on the other hand, have a low concentration of iron as observed in Figure 6.14. Thus, their color is completely clear.



**Fig. 6.15:** Effluents collected stepwise for BC-16 flooded with 2D\*SB<sub>citric</sub>

It is believed that due to the improvement of the rock properties (porosity and permeability) the use of citric acid would decrease very much after some time. In order to test this hypothesis a second flood test was scheduled for BC-15<sub>citric</sub>. The impedance change for 2D\*SB is presented in Figure 6.16. It can be observed that the impedance value is less than 1 for the first and second zones, which indicates that the injectivity has been improved considerably.



**Fig. 6.16:** Impedance change for 2D\*SB flooded into BC-15<sub>citric</sub>

It can be observed in Table 6.7 that the rock properties of BC-15 previously flooded with citric acid were indeed improved. The initial brine permeability ( $k_0$ ) was about 20 mD. This value was further improved during the first and second injections with values of 42 and 52 mD, respectively. Consequently, the injection of a half diluted geothermal brine with citric acid could be a good choice to overcome the very often problems related with scaling that normally occurs in the reinjection wells.

**Table 6.7:** Brine permeabilities for 2D\*SB flooded into BC-15<sub>citric</sub>

sample	$k_0$ (mD)	$k_{B1}$ (mD)	$k_{B2}$ (mD)
BC-15 <sub>citric</sub>	20.4	42.3	52.2

## References

- [1] M. Alkhalidi, H. Nasr-El-Din, and H. Sarma, “Application of citric acid in acid stimulation treatments,” in *Canadian International Petroleum Conference, Calgary, Alberta*, 2009, p. 16.
- [2] K. C. Khilar and H. S. Fogler, “Water sensitivity of sandstones,” *Society of Petroleum Engineers Journal*, vol. 23, pp. 55–64, 02 1983.
- [3] J. E. Cobos and E. G. Søgaaard, “Study of geothermal brine reinjection by microcalorimetry and core flooding experiments,” *Geothermics*, vol. 87, p. 101863, 2020.
- [4] J. E. Cobos and E. G. Søgaaard, “Impact of compositional differences in chalk and water content on advanced water flooding: A microcalorimetric assessment,” *Energy & Fuels*, vol. 34, no. 10, pp. 12 291–12 300, 2020. [Online]. Available: <https://doi.org/10.1021/acs.energyfuels.0c02108>
- [5] J. E. Cobos, P. Westh, and E. G. Søgaaard, “Isothermal titration calorimetry study of brine oil rock interactions,” *Energy & Fuels*, vol. 32, no. 7, pp. 7338–7346, 2018.
- [6] K. Khilar, H. Fogler, and J. Ahluwalia, “Sandstone water sensitivity: Existence of a critical rate of salinity decrease for particle capture,” *Chemical Engineering Science*, vol. 38, no. 5, pp. 789 – 800, 1983.
- [7] S. Kia, H. S. Fogler, and M. Reed, “Effect of salt composition on clay release in berea sandstones,” *Society of Petroleum Engineers*, p. 11, 02 1987.
- [8] R. Mancinelli, A. Botti, F. Bruni, M. A. Ricci, and A. K. Soper, “Perturbation of water structure due to monovalent ions in solution,” *Phys. Chem. Chem. Phys.*, vol. 9, pp. 2959–2967, 2007.
- [9] M. A. Oliveira, A. S. Vaz, F. D. Siqueira, Y. Yang, Z. You, and P. Bedrikovetsky, “Slow migration of mobilised fines during flow in reservoir rocks: Laboratory study,” *Journal of Petroleum Science and Engineering*, vol. 122, pp. 534 – 541, 2014.
- [10] M. Valiskó, D. Boda, and D. Gillespie, “Selective adsorption of ions with different diameter and valence at highly charged interfaces,” *The Journal of Physical Chemistry C*, vol. 111, no. 43, pp. 15 575–15 585, 2007.



# Conclusions

In this study, microcalorimetry has been shown as a powerful apparatus to characterize rock-fluid systems in an accurate and reproducible manner. The normal application of microcalorimetry is on biological science research for characterizing the metabolic activities of living systems and bio-molecular interactions. Based on the experimental results in this study, the overall conclusions are summarized in the following sections.

## Wettability Alteration

Isothermal titration calorimetry can be used to characterize the wettability alteration in carbonate rocks. This technique gives the heat released or adsorbed upon rock-fluid and fluid-fluid interactions. Based on the results following conclusions were drawn:

- The thermograms for different chalk+formation brine+oil systems show that the wetting energies for 10 times diluted seawater (10D\*SW) are well above than for seawater spiked with sulfate or smart water.
- The performance of an advanced fluid depends slightly on the mineral depositions and compositional conditions of different chalk samples, a small fraction of metal oxides ( $\text{Al}_2\text{O}_3$ ,  $\text{SiO}_2$ ),  $\text{MgCO}_3$  are believed to be responsible for the observed differences.
- Different competitive processes take place at the interface when crude oil contact a non-organic fluid (brine). Those interactions are endothermic and require energy from the surroundings to proceed.
- Micro-dispersions at the crude oil-liquid interface, due to a high entropy production, makes the endothermic processes to proceed spontaneously. The total energy required to create those micro-emulsions for salts that contain  $\text{Cl}^-$  follows:  $\text{Mg}^{2+} > \text{Ca}^{2+} > \text{Na}^+$ . The order for salts that contain  $\text{Na}^+$  is:  $\text{HCO}_3^- > \text{SO}_4^{2-}$ .
- A pair creation process affects fluid-fluid interactions. Due to the hydrophobic effect, it is easier for water molecules to push away ion pairs with a neutral charge into the oil

phase than to disrupt the existing hydrogen bonding (HB) network.

- Supplying fresh crude oil during the aging procedure to a rock sample causes the greatest wettability change. Exothermic peaks were observed in further crude oil injections into the limestone+formation brine system. Therefore, dynamic aging is more efficient in the wettability alteration of outcrop limestone rocks than the static aging method.

## Brine Reinjection

The injection feasibility of a half diluted geothermal brine back to the same reservoir was explored by a combination of microcalorimetry and core flood tests. The main conclusions of this study are shortly summarized as:

- Isothermal Titration Calorimetry shows that a geothermal brine (highly saline fluid) that has been diluted can still stabilize loosely attached particles inside the porous media, those observations were confirmed by core flooding experiments.
- The major problem with half diluted brines coming from SaltPower electricity generation is not the dilution but the oxidation and precipitation of iron oxides inside the porous media. This problem could be solved by the addition of citric acid.
- Half diluted geothermal brine with citric acid improves the rock properties due to the dissolution of the material that clogs the pore space and iron carbonate cement. This fluid could be used as a good choice to overcome scaling problems in geothermal wells. The results are very promising because the injection of half diluted geothermal brine in a core flooded previously with citric acid has an improvement. Therefore, the use of citric acid could be decreased over time.



# Future Perspectives

The experimental work presented in this thesis has given a systematic procedure for analysis of rock-fluid and fluid-fluid interactions for wettability alteration studies and geothermal brine reinjection through microcalorimetry. In light of the interesting results, the following studies should be conducted:

- In this work the potential of two advanced fluid (diluted seawater and modified seawater) was investigated using different types of outcrop chalk rocks and crude oil. But this work should be extended to reservoir rocks, and other outcrop rocks, such as limestone, dolomite, and sandstone.
- In the current study most wettability studies were performed at 75 °C, but other temperatures should also be considered (23, 50, and 100 °C). At high temperatures, the heat flow registered in the calorimeter should be corrected for the vaporization of light crude oil fractions.
- Identify the role of crude oil with different acid and base numbers on adsorption energies. Develop a database to find possible correlations among key important parameters for wettability reversal (oil-wet towards less oil-wet conditions).
- The role of pH change upon each injection of low salinity water could be explored while measuring heat flow. For that purpose, a special sensor is needed.
- Extend the dynamic aging procedure to other rocks, such as dolomite, and sandstone.
- In the current work, outcrop sandstone core plugs were used to evaluate the reinjection of half diluted geothermal brine coming from SaltPower electricity generation but the flood tests should be extended to real reservoir rocks.
- Evaluate different options to keep iron in solution to avoid formation damage in geothermal reservoirs.

ISSN (online): 2446-1636  
ISBN (online): 978-87-7210-849-0

AALBORG UNIVERSITY PRESS